



Evaluation of a peptidomimetic targeting the receptor NRP-1 for treatment of medulloblastoma

Caifeng Gong

► To cite this version:

Caifeng Gong. Evaluation of a peptidomimetic targeting the receptor NRP-1 for treatment of medulloblastoma. Human health and pathology. Université de Lorraine, 2018. English. NNT : 2018LORR0115 . tel-01902449

HAL Id: tel-01902449

<https://hal.univ-lorraine.fr/tel-01902449>

Submitted on 13 Jan 2022

HAL is a multi-disciplinary open access archive for the deposit and dissemination of scientific research documents, whether they are published or not. The documents may come from teaching and research institutions in France or abroad, or from public or private research centers.

L'archive ouverte pluridisciplinaire **HAL**, est destinée au dépôt et à la diffusion de documents scientifiques de niveau recherche, publiés ou non, émanant des établissements d'enseignement et de recherche français ou étrangers, des laboratoires publics ou privés.



AVERTISSEMENT

Ce document est le fruit d'un long travail approuvé par le jury de soutenance et mis à disposition de l'ensemble de la communauté universitaire élargie.

Il est soumis à la propriété intellectuelle de l'auteur. Ceci implique une obligation de citation et de référencement lors de l'utilisation de ce document.

D'autre part, toute contrefaçon, plagiat, reproduction illicite encourt une poursuite pénale.

Contact : ddoc-theses-contact@univ-lorraine.fr

LIENS

Code de la Propriété Intellectuelle. articles L 122. 4

Code de la Propriété Intellectuelle. articles L 335.2- L 335.10

http://www.cfcopies.com/V2/leg/leg_droi.php

<http://www.culture.gouv.fr/culture/infos-pratiques/droits/protection.htm>

Thèse

Présentée et soutenue publiquement pour l'obtention du titre de

DOCTEUR DE L'UNIVERSITÉ DE LORRAINE

Mention: «Sciences de la vie et de la Santé»

Par **Caifeng GONG**

**Intérêt de l'utilisation d'un peptidomimétique ciblant le récepteur
NRP-1 pour le traitement du médulloblastome**

**Evaluation of a peptidomimetic targeting the receptor NRP-1 for
treatment of medulloblastoma**

Le 21 septembre 2018

Travaux encadrés par Cédric BOURA et Pascal CHASTAGNER

Membres du jury :

Rapporteurs :

BALOSSO Jacques
DONTENWILL Monique

PU-PH, Crlcc Francois Baclesse, Caen
DR CNRS, Université de Strasbourg

Examineurs:

LEBLOND Pierre
PELLEGRINI-MOÏSE Nadia

PH, Crlcc Oscar Lambret, Lille
MCF-HDR, Université de Lorraine

Directeur de thèse:

CHASTAGNER Pascal

PU-PH, CHRU-Nancy, Université de Lorraine

Co-directeur de thèse:

BOURA Cédric

MCF, Université de Lorraine

Résumé

Titre : Intérêt de l'utilisation d'un peptidomimétique ciblant le récepteur NRP-1 pour le traitement du médulloblastome

Le médulloblastome (MB) est la plus fréquente des tumeurs cérébrales malignes pédiatriques qui représentent la première cause de mortalité par cancer chez l'enfant. Malgré les avancées des nouveaux traitements, les risques de récurrence, séquelles et décès après traitement restent importants. Le récepteur de neuropiline-1 (NRP-1) a été récemment impliqué dans la progression tumorale des MBs et semble jouer un rôle important dans le phénotype des cellules souches cancéreuses (CSCs). Le ciblage de cette molécule pourrait ainsi présenter un intérêt thérapeutique dans le traitement des MBs. Nous avons sélectionné des cellules souches de MB capables de former des médullosphères (MS) à partir de 3 lignées cellulaires (DAOY, D283-Med et D341-Med). Ces modèles ont été caractérisés par l'expression de neuropilines (NRP-1 and NRP-2) et de marqueurs phénotypiques (CD133, CD15 et NF-M). Les résultats ont montré une augmentation significative de l'expression de NRP-1 par les cellules cultivées en médullosphères confortant notre stratégie de ciblage. L'impact du traitement de ces cellules par un composé innovant ciblant spécifiquement NRP-1, le MR438, a été ensuite évalué *in vitro* seul et en association avec la radiothérapie notamment sur l'étude de la capacité d'auto-renouvellement des CSCs de MBs. Nous avons mis en évidence une diminution de la capacité d'autorenouvellement des cellules souches de MBs après exposition au MR438 avec une radiosensibilité augmentée pour les 3 modèles cellulaires. *In vivo*, le composé MR438 a été évalué sur des modèles de xénogreffes hétéotopiques chez la souris nude et montre un effet radiopotentialisant significatif pour les tumeurs issues de la lignée Daoy avec une tendance à la diminution de la progression tumorale pour les 2 autres lignées. De façon intéressante, le composé MR438 induit une diminution significative du nombre de cellules souches pour l'ensemble de nos modèles. Par conséquent, le composé semblerait induire les cellules souches vers un phénotype différencié au moins pour la lignée DAOY, même si les mécanismes n'ont pas pu être clairement élucidés. En conclusion, l'inhibition de NRP-1 *via* MR438 semble stimuler la différenciation des cellules souches cancéreuses pouvant à terme réduire la progression du MB et apporter un bénéfice en association avec la radiothérapie. L'évaluation du composé sur des modèles orthotopiques de MB permettrait d'obtenir des informations quant à son efficacité sur des modèles plus proches de la physiopathologie tenant compte de sa distribution au niveau cérébral.

Mots-clés: Médulloblastome; Neuropiline-1; Cellule souche cancéreuse; Peptidomimétique; Radiothérapie

Abstract

Title: Evaluation of a peptidomimetic targeting the receptor NRP-1 for treatment of medulloblastoma

Medulloblastoma (MB) is the most common malignant pediatric brain tumors which is the leading cause of cancer death in children. Despite the progress of new treatments, the risk of recurrence, morbidity, and death after treatment remain important. The neuropilin-1 receptor (NRP-1) has recently been implicated in tumor progression of MBs, which seems to play an important role in the phenotype of cancer stem cells (CSCs). Targeting this molecule could thus present an interesting therapeutic value in the treatment of MB. We have selected cancer stem like cells of MBs in the form of medullospheres (MSs) from 3 cell lines (DAOY, D283-Med and Med-D341). These models were characterized by expression of neuropilins (NRP-1 and NRP-2) and phenotypic markers (CD133, CD15 and NF-M). Results showed a significant increase of the expression of NRP-1 by our CSCs models cultured in MSs that confirms our targeting strategy. The impact of the treatment of these cells with an innovative compound specifically targeting NRP-1, MR438, was then evaluated *in vitro* alone and in association with radiotherapy, especially on the study of the capacity for self-renewal. A decrease of self-renewal capacity for MB stem cells after exposition of MR438 with an increase of radiosensitivity for the 3 cell models *in vitro* was demonstrated. *In vivo*, MR438 was evaluated on heterotopic xenograft models in nude mice and showed a significant augmentation of radiosensitivity for DAOY tumors with a tendency to decrease tumor progression for the other 2 cell lines. Interestingly, the compound MR438 induced a significant decrease in the number of stem cells for all of our models. The compound appeared to induce CSCs to a differentiated phenotype at least for the DAOY cells, although mechanisms could not be clearly elucidated. In conclusion, inhibition of NRP-1 via MR438 seems to stimulate the differentiation of CSCs that may eventually reduce the progression of MB and bring a benefit in association with radiotherapy. Evaluation of this compound on orthotopic models of MB would provide information on its effectiveness on models closer to the physiopathology taking into account its distribution at the cerebral level.

Key words: Medulloblastoma; Neuropilin-1; Cancer stem cells; Peptidomimetic; Radiotherapy

Acknowledgements

Words can't describe my gratitude for everyone who has helped and supported me during my studies.

Firstly, I would like to express my heartfelt gratitude to my supervisors, Pr. Pascal CHASTAGNER and Dr. Cédric BOURA, for giving me the opportunity to study here and their guidance, patience and all useful suggestions on my thesis and experimentations. Without their consistent and illuminating instruction, this thesis could not have been completed. I would also like to thank Dr. Nadia Pellegrini-Moïse from L2CM7053 to provide us the peptidomimetics.

I must thank all members of our laboratory: Sophie, Alicia, Muriel, Valérie, Alain, Noémie, Dominique, Héna, Lorraine, Karima, Tiphaine, Magalie, Meriem, Mickaël and Denise. Thanks to Sophie for her constructive suggestions, to Alicia for teaching me experimental techniques, to Valérie for helping me to use the flow cytometry, to Paul for assisting me with radiotherapy at CHU-Nancy Brabois, for all their supportive and encouraging help.

I'm grateful to Mr. Jean-françois PLENAT for his carefully and meticulously observation of all our samples, and for the histological courses to improve our experimental skills. I would like also to thank two interns Abudullat and Naïma for their help to my experimentations.

I would like to extend my gratitude to Pr. Jean-François STOLTZ, Pr. Yunfeng ZHOU, Pr. Gilbert FAURE, Pr. Jacques HUBERT, Pr. Yan ZHAO and Pr. Alain

GERARD, who have spent much time and efforts to the France-China collaboration.
Thanks to their friendly cooperation and helpful advices.

Thanks for our neighbor Lab of all colleagues, for their instruments support and friendly help.

I would also like to thank all my Chinese friends in France for their help and support in life, and for just everything.

I feel grateful to all the teachers, friends and colleagues. Last but not least, thanks also to my family who has been assisting, supporting and caring for me all of my life.

List of Abbreviations

ADAM	A disintegrin and metalloprotease
AKT	Protein kinase B
APC	Adenomatous polyposis coli
BBB	Blood Brain Barrier
BET	Bromodomain and extra-terminal domain
BTIC	Brain tumor initiating cells
BTSCs	Brain tumor stem cells
CNS	Central Nervous System
CSCs	Cancer stem cells
CSF	Cerebrospinal fluid
CSI	Craniospinal irradiation
CTNNB1	Beta-catenin
DMF2	Dose modified factor at 2 Gy
DHH	Desert Hedgehog
DNA	Dexoyribonucleic acid
DSH	Dishevelled
EGF	Epidermal growth factor
EGPO	Endogenous peroxidase
FBS	Fetal bovine serum
FGF-2	Fibroblastic growth factor 2
GF	Growth factor
GLI	GLI-Krüppel family member
GPCR	G-protein coupled receptor
IHH	Indian Hedgehog
HBSS	Hank's Balanced Salt Solution
Hes	Hairy and enhancer of split
H&E	Hematoxylin and eosin
HGF	Hepatocyte growth factor
IHC	Immunohistochemistry
IHH	Indian Hedgehog
LCA	Large cell/anaplastic
MAPK	Mitogen Activated Protein Kinases
MB	Medulloblastoma
MS	Medullosphere

MKI	Multikinase
MRI	Magnetic resonance imaging
MYC	Myelocytomatosis oncogene
NPR3	Natriuretic peptide receptor 3
NRP-1	Neuropilin 1
NRP-2	Neuropilin 2
NECD	Notch extracellular domain
NICD	Notch intracellular domain
NTM	Notch transmembrane domain
Oct4	Octamer-binding transcription factor 4
PBS	Phosphate Buffered Saline
PCR	Polymerase chain reaction
PDE4D	Phosphodiesterase 4D
PDGF	Platelet Derived Growth Factor
PI3K	Phosphoinositide 3-kinase
PIGF	Placental growth factor
PNET	Primitive neuroectodermal tumor
PTCH	Patched
RFP	Red fluorescent protein
RNA	Ribonucleic acid
RT	Radiotherapy
SF2	Surviving fraction at 2 Gy
SHH	Sonic Hedgehog
SMO	Smoothened
SUFU	Suppressor of fused
TBS	Tris-Buffered Saline
TBST	Tris-Buffered Saline + Tween 20
TGF-β	Transforming growth factor beta
TRP53	Transformation-related protein 53
TP53	Tumor protein 53
VEGF	Vascular endothelial growth factor
VEGFR	Vascular endothelial growth factor receptor
WHO	World Health Organization
WNT	Wingless
WT	Wild-type

List of Figures

Figure 1.1: The comparison of 4 main molecular subtypes of MB includes their molecular and clinical characteristics.....	15
Figure 1.2: Summary of the seven primary medulloblastoma subgroups.	19
Figure 1.3: Therapeutic strategies according to different prognostic factors.	22
Figure 1.4: Isolation and perpetuation of brain tumor stem cells <i>in vitro</i> culture.	30
Figure 1.5: Germinal zones in the developing cerebellum and their mechanism of development.	32
Figure 1.6: Key signaling pathways involved in Medulloblastoma.	34
Figure 1.7: Overview of Sonic hedgehog signaling.....	36
Figure 1.8: The canonical Wnt signaling pathway.....	38
Figure 1.9: Canonical Notch signaling involved current targeted therapies.....	41
Figure 1.10: Structural domains of Neuropilins.....	43
Figure 1.11: Co-receptors involved in main signaling pathways and functions regulated by Neuropilins.....	44
Figure 1.12: Strategies to target NRP-1.....	48
Figure 1.13: Structures of compounds peptide and peptidomimetic.	51
Figure 2.1: Scheme of the design of the experimental procedures <i>in vitro</i>	59
Figure 2.2: Phenotypic proteins and transcripts expression of MB stem cells models.....	67
Figure 2.3: Effect of MR438 and Tuftsin on expression of Sox2 for DAOY.	68
Figure 2.4: NRP-1 and NRP-2 proteins expression of MB stem cell models of DAOY, D283 and D341 by Western blot.....	69
Figure 2.5: Effects of MR438 or Tuftsin on cytotoxicity and on spheres formation for MB stem cell models of DAOY, D283-Med and D341-Med.	71
Figure 2.6: Effects of MR438 or Tuftsin on self-renewal ability by clonogenic assay for DAOY, D283 and D341 stem cells.	73
Figure 2.7: Effects of MR438 or Tuftsin on proteins and transcripts expression of neuropilin receptors and stem cell markers.	75
Figure 2.8: Effect of MR438 or Tuftsin on expression of NRP-1 and CD15 by flow cytometry for the 3 MB stem cells models.....	76
Figure 2.9: Effects of MR438 or Tuftsin on invasive ability of MB stem cells derived from DAOY and D283 cell lines.	78
Figure 2.10: Invasive test for MB stem cells derived from D341 cell lines.....	79
Figure 3.1: Scheme of experimental procedures to evaluate the irradiation effects on MB stem like cells models <i>in vitro</i>	89
Figure 3.2: Timeline of the MR438 tolerance assay.....	91
Figure 3.3: Irradiation schedule for heterotopic xenograft nude mice.....	94

Figure 3.4: Effect of MR438 on tumor radiosensitization for cancer stem like cells of MB <i>in vitro</i> .	99
Figure 3.5: Macroscopic view of dissected organs from a mouse of 10mg/kg group and 1mg/kg group: brain, liver, kidneys, adrenals, heart, spleen, lung and gut.	101
Figure 3.6: Microscopic views of different organs from mice treated with MR438.	102
Figure 3.7: High-performance liquid chromatography (HPLC) reading graphs for detecting the presence of MR438 molecule in the serum 2 hours post injection at the dose 10 mg/kg.	103
Figure 3.8: Effect of MR438 on tumor growth following irradiation with xenograft nude mice <i>in vivo</i> .	105
Figure 3.9: Endpoint time for mice with three subtype MB tumor.	106
Figure 3.10: Effect of MR438 on cell viability and colony formation assay after tumor dissociation.	107
Figure 3.11: Representative images of macroscopic view for 3 subgroup tumors: DAOY, D283 and D341 ctrl groups showed the different form, homogeneity and vascularization.	109
Figure 3.12: Microscopic views of MB tumors by HE staining.	110
Figure 3.13: Effect of MR438 on NRP-1 expression in xenografted MB tumor by immunohistochemistry.	112
Figure 3.14: Effect of MR438 and Tuftsin on CD15 expression in xenografted MB tumor by immunohistochemistry.	114
Figure 4.1: Nervous System Tumor Models.	125
Figure 4.2: Orthotopic transplantation with Stereotaxic Instrument.	126
Figure 4.3: Histological presentation of tumors <i>in vivo</i> from different cell lines.	131
Figure 4.4: An invasive tumor of D341Med cell line.	132
Figure 4.5: Immunohistochemistry of vimentin human antibody in DAOY tumor.	132
Figure 4.6: Transduction of RFP for 3 cell lines	134

List of Tables

Table 1.1: Clinical stage of medulloblastoma.....	13
Table 1.2: Characteristics of the 3 MB cell lines: DAOY, D283-Med and D341-Med.	27
Table 2.1: Sequences and annealing temperatures of primers used in qRT-PCR.....	64
Table 3.1: Evaluation score followed up for tolerance assay	92
Table 3.2: Animals tested with two doses of MR438: 1 mg/kg and 10 mg/kg.	100
Table 4.1: Time of tumor apparition after cell transplantation following different cell culture method and amount of transplanted cells.....	136

Table of Contents

Acknowledgements.....	I
List of Abbreviations	III
List of Figures	V
List of Tables	VII
Table of Contents.....	VIII
Résumé en français de la thèse	1
Chapter 1 :	
General introduction	10
Medulloblastoma.....	11
Epidemiology and survival	11
Clinical advances with molecular subgroups.....	14
Current and prospective therapies.....	20
Preclinical models of MB	25
Cancer stem cells	28
Brain tumor stem cells	28
Isolation and identification of cancer stem cells.....	29
Cancer stem cell signaling pathways in medulloblastoma	33
Neuropilins.....	42
Structure and co-receptors of neuropilins	42
Role of NRP-1 in cancer and involved signaling pathways	43
Different approaches envisaged to target NRP-1.....	47
Hypotheses and objectives.....	51
Chapter 2 :	
Stimulation of medulloblastoma stem cells differentiation by a peptidomimetic targeting Neuropilin-1	54
Introduction.....	55
Materials and methods	58
Cell culture of MB stem like cells	58
Sphere formation and Cells viability	59
Clonogenic assay	60
Transwell invasion assays.....	61
Analysis of proteins expression by western blot.....	61
Gene expression of phenotypic markers by quantitative PCR.....	62
Expression of NRP-1 and CD15 by flow cytometry	65
Statistical analysis	65
Results.....	66
Phenotypic characteristics of stem cell MB models	66
Protein expression of neuropilins by MB stem cell models	68
Effect of peptidomimetic MR438 on spheres formation and cell viability	70
Effect of peptidomimetic MR438 on self-renewal capacity	72

Effect of peptidomimetic MR438 on expression of neuropilins and phenotypic markers by western blot and qRT-PCR	73
Effect of peptidomimetic MR438 on invasive capacity of medullosphere cells.....	77
Effect of peptidomimetic MR438 on the key proteins involved in the neuropilin pathways	79
Discussion and conclusion.....	81
Chapter 3:	
MR438 increases radiopotentialization of medulloblastoma cells <i>in vitro</i> and <i>in vivo</i> (Heterotopic xenografts models)	86
Introduction.....	87
Materials and methods	89
Cell culture and drug solutions	89
Tolerance assays <i>in vivo</i>	90
Animal models	92
Irradiation.....	93
Tumor dissociation.....	95
Clonogenic assay	95
Sphere formation and Stem cell survival assay	96
Histological analysis	97
Statistical analysis	97
Results.....	98
Effect of MR438 <i>in vitro</i> on radiosensitivity of cancer stem like cells.....	98
Tolerance and blood levels assays of MR438.....	100
Effect of MR438 on tumor growth following irradiation <i>in vivo</i>	103
Effect of MR438 on cell viability and colony formation assay after tumor dissociation.....	106
Histological analysis of MB animal models treated by MR438	108
Discussion and conclusion.....	115
Chapter 4:	
Elaboration of orthotopic models of medulloblastoma obtained from cell lines DAOY, D283-Med and D341-Med	120
Introduction.....	121
Materials and methods	123
Cell culture and cancer stem cell preparation	123
Orthotopic xenografts of medulloblastoma stem cells.....	123
Histological preparation of H&E tumor sections.....	126
Immunohistochemistry of tumor sections.....	127
<i>In vitro</i> transfection of Luciferase-RFP in MB cells	128
Results.....	129
Animal models of orthotopic transplantation experiments.....	129
RFP /Luciferase models of MB cell lines	133
Discussion and conclusion.....	135
Chapter 5:	
General Discussion.....	139
References.....	146
Appendix.....	164

Résumé en français de la thèse

Contexte général du projet de thèse

Le médulloblastome (MB) est une tumeur embryonnaire qui représente la première cause de tumeurs malignes du système nerveux central chez l'enfant. Le taux de survie des enfants atteints de médulloblastome a considérablement été amélioré au cours de ces dernières années en raison des progrès de la chirurgie et des schémas de chimio-radiothérapie. Cependant, malgré ces avancées thérapeutiques qui permettent d'atteindre un taux de survie à 5 ans de 65 % (source rapport de l'Inca 2014), les récurrences sont fréquentes dues à la présence de métastases dans 30 % des cas. Les enfants atteints de MB souffrent également de dysfonctionnements cognitifs et physiques permanents attribués à l'impact des traitements sur le système nerveux en développement. Les études moléculaires du MB ont récemment montré la présence de plusieurs sous-groupes distincts qui diffèrent dans le pronostic vital. Le consensus récent de cette nouvelle classification moléculaire se compose de quatre sous-types. Les sous-types Wnt et Sonic Hedgehog (SHH), qui sont associés à un meilleur pronostic, par rapport aux sous-types 3 et 4, qui sont plus agressifs, résistants aux modalités de traitement actuelles et caractérisés par une plus grande propension à une dissémination métastatique¹.

¹ Ellison DW. Childhood medulloblastoma: novel approaches to the classification of a heterogeneous disease. Acta Neuropathol. 2010; 120(3):305-16.

L'existence des cellules initiatrices de tumeurs également appelées cellules souches cancéreuses (CSC) a été montrée dans les tumeurs cérébrales, et en particuliers dans le MB, par les travaux de Singh *et al* en 2003². Ces travaux suggèrent qu'une fraction relativement faible de cellules tumorales a la capacité de proliférer et de maintenir la croissance de la tumeur. Ceci contrairement aux autres cellules de la tumeur, caractérisées par une capacité de prolifération limitée et par un phénotype plus spécifique de cellules différenciées et matures. Plus précisément, une CSC de MB maintiendrait deux propriétés essentielles: l'auto-renouvellement et la capacité à se différencier dans tous les types cellulaires de la tumeur³. Plus récemment, il a été démontré que cette population particulière de cellules serait hautement radio et chimio-résistantes et serait fortement impliquée dans les phénomènes de récurrence⁴.

La voie de signalisation de la neuropiline-1 (NRP-1) a été montrée comme étant impliquée dans la progression du médulloblastome⁵. Neuropiline-1 est une protéine transmembranaire qui agit comme co-récepteur avec les récepteurs des sémaphorines 3 (sema3) et des facteurs de croissance de l'endothélium vasculaire (VEGFRs). En plus de son rôle crucial dans le développement des systèmes nerveux et

² Singh SK et al. Identification of a cancer stem cell in human brain tumors. *Cancer Res.* 2003; 63(18):5821-8.

³ Manoranjan B et al. Medulloblastoma stem cells: modeling tumor heterogeneity. *Cancer Lett.* 2013 ;338(1):2331.

⁴ Tang X et al. Differential proliferative index of cancer stem-like cells in primary and recurrent medulloblastoma in human. *Childs Nerv Syst.* 2012; 28(11): 1869-77.

⁵ Snuderl M et al. Targeting placental growth factor/neuropilin 1 pathway inhibits growth and spread of medulloblastoma. *Cell.* 2013; 152(5):1065-76.

cardiovasculaire, NRP-1 est impliqué dans des processus physiopathologiques impliquant ses ligands classiques comme les molécules de la famille du VEGF ou plus récemment le TGF- β 1 et le PDGF.

Les travaux de Hamerlick et coll.⁶ ont démontré récemment que NRP-1 était exprimé par les cellules souches de gliome et jouait un rôle dans leur survie. Ces auteurs ont identifié un double rôle pour NRP-1 dans la promotion du caractère souche par stimulation de l'angiogénèse d'une manière paracrine et via directement les cellules souches cancéreuses grâce à une boucle autocrine. En effet, l'inhibition de NRP-1 réduit fortement la transduction du signal de Sonic Hedgehog et par conséquent la transcription de gènes cibles tels que Gli1 (facteur de transcription impliqué dans le maintien du phénotype souche).

Objectifs

Les objectifs du projet étaient :

1) De conforter et valider les effets *in vitro* du composé MR438 sur des modèles de cellules souches de médulloblastome de différents sous-groupes (partie 2),

2) D'évaluer les effets *in vitro* et *in vivo* du composé en association avec la radiothérapie (partie 3),

⁶ Hamerlik P et al. Autocrine VEGF-VEGFR2-Neuropilin-1 signaling promotes glioma stem-like cell viability and tumor growth. J Exp Med. 2012;209(3):507-20.

3) Développer des modèles orthotopiques de médulloblastomes à partir de cellules souches de médulloblastomes (partie 4).

Méthodologie et Résultats obtenus

Pour mener à bien ce projet, nous avons utilisé trois lignées cellulaires de médulloblastome (DAOY, D283-Med et D341-Med) afin d'enrichir in vitro des cellules souches cancéreuses, puis nous avons testé les effets du composé MR438 par comparaison à ceux engendrés par la Tuftsiine (TKPR) connue pour être un inhibiteur spécifique et naturel de NRP-1. En collaboration avec le Dr N. Pellegrini-Moïse du Laboratoire Lorraine en Chimie Macromoléculaire (L2CM, UMR CNRS-UL 7053), nous avons évalué différents composés peptidomimétiques à base de sucre qui se sont révélés affins pour NRP-1⁷. Par la suite, le composé peptidomimétique MR438 a été retenu pour son effet sur l'inhibition de la capacité d'autorenouvellement de 3 modèles différents de cellules souches de médulloblastome dérivées des lignées DAOY (groupe SHH), D283-Med (groupe 4) et D341-Med (groupe 3).

Effets in vitro du composé MR438 sur des modèles de cellules souches de médulloblastome de différents sous-groupes

En effet, le composé MR438 inhibe non seulement l'expression de NRP-1 mais semble induire également un effet différenciant in vitro observable par la diminution

⁷ Richard et al, Bioorg Med Chem. 2016

de l'expression de CD15, ainsi que de CD133 et Sox2. Nous avons tenté également de comprendre les effets de l'inhibition de l'expression NRP-1 par le composé MR438 sur l'activation des voies de signalisation AKT (voie de la survie cellulaire) et ERK (voie mitogène) impliqués notamment dans la viabilité et la prolifération cellulaire. L'exposition au MR438 ou à la Tuftisine induit une diminution significative de l'activation des voies AKT et ERK en moyenne de 75 et 50% respectivement, pour la lignée DAOY. Pour les 2 autres modèles cellulaires (D283-Med, D341-Med) aucune variation significative du ratio de l'expression protéique de pERK/ERK et pAKT/AKT n'est observée. Nous avons également exploré la voie Smad (lié au récepteur du TGFβ) qui ne semble pas être perturbée par l'exposition au MR438.

Effets in vitro et in vivo du composé MR438 en association avec la radiothérapie

Nous avons ensuite évalué les effets du composé MR438 en association avec la radiothérapie. Les cellules souches de médulloblastome ont été irradiées à 2, 4, 8 et 10 Gy sur un irradiateur expérimental (XRad 320, Precision X Ray) afin d'évaluer l'effet de l'association thérapeutique sur la capacité des cellules souches de médulloblastome à conserver leur capacité d'auto-renouvellement. L'association montre un bénéfice statistiquement significatif en terme de diminution de la capacité clonogénique à 2Gy en association avec le MR438 quel que soit l'origine des cellules même si l'effet semble plus marqué pour les cellules du sous-groupe SHH (Daoy).

Le calcul du pouvoir radiosensibilisant a été calculé avec le facteur modifiant la dose à 2 Gy (DMF2) et évalué à 0,74, 0,89 et 0,88 respectivement pour les cellules Daoy, D283-Med et D341-Med.

Les résultats *in vitro* sur l'association avec la radiothérapie ont montré des effets potentiellement intéressants et nous ont amené à poursuivre les expérimentations sur des modèles *in vivo* chez la souris nude xénotreffés au niveau hétéotopique.

Les résultats *in vivo* sur des modèles hétéotopiques montrent un bénéfice de l'association radiothérapie avec le composé MR438 caractérisé par un ralentissement statistiquement significatif de la croissance tumorale par rapport à la radiothérapie seule en particulier pour les tumeurs issues de la lignée Daoy. Nous avons également évalué la persistance des cellules souches de médulloblastome après dissociation tumorale. De façon intéressante, le traitement MR438 + radiothérapie engendre une diminution du nombre de cellules souches par rapport à la radiothérapie seule pour l'ensemble des modèles évalués.

Développement des modèles orthotopiques de médulloblastome

L'objectif de la partie 4 était de développer des modèles de médulloblastome orthotopiques par injection intracérébelleuse d'une population cellulaire enrichie en cellules souches de médulloblastome (médullosphères). Les premières expériences suite à l'administration des cellules de médulloblastomes montrent un taux de prise important quelle que soit la lignée de 70 à 90 % avec des profils de dissémination cohérents avec l'origine de la tumeur. Nous avons poursuivi le développement de ces modèles en transfectant nos modèles cellulaires avec une particule virale permettant

l'intégration de la Red Fluorescent Protein et de la luciférase au niveau génomique. Ces modèles permettront à terme un suivi longitudinal des animaux xéno greffés en orthotopique pour l'évaluation de l'association Radiothérapie et MR438.

Discussion et Conclusion

Le médulloblastome est la plus fréquente des tumeurs cérébrales pédiatriques malignes et représente la première cause de mortalité par cancer chez l'enfant. Malgré une amélioration de la survie grâce au développement des nouveaux traitements, il s'agit d'une tumeur invasive, à fort potentiel métastatique, et dont le pronostic est grevé par un risque important de récurrence. Pour faire face à ce risque, les traitements entrepris sont souvent agressifs (chirurgie, radiothérapie et chimiothérapie parfois à haute dose, associée à une greffe de cellules souches hématopoïétiques) et entraînent régulièrement des séquelles de type endocriniennes (retard de croissance et pubertaire) et cognitives (retard de développement, troubles des apprentissages), responsables d'une grande morbidité. Des travaux récents ont montré que les cellules souches cancéreuses jouent un rôle très important dans la progression tumorale et la résistance aux traitements. Il a été également montré que le récepteur NRP-1 était impliqué dans la progression tumorale des médulloblastomes. NRP-1 pourrait ainsi constituer une cible thérapeutique intéressante dans le traitement des médulloblastomes.

Au cours des dernières années, des progrès importants ont été réalisés dans la compréhension des mécanismes moléculaires permettant de subdiviser en 4 sous-groupes distincts les médulloblastomes et ainsi d'envisager de nouvelles approches

thérapeutiques Dans notre travail, nous avons utilisé comme modèle trois lignées cellulaires de médulloblastome, les lignées Daoy, D283-Med et D341-Med, qui correspondraient respectivement aux sous-groupes SHH, 3 et 4. Ces cellules ont été cultivées dans un milieu spécifique permettant l'obtention de médullosphères, et donc l'enrichissement en cellules progénitrices/souches de médulloblastome. Nous avons pu mettre en évidence une augmentation significative de l'expression de NRP-1 par ce mode de culture en médullosphères confortant notre stratégie de ciblage.

Dans un second temps, nous avons évalué l'impact du traitement des cellules cultivées en médullosphères par un composé innovant ciblant spécifiquement NRP-1, le composé MR438. Ce composé a montré un effet intéressant sur la capacité d'autorenouvellement des cellules issues des médullosphères avec une diminution de marqueurs phénotypiques des cellules souches de médulloblastomes. Cet effet est probablement dû à une inactivation de la voie de signalisation AKT/ERK pour les cellules Daoy.

Nous nous sommes donc efforcés dans la suite de ce travail de comprendre les effets de ce composé sur les cellules souches de médulloblastome de différents sous-groupes en association avec la radiothérapie. Les résultats *in vitro* et *in vivo* montrent un effet plus intéressant en terme de radiosensibilité et de progression tumorale sur le modèle Daoy par rapport à deux autres qui pourrait s'expliquer par le statut p53 des cellules Daoy qui est non mutées par rapport aux cellules des lignées D283-Med et D341-Med. Cependant le composé MR438 induit en association avec la radiothérapie une diminution du nombre de cellules souches de médulloblastomes pour l'ensemble des modèles confirmé par nos premiers résultats sur l'expression de CD15, marqueur

des progéniteurs neuronaux. Le développement de modèles orthotopiques nous permettra d'aller plus loin dans l'évaluation du composé en prenant en compte sa distribution au niveau cérébrale et son passage au niveau des barrières méningées.

En conclusion, nous avons trouvé que l'inhibition de NRP-1 via MR438 semble stimuler la différenciation des cellules souches pouvant à terme réduire la progression des médulloblastomes, avec une implication probable des voies de signalisation PI3K/AKT et MAPK pour les cellules du sous-groupe SHH. Même si les mécanismes induisant une diminution de la capacité d'autorenouvellement ne sont pas encore clairement élucidés. L'utilisation de molécules ciblant NRP-1 nous semble pertinente pour atteindre les cellules souches de médulloblastomes, favoriser leur différenciation et probablement leur radio-chimio-sensibilité. Nous tenterons dans un futur proche de confirmer ces résultats sur des modèles de xéogreffes orthotopiques chez la souris nude.

Chapter 1 :

General introduction

Medulloblastoma

Epidemiology and survival

Medulloblastoma (MB) is the most common pediatric malignant brain tumor, which is the leading cause of cancer related deaths in children. It accounts for about 2% of primary brain tumors and 15-20% of all pediatric brain tumors (Kumar *et al.*, 2017, Klein *et al.*, 2015). As one of the embryonal tumor, children are more likely to be affected than adults. The incidence of MB for children from 1 to 9 years ages is 6.0 per million in the USA and 0.6 per million for adults (Smoll *et al.*, 2012), while there are 5 to 10 cases per million in France (Klein *et al.*, 2015). The American epidemiological surveillance reported that the incidence of MB decreased while the incidence of primary neuroectodermal tumors in supratentorial localizations has been increasing. Boys are more often affected than girls (sex ratio 1.5: 1). The five-year survival rate is in the range of 75% ~ 80% without metastases. The median age at diagnosis is around 9 years old and the peak incidence occurs in children from ages 3~4 or 8~9 years old (Crawford *et al.*, 2007), but this tumor exists from birth to adulthood. Normally, it is a tumor occurring sporadically in isolation from a family. Pathologies have been described to favor the apparition of MB like Li Fraumeni syndrome, Gorlin syndrome, ataxia-telangiectasia, Rubinstein-Taybi syndrome or SUFU mutation (Bourdeaut *et al.*, 2011).

The current treatment of MB is mainly with non-specific therapies including surgery with aggressive chemotherapy and radiotherapy (RT). The prognostic factors

currently used to define post-operative treatments are initial extension of the disease, quality of excision, subtype of MB and biological criteria (Orbach *et al.*, 2012). In general, clinical staging determines the choice of treatment and affects patients' prognosis, so as MB (Table 1.1). Stage T has little effect on survival time, while Stage M is a high risk factor for MB. Jenkin *et al.* showed that the 5-year survival was 78% for stage M0 + M1 and 21% for M2 + M3, respectively (Jenkin *et al.*, 2000). Recent research is devoted to study molecular subgroups, which is an important challenge in the near term for the pediatric neuro-oncology community (Ramaswamy *et al.*, 2017). Moreover, age is another vital prognostic factor for MB, prognosis is worse if the child is less than 3 years old, degree of resection is inadequate, or if any cerebrospinal fluid (CSF) spinal, supratentorial, or systemic spread occurs. The combination of these various factors makes it possible to choose one appropriate treatment strategy.

Table 1. 1 : Clinical stage of medulloblastoma

Stage		Parameters
T stage	T1	Tumor < 3cm in diameter
	T2	Tumor \geq 3cm in diameter
	T3a	Tumor > 3cm and with extension into aqueduct of sylvius or foramen of luschka
	T3b	Tumor > 3cm and with unequivocal extension into brainstem
	T4	Tumor > 3cm with extension past the aqueduct of sylvius or past foramen magnum
M stage	M0	No evidence of metastasis
	M1	Tumor cells in the spinal fluid
	M2	Tumor spread within the brain
	M3	Tumor spread into the spine
	M4	Tumor spread away from the brain and spine

The survival rate of children with MB is around 69%, and the cumulative relative survival rate was 60%, 52%, and 47% at 5 years, 10 years, and 20 years, respectively (Smoll *et al.*, 2012). The treatments are therefore aimed at maintaining or even increasing the survival rate while decreasing the high frequency of sequelae like neurocognitive, hormonal, growth, auditory disorders (Frange *et al.*, 2009). It is essential to find more selective and less aggressive individual therapy aiming to reduce mortality and improve the patient quality of life.

Clinical advances with molecular subgroups

The 2016 World Health Organization (WHO) classification of the central nervous system (CNS) tumors includes four histological variants of MB: classic (about 70%), desmoplastic/nodular (about 15%), MB with extensive nodularity and large cell/anaplastic (LCA) (Louis *et al.*, 2016). The prognosis of MBs remains disparate according to the histological type, and this histological classification is not sufficient to determine the prognosis and decide the choice of the treatment (Klein *et al.*, 2015). Even within the same histopathology, patients have greatly different responses to treatments because of the biological heterogeneous group of tumors.

Recent integrated genomic studies have showed that MB is composed of four essential molecular subgroups: WNT (Wingless), SHH (Sonic Hedgehog), Group 3 and Group 4 (non-WNT/non-SHH groups), which correspond to different molecular and clinical characteristics (Figure 1.1). This molecular classification was added in the 2016 WHO classification of brain tumors. Also for the first time, the WHO classification of MB is defined by both histology and molecular features, including WNT-activated, SHH-activated, TP53-mutant or TP53-wildtype, non-WNT/non-SHH Group 3 and Group 4 (Louis *et al.*, 2016). The WNT and SHH groups were thus named in connection with signaling pathways that appear to play important roles in the pathogenesis of these subgroups. Subgroup 3 and 4 are related to a high incidence of recurrence and metastasis and lead to a poorer prognosis (Taylor *et al.*, 2012, Northcott *et al.*, 2011).





















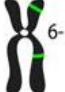

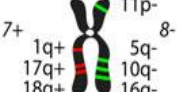
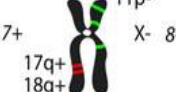
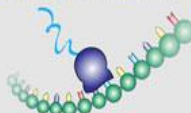
Molecular Subgroups of Medulloblastoma				
CONSENSUS	WNT	SHH	Group 3	Group 4
Cho (2010)	C6	C3	C1/C5	C2/C4
Northcott (2010)	WNT	SHH	Group C	Group D
Kool (2008)	A	B	E	C/D
Thompson (2006)	B	C ¹ , D	E, A	A, C
DEMOGRAPHICS				
Age Group:   	  	    	  	    
Gender: ♀ ♂	♂ ♂ : ♀ ♀	♂ ♂ : ♀ ♀	♂ ♂ : ♀	♂ ♂ : ♀
CLINICAL FEATURES				
Histology	classic, rarely LCA	desmoplastic/nodular, classic, LCA	classic, LCA	classic, LCA
Metastasis	rarely M+	uncommonly M+	very frequently M+	frequently M+
Prognosis	very good	infants good, others intermediate	poor	intermediate
GENETICS				
	 CTNNB1 mutation	 PTCH1/SMO/SUFU mutation GLI2 amplification MYCN amplification	 i17q MYC amplification	 i17q CDK6 amplification MYCN amplification
GENE EXPRESSION				
	WNT signaling MYC +	SHH signaling MYCN +	Photoreceptor/GABAergic MYC +++	Neuronal/Glutamatergic minimal MYC / MYCN

Figure 1. 1: The comparison of 4 main molecular subtypes of MB includes their molecular and clinical characteristics.

MB is composed of four essential molecular subgroups: WNT, SHH, Group 3 and Group 4, which correspond to different molecular and clinical characteristics. The methods of classification for the molecular subgroups depend on recent integrated genomic analysis. MB: Medulloblastoma; WNT: Wingless; SHH: Sonic Hedgehog; LCA: Large cell/anaplastic. Figure taken from Taylor *et al.*, 2012

WNT subgroup

The MB of WNT subgroup (about 15% of cases) has a very good prognosis (survival > 90%, metastases in 5-10% of cases). This subgroup is identified by the expression of genes present during activated WNT signaling pathway: DKK1, DKK2, WIF1, filamin-A, YAP-1 and β -catenin (+/- nuclear cytoplasmic expression). More than 75% of WNT tumors have the mutation on exon 3 (CTNNB1) of the β -catenin gene. The genome of WNT tumors is relatively stable compared to other subgroups and well-defined by different approaches (Schroeder *et al.*, 2014).

SHH subgroup

The SHH subgroup has 25% of patients with overall survival about 75% and the risk of metastasis is 15-20%. Its name is according to the activation of SHH pathway, which is easily identified with the expression of GAB1, SFRP and Gli1-3. This tumor subtype is initiated by the amplification or deletion of genes that are components of the SHH pathway: PTCH1/2 (somatic or germinal mutation), SUFU (somatic or germinal mutation), Smoothened (SMO, [somatic mutation]), and GLI2 (amplification).

Group 3

Group 3 human tumors approximately 25% of the cases with a high incidence of metastasis at the time of diagnosis (poor prognoses with survival <50%, metastases in 40-45% of cases). The expression of the natriuretic peptide receptor 3 (NPR3) has been reported as the group 3 marker, characterized also by Myc overexpression or

amplification. Many studies have validated the functional role of Myc overexpression in tumorigenesis and invasion. There is no known stable germinal mutation associated with this subgroup in the current studies.

Group 4

As the most common but least characterized subtype, Group 4 constitutes 35% of cases with a survival less than 75% and metastases observed in 35-40% of the cases. This group could be identified by the amplification of MYCN (Kool *et al.*, 2012). There is no known germinal mutation and its pathogenesis remains poorly understood.

These 4 subgroups support current disease subclassification and initial molecular subgroup-directed therapies in advanced clinical trials. However, substantial biological heterogeneity and differences in survival for each subgroup are still manifest. More recently, additional age and risk factor features to molecular subgroups within childhood MB lead to improve disease subclassification and prognosis predictions (Schwalbe *et al.*, 2017). In this retrospective cohort study, 428 primary MB samples were collected and identified within seven robust and reproducible primary molecular subgroups of childhood MB. High-risk clinical factors included as described above pathology of large cell and anaplastic (LCA), metastasis (M+), incomplete surgical resection (R+) and MYC or MYCN amplification. MB subgroup WNT remained unchanged and other 3 subgroups were divided in two according to high-risk clinical factors and age: subgroup SHH divided into SHH-Child (>4.3 years) and SHH-Infant (<4.3 years), subgroup 3 and 4 were

separated into high-risk (MBGrp3-HR and MBGrp4-HR) and low-risk subgroup (MBGrp3-LR and MBGrp4-LR) (Figure 1.2). This discovery of seven novel, clinically significant subgroups improves disease risk-stratification and could better inform treatment decisions in the future. More additional subgroups were proposed for clinical application, taking clinical and therapeutic information of the treated patients into account and considering the genetic prognostic factors like TP53 mutation, MYC amplification and chromosome 11 and 13 loss.

	WNT	MB _{SHH-Child}	MB _{SHH-Infant}	MB _{Grp4-HR}	MB _{Grp4-LR}	MB _{Grp3-LR}	MB _{Grp3-HR}
Demographics							
Infant disease % (<3 years)	0	5	78	5	3	54	17
Male %	48	63	55	67	66	68	77
n	33	38	65	85	73	50	65
Clinical features							
Histology (%)	86:3:10	32:26:41	35:55:10	86:5:9	85:6:9	90:2:8	61:4:35
CLAS:DN:LCA							
Metastasis (%)	3	16	28	30	23	41	33
Sub-total resection (%)	10	17	26	35	28	24	25
10 year overall survival (95% CI)	72% (66–100)	48% (29–80)	58% (46–75)	36% (22–59)	72% (59–88)	69% (55–87)	22% (10–46)
Molecular features							
Mutation	CTNNB1, TP53	TP53, TP53 GL, TERT, SUFU, PTCH1	SUFU, PTCH1				GFI1
Cytogenetics							
Gene expression*		↑ RUNX3, HCAR1, HCAR2, FOXG1	↑ TRABD2A, TTC9, SLFN11, CHRM2	↑ ESYT2, WDR60, DAPK2, PRDM6	↑ BMP5, SPTLC3, COL9A3, ZIC5	↑ FGD6, BRMS1L, FAM122B, REV3L	↑ PVT1, TRAP1, NMRAL1, CNTLN Ribosome biogenesis genes
DNA methylation							
Global	↓ vs CB	↓ vs CB ↑ vs MB _{SHH-Infant}	↓ vs CB ↓ vs MB _{SHH-Child}	↓ vs CB ↓ vs MB _{Grp4-LR}	↓ vs CB ↑ vs MB _{Grp4-HR}	↓ vs CB ↑ vs MB _{Grp3-HR}	↓ vs CB ↓ vs MB _{Grp3-LR}
Probe level*	PI3K-Akt, Ras signalling pathways	Ras signalling pathway	Hippo signalling pathway	PI3K-Akt signalling pathway			PI3K-Akt signalling pathway
Gene level*		↑ vs MB _{SHH-Infant} CB DLX6-AS1, ACTA1, GCM2, FEZF2			↑ vs MB _{Grp4-HR} CB HLA-DRB5, NXK2-5, ABLIM1, HOXC6	↑ vs MB _{Grp3-HR} CB PRKCZ, MCF2L, MIR662	↑ vs MB _{Grp3-LR} CB GALNT9, MIR662

Figure 1. 2: Summary of the seven primary medulloblastoma subgroups.

Demographic, clinicopathological, and molecular features are summarized for the 7 novel clinical depended subgroups. CB: Normal cerebella. CLAS: Classic histological subtype. DN: desmoplastic nodular. LCA: large-cell anaplastic. Figure taken from Schwalbe *et al.*, 2017.

Gene TP53 and its protein p53 have been studied dramatically with a number of different tumors. Early research found that more than 40% MB samples have frequently changed the isochromosome 17q (Biegel *et al.*, 1992), which maybe highly associated with TP53. But later studies showed that 17p and 17p loss and TP53 mutations are unrelated with tumor initiation, but associated with prognosis (Adesina *et al.*, 1994, Pfaff *et al.*, 2010). The prognostic effect of TP53 mutations for MB

depends on different molecular subgroup. SHH subgroup of MB are divided into TP53-mutant and TP53-wildtype in 2016 WHO classification. TP53 mutations as the high risk prognostic factors are associated with the majority of treatment failures in SHH MB (Ramaswamy *et al.*, 2016). Because of local recurrence observed frequently for the majority of SHH MB, a potential explanation for the poor prognosis in TP53-mutated SHH subgroup associates with radiation resistance (Ramaswamy *et al.*, 2013). On the contrary, TP53 mutations are also frequently associated with CTNNB1 mutation in WNT subgroup but related with the best prognosis. It is explained that accumulation of β -catenin protein is down-regulated by activated p53 (Levina *et al.*, 2004). However, p53-associated proteins in group 3 and 4 MB for the prognosis, progression and initiation remain still unclear.

Current and prospective therapies

Conventional therapies

The management is initially neurosurgical surgery: first of all, hydrocephalus is lifted mainly by a ventriculocisternostomy type derivation followed by surgical resection as complete as possible. Future treatments depend on the main prognostic factors: initial extension of the disease (localized or presence of a meningeal diffusion), quality of the excision (macroscopically complete or not), histological type of the MB (favorable character of the nodular subtype desmoplastic or with extensive nodularity, poor prognosis of LCA), biological criteria (favorable aspect of intra-nuclear accumulation of β -catenin, lack of amplification of MYC and MYCN

oncogenes in tumoral cells, ...) (Cho *et al.*, 2011). More recently as presented above, molecular subgroup demonstrates also an important role in prognosis. The combination of these different factors makes it possible to define a stratification of this disease and to define the therapeutic strategy that also relies on the age of the child at the time of diagnosis (Figure 1.3).

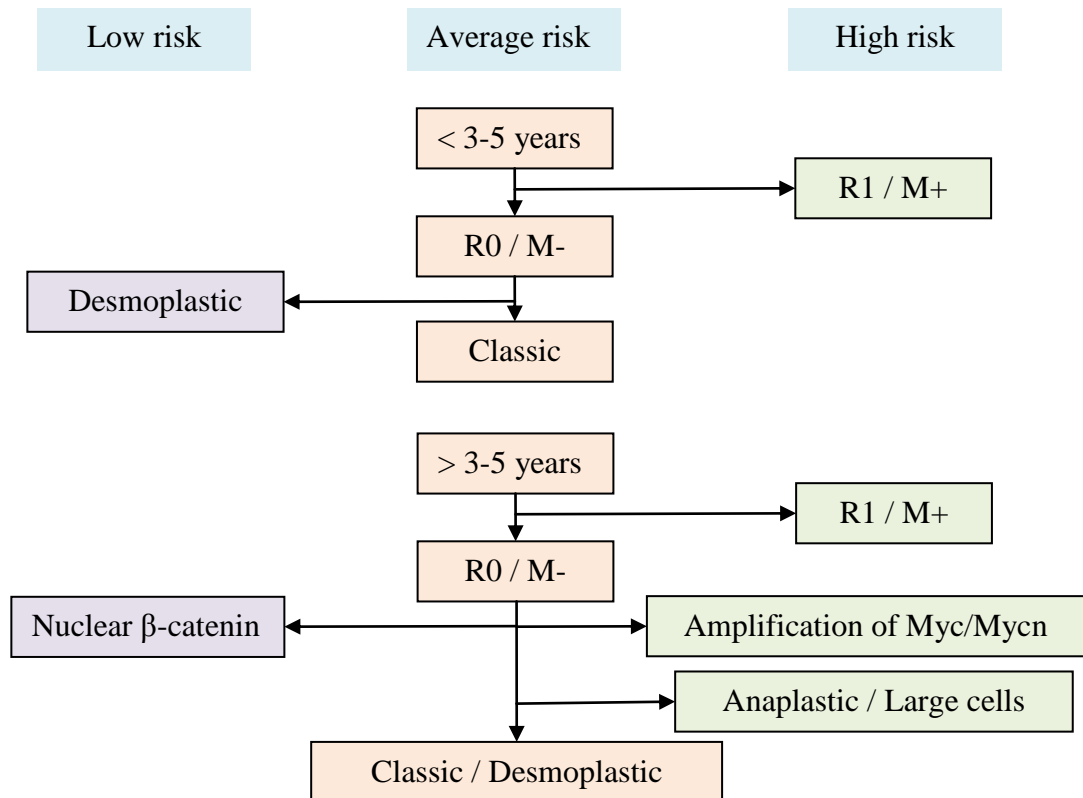


Figure 1. 3: Therapeutic strategies according to different prognostic factors.

Three levels of risk guide to the different strategies: high risk clinical factors include large cell and anaplastic [LCA], metastasis [M+], incomplete surgical resection [R+] and MYC or MYCN amplification. While low risk clinical factors consist in desmoplastic histology and β -catenin subgroup (WNT).

Indeed, post-operative craniospinal irradiation (CSI) is an essential treatment for MB due to the risk of meningeal diffusion, which causes a high risk of neurocognitive sequelae, especially for young patients. The dose of conventional radiotherapy on the whole central nervous system is 36 Gy and up to 54-55 Gy on the tumor bed. In young patients, this treatment is associated with high risk of neurocognitive sequelae. The strategies were therefore proposed to reduce these sequelae by reducing the doses on the cranio-spinal axis to 23.4 Gy under the cover of chemotherapy, reducing the irradiation field to the post-operative tumor volume rather than the entire posterior

fossa, using high-compliance radiotherapy techniques to protect the surrounding organs (cochlea for example), by delaying the date of RT as much as possible or by reducing radiation fields for young patients to avoid as much as possible irradiating an "immature" brain by using prolonged chemotherapy. In addition, different strategies for administering chemotherapy drugs (intravenous, intrathecal, conventional or high doses) are being evaluated to define the most effective treatments with the most acceptable toxicity.

Targeted therapies

The current treatment of MB is mainly composed of non-specific therapies including surgery and aggressive chemotherapy and radiotherapy. Due to the progresses of molecular and genetic biology, the better understanding of tumor development suggested possibility of targeting therapy. The role of targeting therapies is booming and the new treatments under study focus on the targeting of signaling pathways related to molecular subgroups, including the WNT and SHH pathway (Remke *et al.*, 2013).

Biologically, the WNT subgroup is characterized by mutations of CTNNB1, DDX3X and TP53 in the WNT signaling pathway which are therefore potential therapeutic targets. MiR-148a, a micro RNA upregulated in the WNT subgroup tumors, inhibits invasion and tumorigenic potential of MB cells (Yogi *et al.*, 2015). Another study of micro-RNA indicated that miR-219 suppresses the proliferation,

migration and invasion of MB cells by targeting CD164 as a potential therapeutic agent for MB.

The SHH subgroup is the best known and best studied mutations PTCH1 and SUFU, as well as mutations of SMO were found in 10-15% of sporadic MB. Several SMO inhibitors are currently in clinical trials for relapsed MB, specifically, GDC-0449 and LDE225 (Kim *et al.*, 2014, Rodon *et al.*, 2014). In addition, a novel PI3K inhibitor (GDC-0941) is effective *in vitro* and *in vivo* by reducing the expression of phosphorylation of AKT (Ehrhardt *et al.*, 2015). A new regulatory mechanism of SHH pathway proposed that phosphodiesterase 4D (PDE4D) acts downstream of Neuropilins to control SHH signaling pathway and MB growth, which could be a promising target to treat the SHH subgroup tumors (Ge *et al.*, 2015).

Because of the poor prognosis of patients in subgroup 3 and 4, it is urgent to find new therapies to improve efficacy of these 2 subgroups. High level of MYC amplifications is reported to be related with poor prognosis. Some molecular inhibitors of MYC have been proposed, some of which are in early clinical trials (Lin *et al.*, 2010). The original cell of subgroup 4 is still unknown, but a possible preclinical model exists with an overexpression of MYCN. Inhibition of effectors downstream of MYCN corresponds to potential therapeutics, and it has recently been shown that the bromodomain and extra-terminal domain (BET) protein specific inhibition of MYCN is effective in preclinical models of neuroblast (Puissant *et al.*, 2013).

Besides, angiogenesis is crucial for tumor growth and dissemination, and many studies have therefore turned to anti-angiogenic strategies in the treatment of pediatric brain tumors. Pazopanib has recently been identified as a potential new anti-angiogenesis that can target MB via the multikinase (MKI) pathway (Craveiro *et al.*, 2014).

There are more and more targeted anti-tumor therapies in clinical trials for MB, but most ended in failure. The reason may be related to the level of gene mutation that most targets identified in the diagnostic sample are unlikely to be present in the dominant clone at the time of recurrence. Even in recurrent cases, molecular subgroup affiliation is extremely stable at the time of recurrence, suggesting that therapeutic strategies based on susceptibility across a subgroup might be efficacious both upfront and at recurrence (Morrissy *et al.*, 2016).

Preclinical models of MB

The identified molecules of MB subgroup remain stable at the time of recurrence and even in metastatic cases for human (Ramaswamy *et al.*, 2013, Wang *et al.*, 2015). However, a large number of experiments should use cell lines *in vitro* or animal models for important exploratory research. But some methods for detection of the primary tumor could not be used in many models especially for cell lines *in vitro*. Global gene expression profiling helps to classify the molecular subgroup for more approximate models like xenograft mouse models and cell lines of MB. Genes SFRP1, WIF1, NPR3, and KCNA1 are widely used to classify the molecular subgroups of

SHH, WNT, Group 3 and Group 4, respectively (Zhao *et al.*, 2012). Lagerweij used the same genes to classify the cell lines that showed the most used cell line DAOY belong to subgroup SHH and the cell line ICb-1299MB in the subgroup 4 while three cell lines D283-Med, D458-Med and VU371 pertain to the subgroup 3 (Lagerweij *et al.*, 2016). However, the molecular subgrouping has not been all completed studied for all cell lines and sometimes showed the different results. The classification of D283-Med above has been confirmed by some authors to be assigned in Group 3 (Sengupta *et al.*, 2014), but also seems to have the characteristics of Group 4 by others (Snuderl *et al.*, 2013), as well as the cell line UW228. The most of cells in culture maintain the mutation and hold the stability of subgroups like in tissue samples whereas the MED6 cell line reverted to wild type and changed WNT mutation into Group 3 (Othman *et al.*, 2014). The culture and environmental conditions could interact with the phenotypic type to active or silence some mutation and signaling pathways.

The WNT and SHH groups were thus named in connection with signaling pathways which appear to play important roles in the pathogenesis of these subgroups. Subgroups 3 and 4 MB are related to a high incidence of metastasis and lead to a poorer prognosis. Thus, it is important to study as much as possible all the molecular subgroups of MB for a better understanding of this disease. Therefore, in my thesis, we analyzed the three most frequent used cell lines of MB: DAOY, D283-Med and D341-Med, corresponding to the subgroup SHH, subgroup 4 or 3 and subgroup 3, respectively (Xu *et al.*, 2015, Snuderl *et al.*, 2013). A permanent cell line of DAOY and D283 arising from the MB were established and their growth characteristics were

investigated in 1985 (Jacobsen *et al.*, 1985, Friedman *et al.*, 1985). The DAOY line is a human desmoplastic MB, developed in a 4 years old male child. These are adherent cells of polygonal morphology. The cell line D283-Med is derived from a 6 years old boy MB peritoneum metastatic site. These cells grow both in suspension and adherent feature with multicellular aggregates. The morphology of the adherent cells is like the epithelial type. In addition, a new continuous cell line of D341-Med derived from a cerebellar MB of a 3.5 years old male child was identified and demonstrated 20-fold amplification of c-myc. These cells grow in suspension, spheroid morphology (Friedman *et al.*, 1988) (Table 1.2).

Table 1. 2 : Characteristics of the 3 MB cell lines: DAOY, D283-Med and D341-Med.

Cell line	DAOY	D283-Med	D341-Med
Original Site	Medulloblastoma Desmoplastic humain	Medulloblastoma peritoneum metastatic	Medulloblastoma humain
Growth Properties	Adherent cells	Suspended cells + multicellular aggregates + adherent cells	Suspended cells
Morphology	Polygonal	Epithelial	Spheroid
Molecular subgroup	SHH	Group 3 ou 4	Group 3

Cancer stem cells

Brain tumor stem cells

Stem cells are a type of pluripotent cells with self-renewing ability which can differentiate into multiple functional cells. In mammals, there are two essential types of stem cells: embryonic stem cells and somatic stem cells. Self-renewal and potency are 2 properties to define a stem cell. According to the development potential of stem cells, they are divided into three types: totipotent stem cells, pluripotent stem cells, and unipotent stem cells. Based on the similarities observed between stem cells and cancer, the hypothesis of cancer stem cells (CSCs) was proposed, which is now supported by a plethora of recent observations. Cancer arises from a series of mutations that occur in few or even single founder cells. These cells eventually acquire unlimited and uncontrolled proliferation. Two hypothetical models can explain this phenomenon: the stochastic model and the hierarchical model. The first model predicts that all the cells in a tumor have a similar proliferative potential, which is activated asynchronously and at a low frequency in some cells. Conversely, the hierarchical model holds that only a rare subset of cells within the tumour have significant proliferation capacity and, particularly, the ability to generate new tumours, with the remainder of the tumour cells representing differentiating or terminally differentiated cells (Nassar *et al.*, 2016). The appearance of CSCs might be the consequence of somatic mutational evolution (Rozhok *et al.*, 2015).

The CSCs in brain tumors were also identified since Singh *et al* demonstrated in 2003 the existence of a particular undifferentiated cancer cell subpopulation with self-

renewing capacity, expressing the CD133 stem cell marker, and named brain tumor stem cells (BTSCs) (Singh *et al.*, 2003). This subpopulation of BTSCs found in MB was well described in a review of (Vescovi *et al.*, 2006). CSCs are distinguished by different characteristics from those of other tumor cells: self-renewal capacity, pluripotency and capacity of differentiation, as well as an ability to restore tumors identical to the original tumor during orthotopic implantation in mice (Singh *et al.*, 2004).

Isolation and identification of cancer stem cells

Current methods for identifying CSCs include the use of specific stem cell markers such as CD133 or functional criteria in culture (neurosphere formation *in vitro*). In fact, the neurosphere culture is a selective or enriched method with a particular condition without serum and in the presence of appropriate growth factors, such as epidermal growth factor (EGF) and fibroblastic growth factor 2 (FGF-2). Under these conditions, most differentiated cells die rapidly, while CSCs proliferate and form spheres that can be dissociated and repeated to generate secondary spheres with little change in their growth or differentiation characteristics (Figure 1.4).

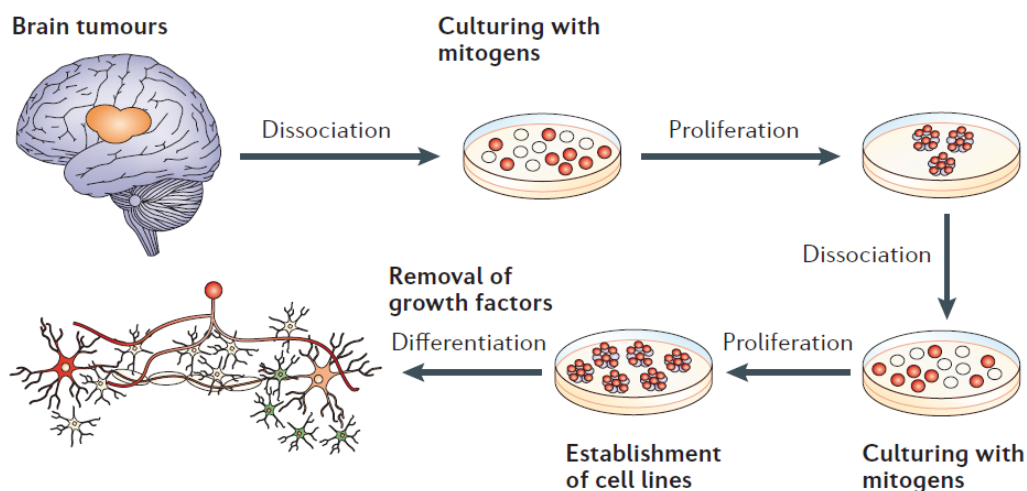


Figure 1. 4: Isolation and perpetuation of brain tumor stem cells *in vitro* culture.

Serum free culture system is used to isolate and receive the CNS-derived stem cells named neurospheres. This system contains the stem cell mitogens EGFR and/or FGR-2. Most cells die due to the lack of serum and the low plating density except those that respond to the stem cell mitogens which stimulate the cell proliferation to form neurospheres in suspension. These neurospheres can be dissociated into a single cell suspension and then re-plated in fresh serum free medium to produce secondary neurospheres. The stem cells will be differentiated into different cell types of CNS system like neurons, astrocytes and oligodendrocytes when removing mitogens. CNS: Central Nervous System; EGFR: Epidermal growth factor; FGR-2: Fibroblast growth factor 2. Figure taken from Vescovi et al., 2006.

CD133, a 117kDa transmembrane glycoprotein, is the most commonly used surface marker for the strain phenotype used to identify CSCs. CD133 is expressed by CSCs from different tumors, such as melanoma, liver cancer, osteosarcoma, colon cancer, glioblastoma and so on. Similarly, it has recently been shown that MB stem cells express also this surface marker. However, CD133 is not a specific identification marker for all types of CSCs and some CD133 negative cancer cells have the ability to form new tumor *in vivo*. Other markers have been identified, in the case of MB, as

the marker CD15 which could be an interesting marker for stem cells of some MB subtypes (Read *et al.*, 2009).

Embryonal brain tumors are aggressive and fast-growing, which can disseminate into the CNS. Recent findings indicate that MB may be developed from granular stem cells or progenitor cells of the cerebellum (Samkari *et al.*, 2015) (Figure 1.5). The discovery of CSCs in MB is a major advance in the field of neuro-oncology research. Stem cells in MB are probably at the origin of the tumorigenesis and Bao *et al.* found that this subpopulation also can lead to resistance to therapy and recurrence (Bao *et al.*, 2006). The identification of new molecular target specific for MB stem cells is a major challenge to improve the management of this pathology.

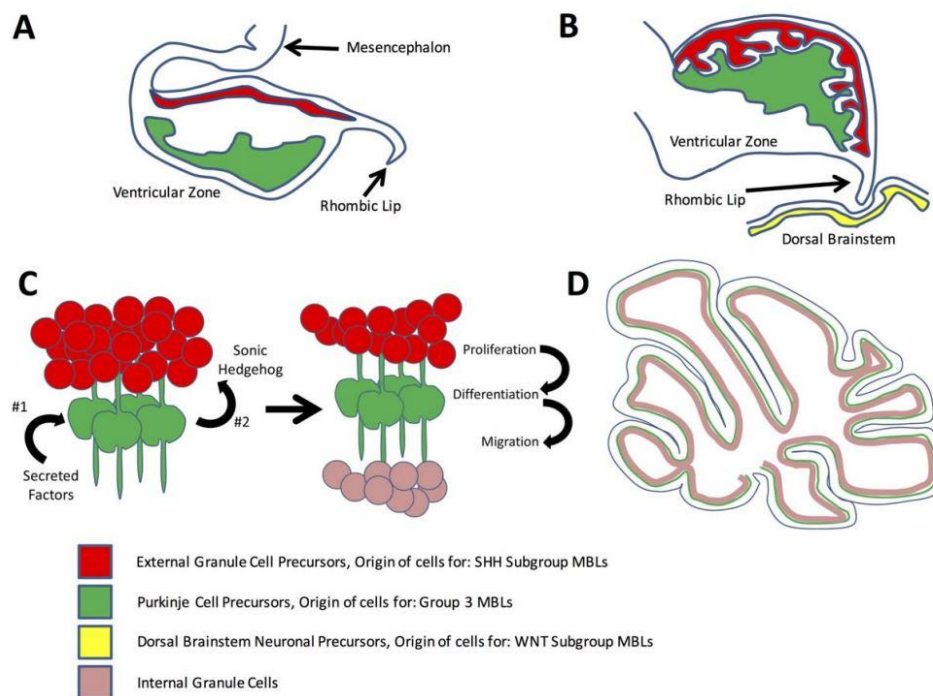


Figure 1. 5: Germinal zones in the developing cerebellum and their mechanism of development.

A: Schematic depicting the initial locations of the Purkinje cell precursors (green) and the external granule cell precursors (red) at approximately embryonic day 10–13. The ventricular zone, the source of GABAergic neurons, houses the Purkinje cell precursors, while the rhombic lip, the source of glutamatergic neurons, houses the external granule cell precursors. The SHH subgroup of MBLs originates from the rhombic lip and external granule cell precursors, and the Group 3 subgroup of MBL originates from precursors in both the rhombic lip as well as the ventricular zone. B: Cerebellum development at embryonic day 16–17. The Purkinje cell precursors, due to paracrine signaling, have migrated to the upper edge of the forming cerebellum, near the external granule cell precursors. C: Snapshot of the signaling pathways occurring in section B. Neuropeptide signaling on Purkinje cells initiates SHH signaling from the Purkinje cells onto the external granule cells. SHH signaling causes rapid proliferation and differentiation of the external granule cells, which then causes them to migrate across the Purkinje cell monolayer and form the internal granule cell layer. D: Final locations of the Purkinje cell layer and the newly formed internal granule cell layer of the fully developed cerebellum at postnatal day 20-adult. Figure taken from Martirosian *et al*, 2016.

Cancer stem cell signaling pathways in medulloblastoma

The signaling pathways related with these subgroups were widely studied for the advanced targeted therapies such as SHH signaling, WNT signaling, Notch signaling, p53, and PI3K (Kumar *et al.*, 2017). Besides, the signaling pathways in group 3 and 4 are not well known, some downstream signaling pathway Bmi1 signaling and other putative brain tumor initiating cells (BTIC) self-renewal genes may be also related with these subgroups. Because these signaling pathways are involved in the MB tumorigenesis and stem like features, their receptors, mediators, transcription factors and oncoproteins may regulate BTIC self-renewal ability and thereby provide potential therapeutic interventions (Manoranjan *et al.*, 2012) (Figure 1.6).

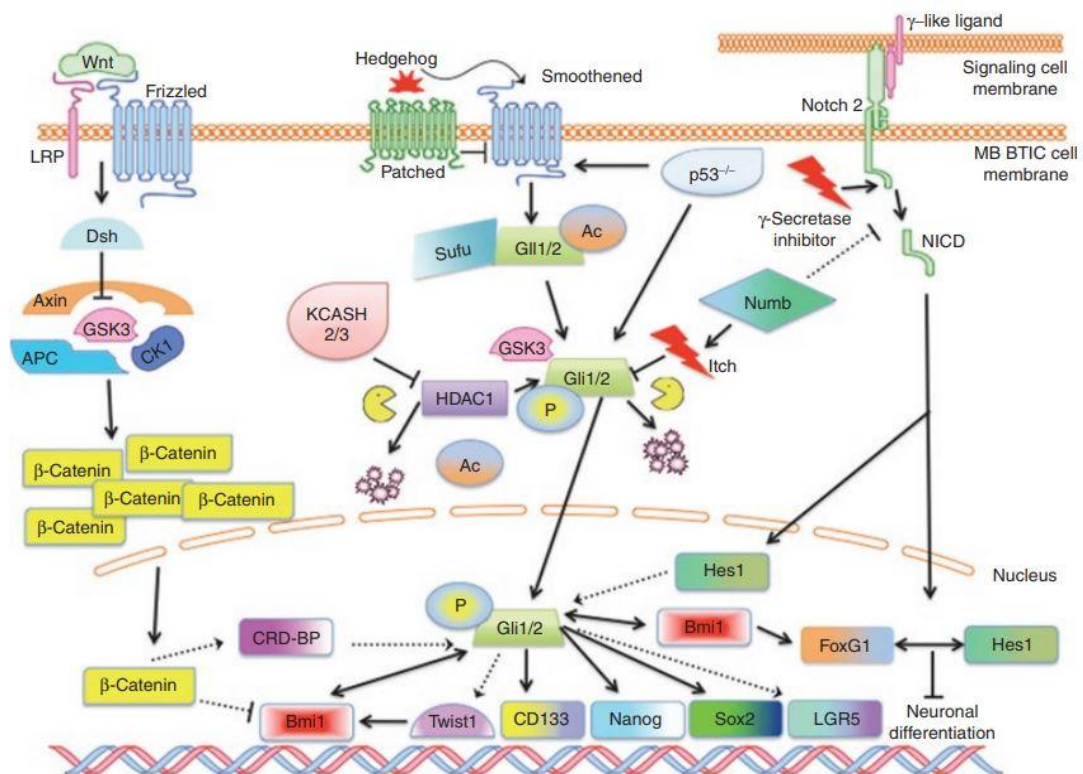


Figure 1. 6 : Key signaling pathways involved in Medulloblastoma.

Signaling pathways reported in maintaining the tumorigenic potential of MB BTICs mainly include Wnt, Shh and Notch signaling pathways. The Wnt and Shh signaling are involved in the molecular subgroup of WNT and SHH. Besides, the signaling pathways in group 3 and 4 are not well known, some downstream signaling pathway Bmi1 signaling and other putative BTIC self-renewal genes may be also related with these subgroups. The key regulators or mediators of these signaling pathways may promote or inhibit BTIC self-renewal ability and thereby provide potential therapeutic interventions. BTIC: Brain tumor-initiating cell; MB, Medulloblastoma; Shh, Sonic hedgehog; Wnt: Wingless. Figure taken from Manoranjan *et al.*, 2012.

SHH signaling

The Hedgehog gene (Hh) encodes a highly conserved glycoprotein that plays an important role in regulating cell differentiation and stem cell maintenance during embryonic development. There are three Hedgehog homologues in humans: Sonic Hedgehog (SHH), Indian Hedgehog (IHH) and Desert Hedgehog (DHH), encoding SHH, IHH, and DHH proteins, respectively (Ingham *et al.*, 2011). SHH is the best studied ligand of the cell signaling pathway in MB. Most of what is known about hedgehog signaling has been established by studying SHH. Thus, the functions of SHH are regulated by PTCH-SMO-GLI signaling (Dray *et al.*, 2010, Taipale *et al.*, 2002), SHH binds to PTCH to relieve its repression of SMO, leading to active the downstream effectors, including GLI1, GLI2 and GLI3 (Figure 1.7).

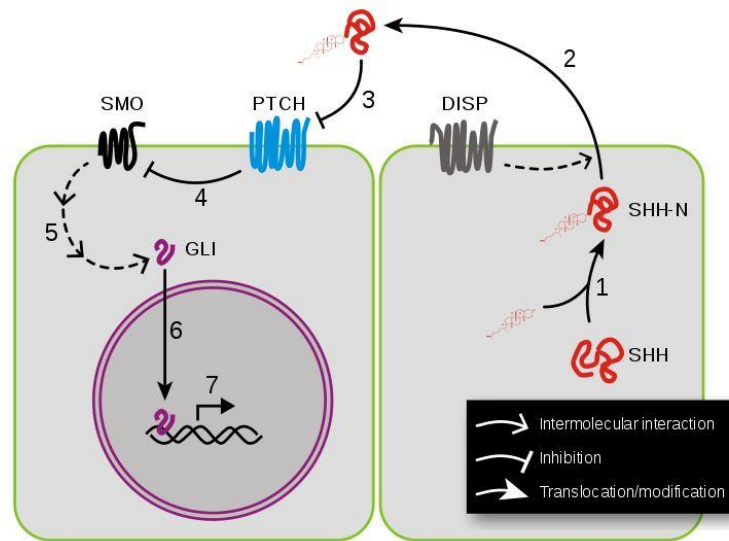


Figure 1. 7: Overview of Sonic hedgehog signaling.

SHH can signal in an autocrine way, affecting the cells in which it is produced. Secretion and consequent paracrine hedgehog signaling require the participation of Dispatched (DISP) protein (Process "1 and 2". SHH binds to the Patched-1 (PTCH1) receptor (Process "3" on Figure 5, the blue molecule). In the absence of ligand, PTCH1 inhibits Smoothened (SMO), a downstream protein in the pathway (Process "4"). It has been suggested that SMO is regulated by a small molecule, the cellular localization of which is controlled by PTCH. The binding of SHH relieves SMO inhibition, leading to activation of the GLI transcription factors (Process "5"): the activators Gli1 and Gli2 and the repressor Gli3. Activated GLI accumulates in the nucleus (Process "6") and controls the transcription of hedgehog target genes (Process "7").

Activation of SHH pathway has been implicated in the development of cancers in various organs, including brain, lung, mammary gland, prostate and skin. MB can also develop due to this activated signaling pathway mainly by the mutations of the repression factors PTCH1, PTCH2 or SUFU (Brugieres *et al.*, 2010, Crawford *et al.*, 2009). Abnormal activation of the pathway probably leads to development of MB through one of the important hypothesis that transformation of adult stem cells into CSCs which contribute the tumor arise (Chen *et al.*, 2002). So the specific inhibitors

of hedgehog signaling could provide an efficient therapy for a wide range of malignancies.

More and more research showed that deregulation of G-protein coupled receptor (GPCR) pathways has been implicated in occurrence and development of MB (He *et al.*, 2014). GNAS was recently identified as a potential tumor suppressor gene encoding the protein Gs α , which inhibited the pathogenesis of an invasive MB driven by Sonic hedgehog protein. Scientists used the Rolipram to treat the GNAS invasive mutant MB mice genetically engineered to not express the GNAS gene. Rolipram treatment increased the level of cAMP molecules in mice and restored the tumor suppressor function of the GNAS-Gs α signaling pathway. This led to shrinking and regression of the tumor. The study also showed that elevating cAMP levels in cells can improve the efficacy of several Sonic hedgehog inhibitors currently tested in clinical trials for combating tumor growth.

WNT signaling

Wnt signaling plays an important role in embryonic development, cell differentiation and proliferation and adult tissue maintenance. The perturbations of Wnt signaling are also identified for its role in carcinogenesis (Nusse *et al.*, 2005). Various proteins involved with different functions are derived in this signaling pathway that could be divided into the canonical pathway, the non canonical pathway and the integrated WNT-Ca²⁺ pathway. β -catenin is the key protein in the canonical Wnt pathway so that it is called β -catenin pathway (Figure 1.8).

Activation of this pathway is relied to the accumulation of β -catenin in the cytoplasm and then translocation into the nucleus to act as a transcription factor after Wnt protein binding to the Frizzled/LRP receptor complex at the cell surface. Mutations in the Wnt pathway cause several hereditary diseases and contribute to the development of cancer involved the interactions of tumor suppressor APC protein (Minde *et al.*, 2013). In human MB, gene CTNNB1 encoding β -catenin serves as the downstream complex with AXIN and APC of WNT signaling and its mutations are frequently observed in WNT subgroup (Thompson *et al.*, 2006).

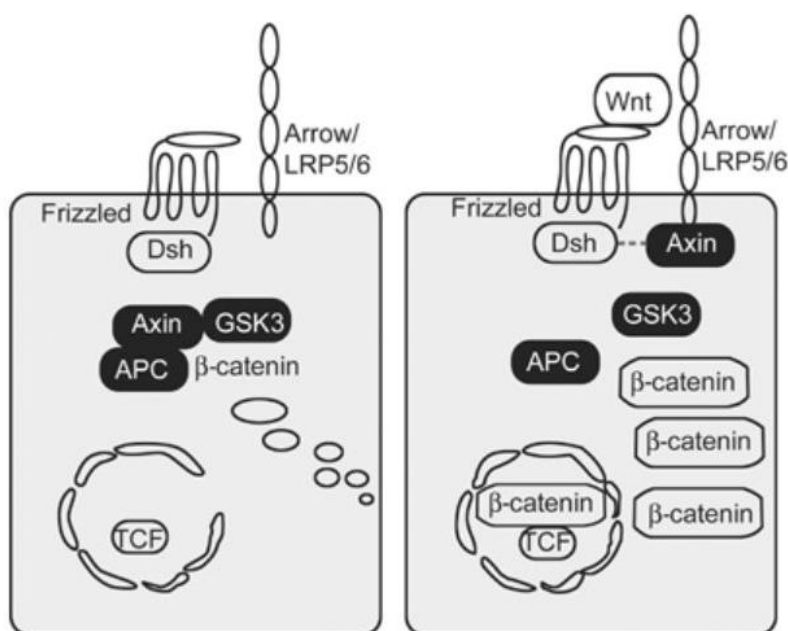


Figure 1. 8 : The canonical Wnt signaling pathway.

Left side showed Wnt signaling at a no activated status, β -catenin is degraded through interactions with Axin, APC, and the protein kinase GSK-3. Right side showed that Wnt proteins bind to the Frizzled/LRP receptor complex at the cell surface and then transmit the signal to Dsh and to Axin, which can inhibit the degradation of β -catenin. The accumulates of β -catenin in the cytoplasm and nucleus interact with TCF to control transcription. Dsh: Dishevelled; Figure taken from Nusse, 2005.

Notch and other signaling pathways

The tumors in subgroup 3 and 4 are more invasive and involved with poorer prognosis, but the signaling pathways in these groups are not well known. Notch may interact with the common downstream factors of other pathways. Notch signaling pathway is a highly conserved cell signaling system presenting in various systems which play an important role in embryonic development, and this pathway also maintains the self-renewal and pluripotency of stem cells or progenitor cells status in preventing their differentiation, particularly in CNS (Ben-Shushan *et al.*, 2015, De la Pompa *et al.*, 1997). Notch family has 4 homologs in mammalian: Notch 1, Notch 2, Notch 3 and Notch 4, and their receptors are all single pass transmembrane proteins. In canonical Notch signaling (Figure 1.9), activation of Notch is closely related to the development and progression of MB by disturbing the common downstream signaling to promote tumor formation and inhibit cancer stem cell differentiation (Teodorczyk *et al.*, 2014). The extracellular Delta/Jagged ligands combine with the Notch receptors and give rise to S2 cleavage on the site of ADAM (a disintegrin and metalloprotease) 10 or 17. Interactions activate the S3 cleavage which leads to the Notch intracellular domain (NICD) binding to a protein γ -secretase-presenilin complex. The stimulated signal then translocates into the nucleus. The transcriptions of hairy/enhancer of split (Hes) and Hey are suppressed by these events (Fischer *et al.*, 2007, Iso *et al.*, 2003). This activated status stimulates the tumor development and also promote the growth of human brain initialing cells (Sarkar *et al.*, 2017). So molecules disturb Notch signaling pathway could be used to treat MB. A gamma secretase inhibitor

RO4929097 of Notch signaling pathway has been already assessed in clinical trials for different tumors (Tolcher *et al.*, 2012, De Jesus-Acosta *et al.*, 2014, Diaz-Padilla *et al.*, 2015) and MK-0752 in refractory or recurrent pediatric CNS tumors (Fouladi *et al.*, 2011). Peptide inhibitors represent potential future treatment modalities in MB by acting function in the late stage of the pathway. The specific signaling pathways remain still unclear for the non SHH/WNT subgroup MB. Recent molecular research of MB found that there is an overexpression of Bmi1 in all subgroups, particularly in the more aggressive subgroups (Leung *et al.*, 2004). Bmi1 is a key stem cell regulatory effector implicated in the pathogenesis of many aggressive cancers, including MB, related with SHH pathway driven tumorigenesis and cell proliferation. The key factor Gli1 as one of the downstream reactor of Shh, can be preferentially binded to the Bmi1 promoter and influence the Gli1 expression. In fact, Shh and Bmi1 were 2 indispensable signaling pathways in MB stem cell maintenance but also be related with each other (Wang *et al.*, 2012). The mediators of Bmi1 signaling and other putative brain tumor stem cell self-renewal genes may provide potential targets for therapeutic interventions.

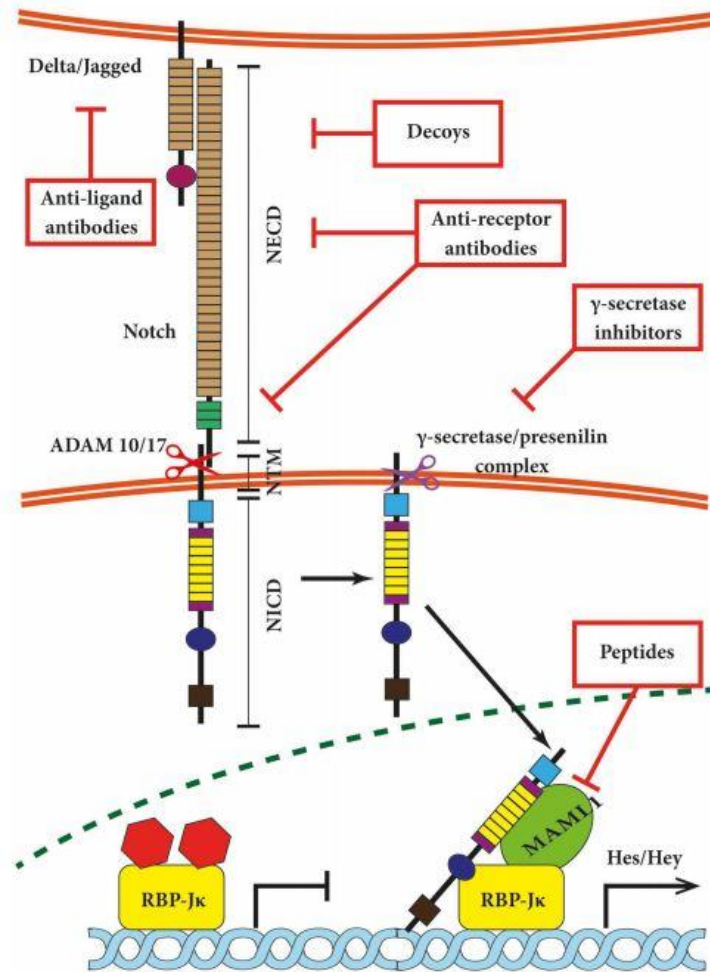


Figure 1. 9 : Canonical Notch signaling involved current targeted therapies.

Figure showed that several stages of the Notch signaling pathway are prone to pharmacological intervention. NICD: Notch intracellular domain, NECD: Notch extracellular domain; NTM: Notch transmembrane domain. Figure taken from Teodorczyk *et al.*, 2014.

Neuropilins

Structure and co-receptors of neuropilins

Neuropilins (Neuropilin-1[NRP-1] and Neuropilin-2 [NRP-2]) are transmembrane glycoproteins that play a very important role in the development of neuronal and vascular systems. They are receptors of the class III semaphorin family, factors of axonal guidance, factors of angiogenesis and receptors of the VEGF family. NRP-1 has 2 fractions including a membrane form of 120 kDa and a soluble fraction at 80 kDa. NRP-2 (105 kDa) is a homolog that shares about 44% similarities of structural and biological properties with NRP-1. They have identical domain structures which are located on different chromosomes (NRP-1 on chromosome 10 and NRP-2 on chromosome 2) (Wild *et al.*, 2012) (Figure 1.10).

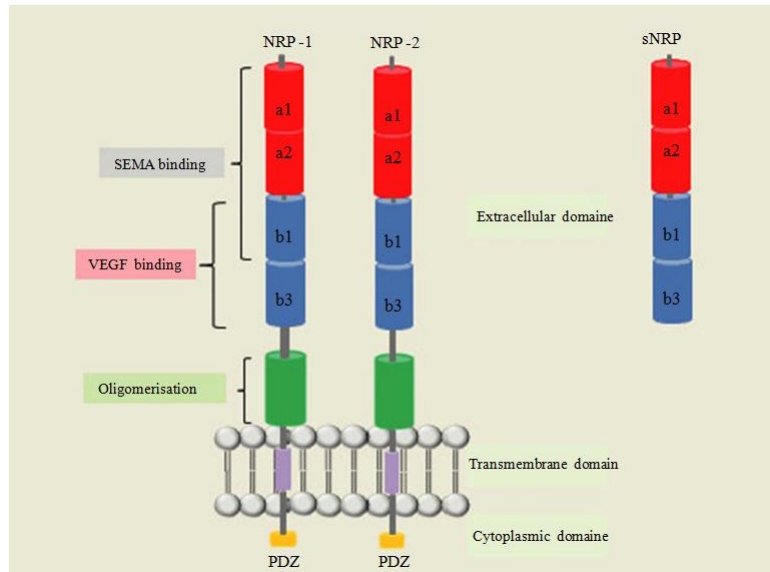


Figure 1. 10 : Structural domains of Neuropilins.

In humans, NRP-2 shares only 44% sequence homology with NRP-1. The two receptors have an identical domain structure, comprising a large N-terminal extracellular domain (835 aa for NRP1, 844 aa for NRP2), a short transmembrane domain (23 aa for NRP1, 25 aa for NRP2) and a small cytoplasmic domain (44 aa for NRP1, 42 for NRP2). The NRP extracellular region is divided into three domains: (1) the a1 /a2 (CUB) domain, which is homologous to complement proteins C1r and C1s, (2) the b1 /b2 domain, which is homologous to coagulation factors V and VIII and (3) the c domain, which is homologous to meprin, A5 and receptor tyrosine phosphatase 1 (hence designated MAM). The PDZ-domain binds the neuropilin interacting protein (NIP). Soluble NRP (sNRP), which contain the extracellular a1 /a2 and b1 /b2 domains and lack the transmembrane -c and cytoplasmic domains function as natural NRP inhibitors. Figure taken from Wild *et al.*, 2012.

Role of NRP-1 in cancer and involved signaling pathways

Neuropilins act as co-receptors by complexing with other transmembrane receptors and thereby increase the binding of extracellular ligands. So far, five major types of soluble mediators that can bind neuropilins have been discovered: TGF- β 1, the VEGF family, HGF, PDGF-BB, and the SEMA III family (Prud'Homme and Glinka, 2012) (Figure 1.11).

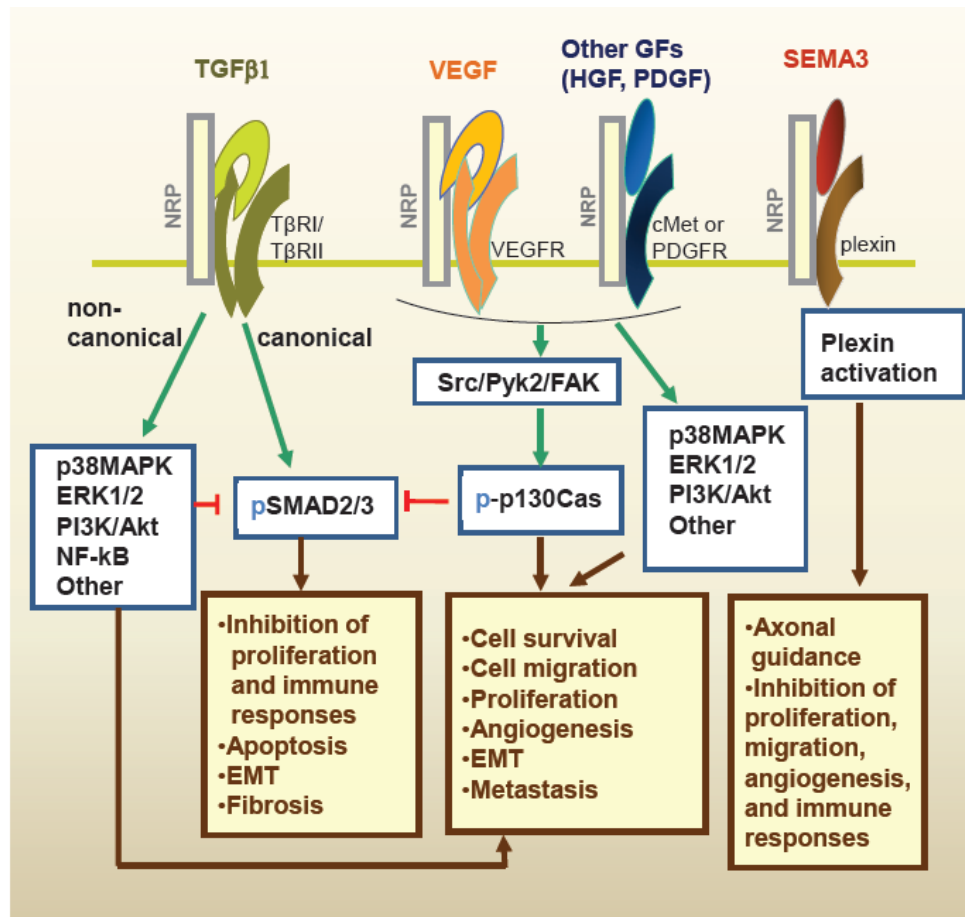


Figure 1. 11 : Co-receptors involved in main signaling pathways and functions regulated by Neuropilins

Receptors and mediators interact in NRP-1-driven signaling pathways including TGF-β1, VEGF family, HGF, PDGF-BB, and the SEMA3 family. The signaling pathway of TGF-β1 is divided into canonical (Smad2/3) and non-canonical signaling. Smad signaling appears to have an anti-proliferative reaction, while TGF-β non-canonical signaling (or other GF pathways) can inhibit Smad2/3 signaling and lead to tumor progression by the adaptor p130Cas. This mediator is in phosphorylated form in response to NRP-1 which binds to GFs, and then interacts in non-canonical signaling pathway. For SEMA3s, the Nrps are not essential for receptor signaling but they enhance the response. SEMA3s interact with Nrps and plexins (the signaling receptors) to activate signaling pathways that regulate axonal guidance, as well as endothelial, immune and tumor cell responses, usually in an inhibitory way. EMT: Epithelial-to-mesenchymal transition; FAK: Focal adhesion kinase; GF: growth factor; HGF: Hepatocyte growth factor; p-: phosphorylated form; p130Cas: Crk-associated substrate; PDGF, platelet-derived growth factor; PDGFR; PDGF receptor; Pyk2, proline-rich tyrosine kinase 2; SEMA3: Class 3 semaphorin; TGF-β: Transforming growth factor-β; TMD: Transmembrane domain; VEGF: Vascular endothelial growth factor; VEGFR: Vascular endothelial growth factor receptor. Figure taken from Prud'Homme *et al.*, 2012

Initially, NRPs were widely described as mediators of axonal guidance but it was later demonstrated that these receptors are also involved in the development of tumor angiogenesis, tumor progression and cancer stem cell stemness by acting via different receptors involving various signaling pathways. VEGFs also play an important role for the self-renewal, survival and tumor-forming ability of CSCs. NRP-1 was first described as an interacting receptor of the VEGF family in 1997. It was showed that the expression of NRP-1 and VEGFR-2 enhanced VEGF165 mediated interactions and induced the mitogenic activity (Soker *et al.*, 1997). In addition, Hamerlik *et al* has shown that VEGFR2 / NRP-1 signaling promoted the survival of cancerous stem cells from brain tumors (Hamerlik *et al.*, 2012). Similarly, Cao *et al.* found that suppression of NRP-1 induced a more differentiated phenotype in a model of renal cell carcinoma with the inhibition of SHH. So that the authors concluded that NRP-1 promoted an undifferentiated phenotype in cancer cells (Cao *et al.*, 2008). Beck *et al* found that blocking NRP-1 decreased VEGF's by affecting CSCs through NRP-1 in an autocrine loop to promote cancer stemness and renewal, caused tumour regression in skin tumors (Beck *et al.*, 2011). NRP-1 acts as the co-receptor of VEGF. They are independent but also interact with each other to affect tumorigenesis, angiogenesis and cancer stemness, therefore, their antagonists may be effective for the treatment of related tumor.

Transforming growth factor- β (TGF- β) is a multifunctional cytokine involved in stem cell differentiation and is also quite commonly expressed by cancers (Beck *et al.*, 2011). The mutations of TGF- β signaling pathway lose the control of normal functions of TGF- β leading to immunosuppression, angiogenesis and even

tumorigenesis (Blobe *et al.*, 2000). Glinka *et al* showed that NRP-1 was a co-receptor of TGF- β and increased the responses of TGF- β related with cancer progression and metastasis (Glinka *et al.*, 2011). The signaling pathway of TGF- β 1 divides into canonical (Smad2/3) and non-canonical signaling. Smad signaling appears to an anti-proliferative reaction, while TGF- β non-canonical signaling (or other GF pathways) can inhibit Smad2/3 signaling and lead to tumor progression by the adaptor p130Cas (Kim *et al.*, 2008). This mediator is in phosphorylated form in response to NRP-1 which binds to growth factors (GFs), and then interacts in non-canonical signaling pathway (Wendt *et al.*, 2009). For SEMA3s, the NRPs are not essential for receptor signaling but they enhance the response. SEMA3s interact with NRPs and active plexins to regulate axonal guidance, as well as endothelial, immune and tumor cell responses, generally in an inhibitory way (Klagsbrun and Shimizu, 2010).

Another pathway could also be considered that NRP-1 control the anti-apoptotic function in endothelial cells (ECs) through the NRP-1 interacting protein (NIP/GIPC) by activating PI3K/Akt and p21, and inactivating p53 pathways and FoxOs (Wang *et al.*, 2007). Furthermore, other authors have reported the possible mechanism in cancer cells, showed a new signaling pathway of NRP-1 that GIPC1/Syx complex in signaling pathway of VEGF-A/NRP1 induced cancer cell proliferation (Yoshida *et al.*, 2015). These signaling pathways contribute to a better understanding of molecular mechanisms of NRP-1 derived angiogenesis and related cancer formation and provide the possibilities for better therapeutic targets.

Different approaches envisaged to target NRP-1

NRP-1 has multifunctions regarded as the co-receptor of different biological molecules. The target action of this receptor is mainly located in its transmembrane fraction (mNRP-1), divided into three domains: a1/a2, which is homologous to the complement proteins C1r/C1s, Uegf and Bmp-1 (CUB); b1/b2, which is homologous to the coagulation factors V and VIII (CF); c, which is homologous to meprin, A5 and receptor tyrosine phosphatase μ (MAM). The cytoplasmic tail (CP) lacks a catalytic activity, but contains a C-terminal SEA sequence that represents a consensus binding motif for proteins containing the PDZ (PSD-95, Dlg, ZO-1) domain, which promotes the formation of complexes with signaling pathway components (Graziani and Lacal., 2015).

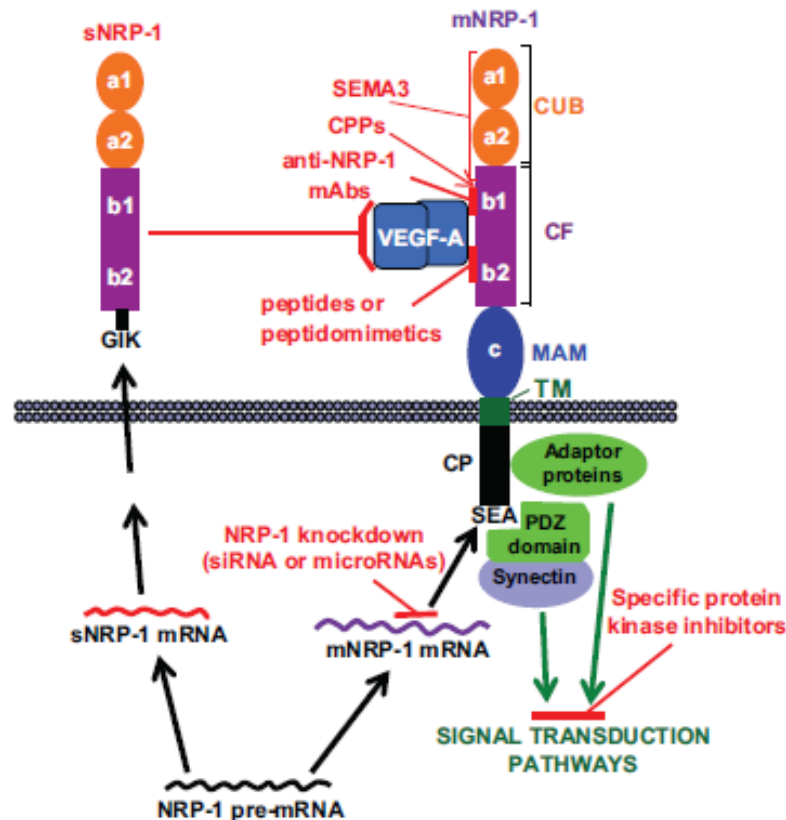


Figure 1. 12 : Strategies to target NRP-1.

Monoclonal antibodies (mAbs), peptides or peptidomimetics block the b domain of NRP-1 binding to VEGF-A. Figure taken from Graziana, *et al.* 2015

Monoclonal antibodies

Because of its important role in tumor angiogenesis and tumor proliferation, different approaches have been recently considered to target NRP-1. Monoclonal antibodies have been used for several years for the treatment of different tumor types, and several antibodies have been developed specifically to target NRP-1. A phase I study of the human monoclonal anti-NRP1 MNRP1685A tested in patients with advanced solid tumors, showed encouraging results (Weekes *et al.*, 2014). It seems

particularly interesting to combine anti-VEGF and anti-NRP-1 antibodies to limit the progression of MB. PlGF is produced in the cerebellar stroma via tumor-derived SHH and shows that a new mechanism noting that placental growth factor (PlGF) acts through NRP-1 and not VEGFR-1 to promote tumor survival, which proposed a new therapy way of MB by targeting PlGF/NRP-1 across MB subtypes-supports (Snuderl *et al.*, 2013). However, some studies have pointed out that proliferation of MB in culture was dependent upon NRP-2, while reducing NRP-1 function had little effect. So NRP2 should be further investigated as a potential target for adjuvant therapy (Hayden *et al.*, 2013).

Peptide-based molecules

NRP-1 was found to be a co-receptor of vascular endothelial growth factor – A165 (VEGF-A165) acting together with vascular endothelial growth factor receptor - 2 (VEGFR-2) via its NRP-1 b1/b2 domain, resulting in increased affinity of VEGF-A165 for the extracellular domain of VEGFR-2. But targeting NRP-1 with small molecules mimicking VEGF-A165 is not very advanced, because of the difficulty to mimic protein–protein interactions. With regard to the peptide-based approach, several peptides have been reported to modulate VEGF-A165/NRP-1 binding.

Tuftsins are natural tetrapeptides (Figure 1.13) (Thr-Lys-Pro-Arg, TKPR, Chemical formula: $C_{21}H_{40}N_8O_6$, Molar mass: 500.593 g/mol) located in the Fc-domain of the heavy chain of immunoglobulin G, known as immunostimulatory factor, which was recently discovered to bind specifically to NRP-1 (Von Wronski *et al.*,

2006). The role of the loops at b1 domain of human NRP-1 as a target binding site for ligand interaction has also been showed in the study of NRP-1 binding with tuftsin (TKPR), which is very similar to the VEGF-A165 C-terminus (DKPRR) (Vander *et al.*, 2007).

The C-terminal arginine of tuftsin contributes to the majority of interactions with NRP-1 and this was confirmed by a molecular modeling approach. Heptapeptide ATWLPPR (A7R), selected by screening a phage display library was described as an effective antagonist binding specifically to NRP-1 and decreased at the same time the angiogenesis and growth of breast cancer *in vivo*, so it can be considered as a potent inhibitor of tumor angiogenesis (Starzec *et al.*, 2007). More and more new peptides structurally related to VEGF-A165 domains were recently designed and synthesized.

However, the stability and bioavailability of peptides are limitations of these compounds, so the design of the more compatible molecules such as peptidomimetic based on carbohydrate moieties have been contemplated and seems an alternative solution. Following these discoveries, our group developed, in collaboration with chemists, some carbohydrate based peptidomimetics taking advantage of functionalities and stereodiversities of sugar derivatives. One of these compounds (MR438) demonstrated inhibition of VEGF-A165 binding to NRP-1 and specificity for NRP-1 over VEGF-R2 (Figure 1.13). Biological evaluations were performed on human umbilical vein endothelial cells (HUVECs) through activation of downstream proteins (AKT and ERK phosphorylation), viability/proliferation assays and *in vitro* measurements of anti-angiogenic abilities (Richard *et al.*, 2016).

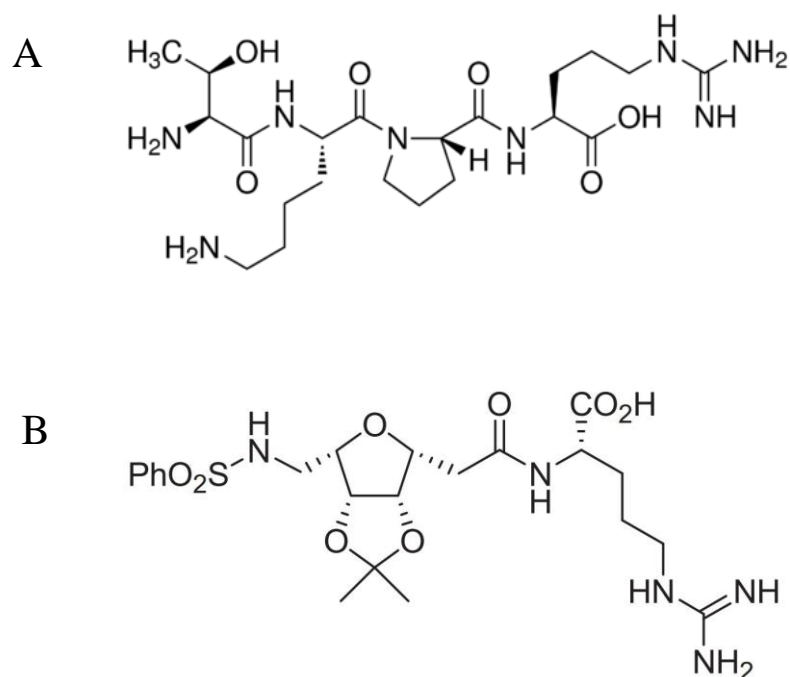


Figure 1. 13 : Structures of compounds peptide and peptidomimetic.
 (A) **Tuftsin**: peptide, Amino acid composition : Thr-Lys-Pro-Arg, TKPR, Chemical formula: C₂₁H₄₀N₈O₆, molar mass: 500.593 g/mol, affinity of NRP-1: 25 mmol/L;(B) **MR438**: peptidomimetic, chemical formula: C₂₂H₃₃N₅O₈S, molar mass: 527..59 g/mol, affinity of NRP-1: 88 mmol/L.

Hypotheses and objectives

The development of peptides aiming to targeting NRP-1 is to use peptidomimetics for their theoretical stability (Richard *et al.*, 2016). We have recently designed and assessed some new sugar-based peptidomimetics targeting NRP-1 (MR563, MR438 and other peptidomimetics provided by Dr. Nadia Pellegrini-Mo ĩe from L2CM 7053). One of them named MR438 presented a relevant *in vitro* affinity

for NRP-1 (IC₅₀ of 88 µmol/L) (Richard *et al.*, 2016). Tuftsin (TKPR: Thr-Lys-Pro-Arg), a natural ligand of NRP-1 with IC₅₀ of 25 µmol/L (Richard *et al.*, 2016) was used in our work as reference compound. Therefore, we investigated the exposition of these two compounds targeting NRP-1 on MB stem cells obtained *in vitro* from 3 cell lines (DAOY, D283-Med and Med-D341) in order to assess their short-term effects as cytotoxicity and cell invasion or their long-term effects as self-renewing ability and change stem cells of phenotypic status.

There are already a plenty of research verified the model of neurospheres as the CSC model *in vitro*, in Chapter 2, we have characterized our 3 MB stem cell models with NRP-1 expression level and stem cell marker features and evaluated the effects of MR438 on CSCs: viability, morphology, self-renewal capacity, invasive capacity and the change of stem cell features. Interestingly, we found that inhibition of NRP-1 seemed to induce the differentiation of MB stem cells, so we continued to study the possible molecular mechanisms related with NRP-1 signaling pathways.

CSCs have better DNA repair capability in comparison with differentiated cells contributing to tumor resistance during radiation. The conventional therapies could kill differentiated tumor cells, but this small population survives and causes tumor progression and recurrence (Singh *et al.*, 2004, Vescovi *et al.*, 2006, Bao *et al.*, 2006). As MR438 could stimulate the differentiated state of CSCs, it might also lead to improve radiosensitivity of resistant cells. We have demonstrated this hypothesis in Chapter 3, in which our results showed that MR438 increased radiosensitivity both for MB CSC cell lines *in vitro* and for heterotopic xenografts models.

The tumor environment is also very important for the development and prognosis of MB, and the blood brain barrier (BBB) is a key valve for the curative effect of treatments for brain tumors. So due to our encouraging results *in vitro* and *in vivo*, we would like to confirm our results in orthotopic models of MB. First of all, we accomplished the elaboration of orthotopic models of MB obtained from DAOY, D283Med and D341Med cell lines and continued to characterize the MB CSC features and further to test the effects of MR438 on orthotopic models.

In brief, our objectives of this study were:

- 1) To support and validate the effects of MR438 with MB stem cell models from different subgroups *in vitro* (Chapter 2).
- 2) To evaluate the effects of the compounds in combination with radiotherapy *in vitro* and *in vivo* (Chapter 3).
- 3) To develop orthotopic models of MBs from CSCs (Chapter 4).

Chapter 2 :

**Stimulation of medulloblastoma stem
cells differentiation by a peptidomimetic
targeting Neuropilin-1**

Introduction

Medulloblastoma (MB) is the most common malignant pediatric brain tumor and affects children at a median age of 9 years (Orbach *et al.*, 2012). Despite the progress of radio- and chemotherapy, the risk of recurrence, frequent cognitive and endocrine sequelae and death after treatment remains important (Bourdeaut *et al.*, 2011, Grill *et al.*, 2005). Recent results showed that MB was composed of four molecular subgroups: WNT (Wingless), SHH (Sonic Hedgehog), Group 3 and Group 4, which correspond to different molecular and clinical characteristics. Indeed, patients of groups 3 and 4, also called non-WNT and non-SHH groups, frequently present metastasis and have a poor prognosis (Taylor *et al.*, 2012, Northcott *et al.*, 2011). MB is classified as an embryonic tumor in which brain tumor stem cells (BTSCs) are present in very low proportion. BTSCs can be characterized by expression of stem cell phenotypic markers such as CD133 or CD15 (Singh *et al.*, 2003, Read *et al.*, 2009) and has a peculiar interest in understanding the progression of MB (Vescovi *et al.*, 2006). This cell population generates tumors through the stem cell patterns of self-renewal and differentiation into multiple tumor cell types. Moreover, these cells have better DNA repair capability contributing to tumor resistance during radiation and chemotherapy. The conventional therapies could kill differentiated tumor cells, but this small population of BTSCs survives and causes tumor recurrence (Singh *et al.*, 2004, Vescovi *et al.*, 2006, Bao *et al.*, 2006).

Neuropilin-1 (NRP-1) is a single-pass transmembrane glycoprotein that plays a very important role in the development of neuronal and vascular systems, and shares about 44% homology with neuropilin-2 (NRP-2). It acts as a co-receptor by complexation with other transmembrane receptors such as VEGFs and Semaphorins, which are involved in neoangiogenesis and tumor progression by activating signaling pathways involved in survival, proliferation or cell migration (Prud'Homme and Glinka, 2012). Recently, Snuderl *et al* demonstrated that PlGF acts through NRP-1 to promote MB cell survival but not through vascular endothelial growth factor receptor 1 (VEGFR-1) (Snuderl *et al.*, 2013). Moreover, NRP-1 seems to favor an undifferentiated phenotype in cancer cells (Cao *et al.*, 2008). Targeting directly this receptor, especially in BTSCs, could thus provide interesting therapeutic value to decrease tumor proliferation or change the stem cells to a differentiated phenotype for improvement of survival and quality of life of MB patients.

Our previous work focused on the development of peptides for targeting NRP-1 and we have proposed to use peptidomimetics for their theoretical stability (Pernot *et al.*, 2011, Benachour *et al.*, 2012). We have recently designed and assessed some new sugar-based peptidomimetics targeting NRP-1 and one of them named MR438 presented a relevant *in vitro* affinity for NRP-1 (IC_{50} of 88 $\mu\text{mol/L}$) (Richard *et al.*, 2016). Tuftsin (TKPR: Thr-Lys-Pro-Arg) is a natural ligand of NRP-1 with a IC_{50} of 25 $\mu\text{mol/L}$ (Nissen *et al.*, 2013, Von Wronski *et al.*, 2006) and it was used in our work as reference compound. Therefore, we investigated the exposition of these two compounds targeting NRP-1 on MB stem cells obtained *in vitro* from 3 cell lines (DAOY, D283-Med and Med-D341) in order to assess their short-term effects as

cytotoxicity and cell invasion or their long-term effects as self-renewing ability and the change of phenotypic status for stem cells. We first characterized the 3 MB stem cell models with an increased NRP-1 expression and stem cell markers and found that inhibition of NRP1 seems to induce the differentiation of MB stem cells.

Materials and methods

Cell culture of MB stem like cells

The human MB cell line DAOY (Jacobsen *et al.*, 1985), D283-Med (Friedman *et al.*, 1985) and D341-Med (Friedman *et al.*, 1988) were purchased from ATCC cell biology collection (Manassas VA, USA). Cells were maintained in MEM (Gibco, Life Technologies Corporation, UK) including 10 % fetal bovine serum (FBS, SIGMA,USA) for DAOY and D283, 20 % FBS for D341-Med, 1% L-glutamine (SIGMA,UK), 1 % non-essential amino acids (Gibco, UK), 1% penicillin/streptomycin (Gibco, UK) and 1 % Sodium pyruvate (GibcoUK) at 37 °C and 5 % CO₂. MB stem like cells cultures were maintained in DMEM/F12 medium (GibcoUK) containing B27 and N2 supplement (Gibco, Life Technologies Corporation, USA), 20 ng/mL of human recombinant epidermal growth factor (EGF) and basic fibroblast growth factor (bFGF) (EGF and FGF from Miltenyi Biotec, Germany). After a 3-day culture in hydrophobic flasks at 37 °C with 5% CO₂ in a humidifier atmosphere, spheres were obtained. MB stem like cells were dissociated from spheres using Accumax (Gibco, Life Technologies Corporation, UK) and seeded in 75 cm² or 25 cm² flasks depending on the experiment. The MB dissociated stem like cells were then exposed to MR438 (Molecular weight: 527.20 g/mol, supplied by the SRSMC laboratory-UMR 7565 in powder form) and Tuftsin (Molecular weight: 500.60 g / mol, BACHEM, Switzerland) at 25 µmol/L during 72h (Figure 2.1).

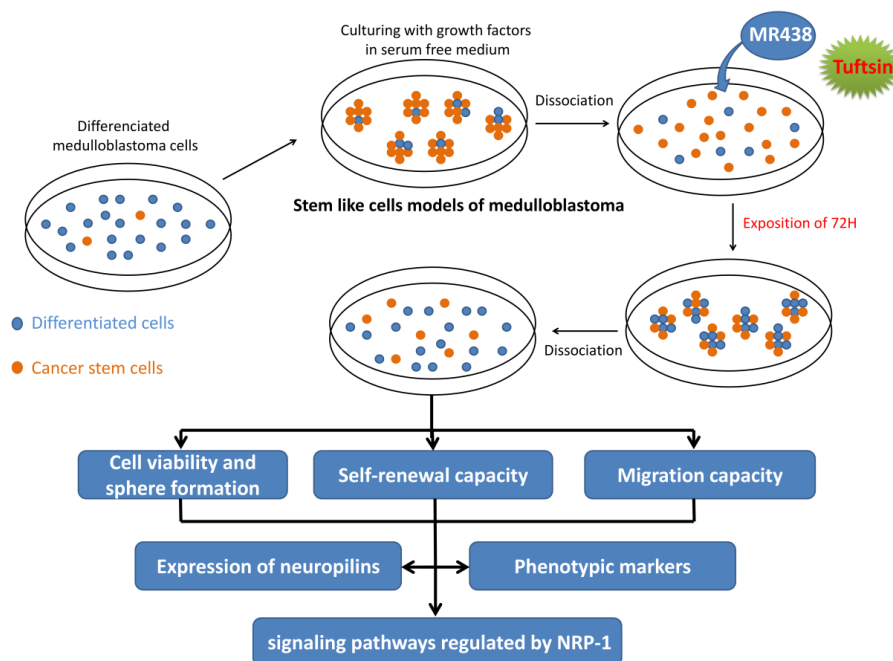


Figure 2.1: Scheme of the design of the experimental procedures *in vitro*.

Experimental procedures to evaluate the peptidomimetic effects on MB stem cells models obtained by *in vitro* enrichment methods. Serum- free medium was used to obtain stem like cells forming medullospheres. Suspension stem like cells were treated with Tuftsin or MR438 during 72H and re-dissociated into suspension cells for further experimentations: cell viability, colony formation, invasive test and the possible mechanism involved in NRP-1.

Sphere formation and Cells viability

We observed the sphere formation of the MB cells after a 72h incubation with the compounds Tuftsin and MR438 at the concentration of 25 $\mu\text{mol/L}$. The cells were seeded in 6 wells plates at a density of 60 000 cells/mL for DAOY-MS and D341-MS and 75 000cells/mL for D283-MS. The number of neurospheres larger than 30 μm was quantified using GelCount™ (Oxford Optronix, UK) to count the number of spheres and to evaluate the efficacy of medullosphere formation. Each experiment was repeated 3 times with 3 independent wells.

The viability of MB stem like cells was evaluated by automated cell counter TC20 (Biorad, France) using the trypan blue exclusion assay in 24 well plates at the same condition of cell density like sphere formation assay. Spheres were previously dissociated with Accumax and cell suspension then rapidly stained with the same volume of 0.4 % trypan-blue solution and deposited in counting chamber slides (TC20, Biorad). The percentage of surviving cells was counted twice and experiment was repeated 6 times.

Clonogenic assay

After exposure of MB stem like cells to MR438 and Tuftsin, clonogenic growth assay using methylcellulose based media was done. Briefly, MB stem like cells (20000 cells / well for DAOY-MS and 50000 cells / well for D283-MS and D341-MS) were suspended in 2 ml of DMEM/F12 containing 1% methylcellulose (SIGMA, USA). The cell suspension was then plated onto 6 well plates and allowed to grow for 8-12 days. Colonies were incubated with 0.5% MTT solution (Thiazolyl blue tetrazolium bromide, 98%, Acros Organics™) and colonies larger than 30 µm in diameter were quantified using GelCount™ (Oxford Optronix, UK). Each experiment was repeated 6 times with 3 independent wells.

Transwell invasion assays

Transwell invasion assays were performed using a transwell insert (Corning Incorporated, Corning, USA) with 4.4% Matrigel® (BD Biosciences, France) coated onto the transwell membrane (8µm pore size, 6.5mm diameter). The lower chambers of the transwell plates were filled with 700µL DMEM/F12 containing 10% FBS. Cells were cultured in the higher chambers (200 000 cells/chambre for DAOY-MS and 1000 000 cells/chamber for D283-MS) onto 24-well plate with 500µL serum free DMEM/F12. After 16 h for DAOY-MS and 48 h for D283-MS in incubators at 37 °C, cells on the upper surface of filters were removed using cotton swabs and those on the lower surface were fixed 10 minutes with 4% paraformaldehyde and staining with 0.05% crystal violet of 30 minutes. Photomicrographs of whole culture surface were taken (Nikon AZ100, Digital Sight DS-Qi1Mc camera, Nikon, France). The coloration was solubilized 10 minutes by placing the inserts in 150 µL of 4% acetic acid and then transferred into 96 well plates. The absorbance was read at 540 nm with a spectrophotometer (Thermo Electron Corporation, Finland).

Analysis of proteins expression by western blot

Western blot was carried out for analysis of NRP-1, NRP-2, CD133, CD15, NF-M and Sox2 protein expression. Total protein cell lysis buffer containing 10% protease (Roche, Germany), 1% Cocktail 2 and 3 (Sigma-Aldrich, Germany) was used to lysis of cells to extraction proteins. Kit Pierce BCA Protein Assay (Thermo scientific, USA) was used to determine protein concentration that reads the

absorbance at 540 nm with a spectrophotometer. Protein aliquots (50 µg) were denatured in the Laemmli buffer containing β mercaptoethanol prior to resolution by SDS polyacrylamide gel electrophoresis. The separated proteins were transferred onto PVDF membranes (Biorad, USA). After blocking the PVDF membrane with Tris base-buffered saline prepared with 0.1% Tween-20 containing 5% bovine serum albumin within 1 hour, the following primary antibodies against NRP-1 (#3725, Cell Signaling, 1:1000 dilution), NRP-2 (#32241, Novus Biologicals, 1:1000 dilution), CD133 (#130-090-422, Miltenyi Biotec, 1:500 dilution), CD15 (#14-0159, eBioscience, 1:1000 dilution), Sox2(#SAB5500176, SIGMA, 1:1000 dilution), NF-M (#2838, Cell Signaling, 1:1000 dilution), p-ERK (#9106, Cell Signaling, 1:2000 dilution), ERK (#9102, Cell Signaling, 1:1000 dilution), p-AKT (#9271, Cell Signaling, 1:1000 dilution), AKT (#9272, Cell Signaling, 1:1000 dilution), p-SMAD (#8828, Cell Signaling, 1:1000 dilution), β-tublin (#2128, Cell Signaling, 1:1000 dilution) and β-actin (#4970, Cell Signaling, 1:1000 dilution) were incubated overnight at 4°C. Quantification of relative band densities was performed using densitometer (LAS Imager FujiFilm) and β-actin or β-tublin was used as internal control.

Gene expression of phenotypic markers by quantitative PCR

To confirm the protein expression, the gene expression of Sox2, Oct4, Nanog, CD133 and CD15 (Table 2.1) for the differentiated cells and stem cells in medullospheres, as well as the impact of MR438 and Tuftsin, were analyzed by

quantitative reverse-transcription PCR (qRT-PCR). Reverse transcribed using the High Capacity cDNA RT Kit (Life Technologies). Total RNA was extracted with All Prep-DNARNA-Mini Kit (Omega). Reverse transcribed to cDNA was synthesized using the iScriptTM cDNA synthesis Kit (BioRad) with conditions of 25 °C for 5 minutes, 42 °C for 30 minutes, 85 °C for 5 minutes, and 12 °C forever. Quantitative PCR amplification was performed with SyberGreen PCR supermix (BioRad) using the CFX96 Real-Time System (BioRad). The qPCR conditions were 95 °C for 2 minutes and 39 cycles of 95 °C for 5 seconds and 63~68 °C for 30 seconds, the hybridization temperature was depended on primers. All values were normalized to RNA pol II and the $\Delta\Delta C_t$ method was used to estimate the fold change expression over control samples.

Table 2. 1: Sequences and annealing temperatures of primers used in qRT-PCR

Fwd: forward, Rev: reverse, Tm: melting temperature, pol: polymerase

Gene	Primer sequence (5'– 3')	Tm (°C)
CD133 Fwd	TCCGGGTTTTGGATACACCCTA	68
CD133 Rev	CTGCAGGTGAAGAGTGCCGTAA	
CD15 Fwd	AGGAGGTGATGTGGACAGCG	67
CD15 Rev	AACTACGAGCGCTTTGTGCC	
Sox2 Fwd	TTTCACGTTTGCAACTGTCC	63
Sox2 Rev	AGTCTCCAAGCGACGAAAAA	
Oct4A Fwd	ACCTGGAGTTTGTGCCAGGGTT	68
Oct4A Rev	CTCCCCTGCCCCCACCCTTT	
Nanog Fwd	GATGGGAGGAGGGGAGAGGA	68
Nanog Rev	TTTGGAAGCTGCTGGGGAAG	
RNA pol II Fwd	TGGGCAAAAGAGTGGACTTC	64
RNA pol II Rev	TTGAAGGGGGTGACAATCTC	

Expression of NRP-1 and CD15 by flow cytometry

Results of NRP-1 and CD15 expression were confirmed by flow cytometry. Cells were dissociated into single cell suspension and fixed with 4% paraformaldehyde and then permeabilized with 0.1% Triton X-100 for 15mins. Non-specific protein-protein interactions were blocked with 5% BSA-PBS for 1 hour at room temperature. The cells were then incubated 1 night with 1/200 dilution of primary antibody NRP-1 (EPR3113, ab81321, Abcam) and CD15 (SAB5500041, Sigma). Anti-rabbit FITC 488 diluted with 1/200 incubated for 1 hour was used as the secondary antibody. 1000 000 suspended cells in 500 μ L of PBS were detected by flow cytometry.

Statistical analysis

All results were given as mean \pm standard error of the mean (SEM). Nonparametric test was employed to determine the statistical significance using SPSS Statistics 5 (SPSS Statistics 19.0, USA) with a minimum of 3 repetitions. For all figures, $p < 0.05$ (marked by *) was considered significant and $p < 0.01$ and $p < 0.001$ were marked by ** and ***, respectively.

Results

Phenotypic characteristics of stem cell MB models

Three cell lines of MBs: DAOY, D283-Med and D341-Med were used *in vitro* to obtain medullospheres (MS) as MB stem cell models (Figure 2.2 A). They correspond to the subgroup SHH, subgroup 4 and subgroup 3, respectively (Northcott *et al.*, 2011, Snuderl *et al.*, 2013, Xu *et al.*, 2015). The medullospheres of DAOY were larger and more regular than the other two cell lines and reached a diameter of about 150 μm after a 72h culture period. These models were characterized by protein expression of stem cell markers which showed, as expected, an increase in the expression of cancer stem cell markers: CD15 for all 3 models and CD133 for D283 and D341 compared to the differentiated cells (Figure 2.2 B and C). A decrease of the neuronal differentiated phenotype marker, Neurofilament-M (NFM), was also observed for the cells obtained from medullospheres compared to the differentiated cells. Furthermore, because expressions of protein CD133 and NF-M for DAOY cells were very weak, we evaluated Sox2, another stem cell marker, which increased for the DAOY stem cells (Figure 2.3). These results were confirmed by qRT-PCR and showed an increase of gene level expression of CD15 and Sox2 for all models of MB stem cell and of CD133 for DAOY and D341 compared to their respective differentiated cells (Figure 2.2 D).

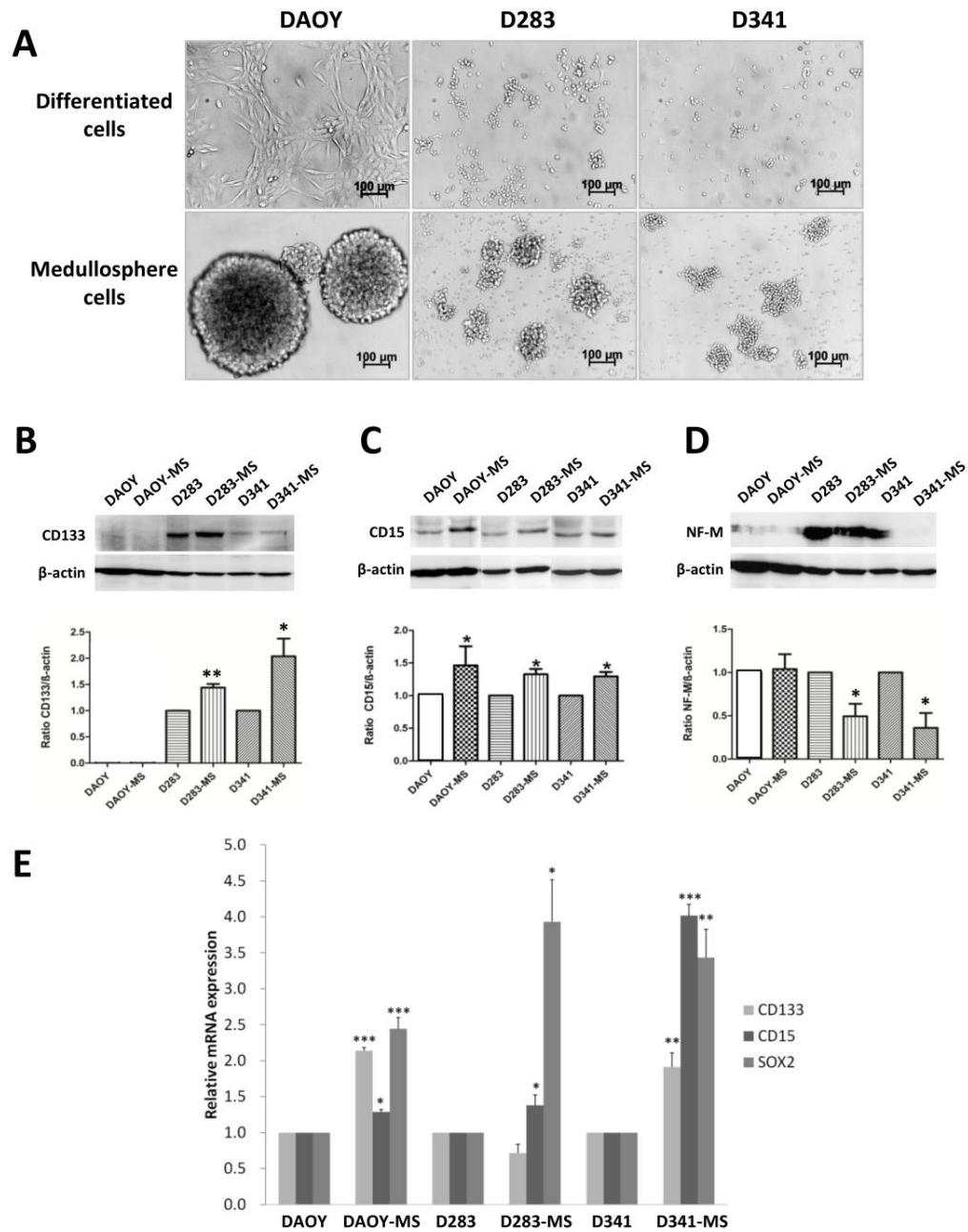


Figure 2. 2: Phenotypic proteins and transcripts expression of MB stem cells models. (A) Images of medullospheres obtained in serum free condition *in vitro* to enrichment of MB stem cells from cell lines: DAOY, D283-Med and D341-Med ($\times 40$ magnification, Bars:100 μ m). Expression of CD133 (B), CD15 (C) and NF-M (D) between differentiated cells and MB stem cells by Western blot were normalized by β -actin expression. (E) Gene expression of phenotypic transcripts of CD133, CD15 and Sox2 of differentiated cells and MB stem cells were normalized by RNA pol II expression. * $p < 0.05$, ** $p < 0.01$, *** $p < 0.001$, $n = 3$.

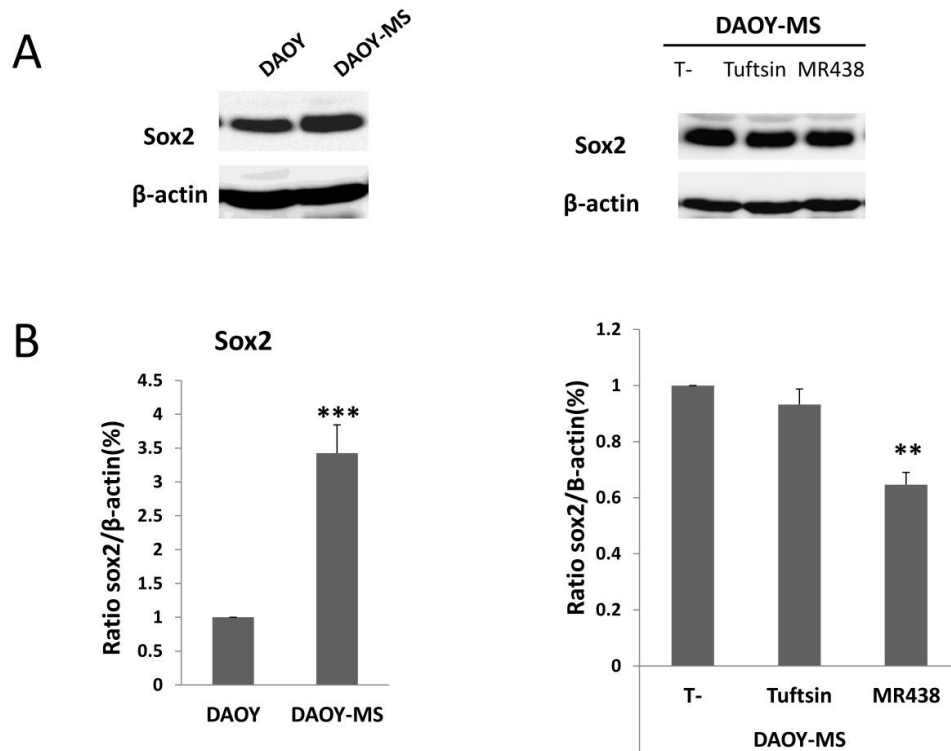


Figure 2. 3: Effect of MR438 and Tuftsin on expression of Sox2 for DAOY.
 (A) Representative images of expression of Sox2 for DAOY exposed to MR438 or Tuftsin by Western blot. (B) Ratio of Sox2 expression to β -actin protein for MB stem cells treated by MR438 or Tuftsin for DAOY. *p<0.05, ** p<0.01, n=3.

Protein expression of neuropilins by MB stem cell models

NRP-1 and NRP-2 play an important role in the development of neuronal and vascular systems. NRP-2 is a homologous protein that shares a sequence similarity of 44% in structural and biological properties with NRP-1 (Wild *et al.*, 2012). In our study, NRP-1 and NRP-2 were expressed by all cell lines of MB (Figure 2.4). Meaningfully, there was a significant increase in the expression of NRP-1 protein (120 kDa) by MB stem cells compared to differentiated cells. A decrease of NRP-2

expression was observed for D283 and D341 stem cells compared with the differentiated cells, which played a part as the competitive receptor of NRP-1.

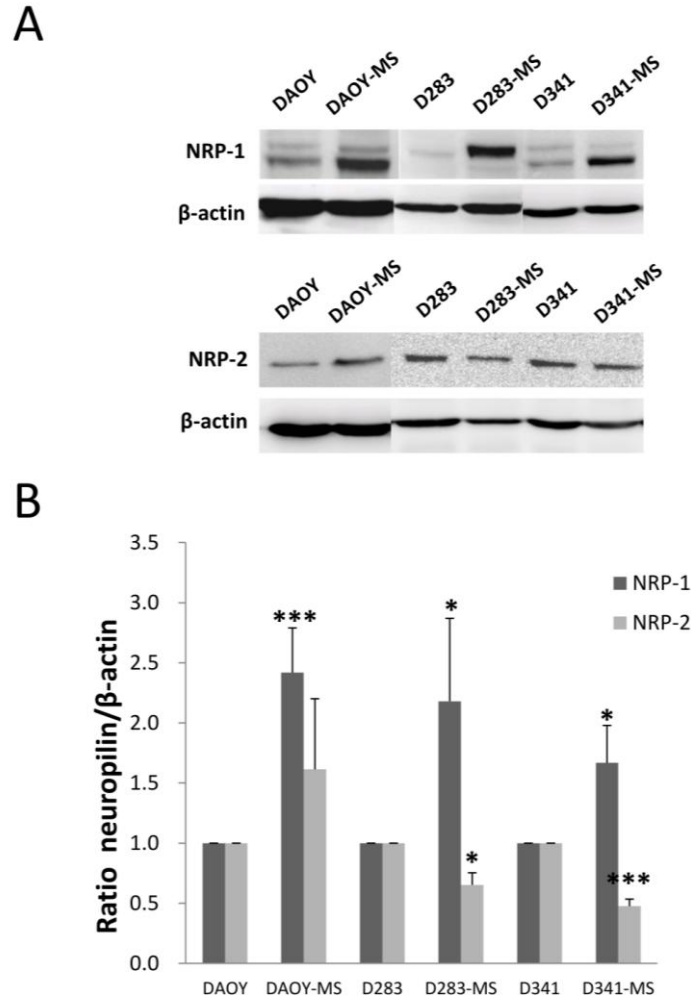


Figure 2. 4: NRP-1 and NRP-2 proteins expression of MB stem cell models of DAOY, D283 and D341 by Western blot.

(A) Representative results of expression of NRP-1 and NRP-2 for differentiated cells and MB stem cells. (B) Ratio of NRP-1 and NRP-2 expression to β -actin protein for differentiated cells and MB stem cells. * $p < 0.05$, *** $p < 0.001$, $n = 4$.

Effect of peptidomimetic MR438 on spheres formation and cell viability

To detect the short-term effects of these compounds on medullospheres, we evaluated the ability of sphere formation (number and diameter of spheres) as well as the cell viability after 72 hours of treatment (Figure 2.5). DAOY rapidly formed numerous large spheres in serum free condition contrary to D283 and D341, but MR438 or Tuftsin were not able to influence the cell ability to form spheres for all cell lines (Figure 2.5 A and B). In the same way, no significant difference was observed in cell viability for the different cell lines (DAOY-MS, D283 and D341-MS-MS) (Figure 2.5 C).

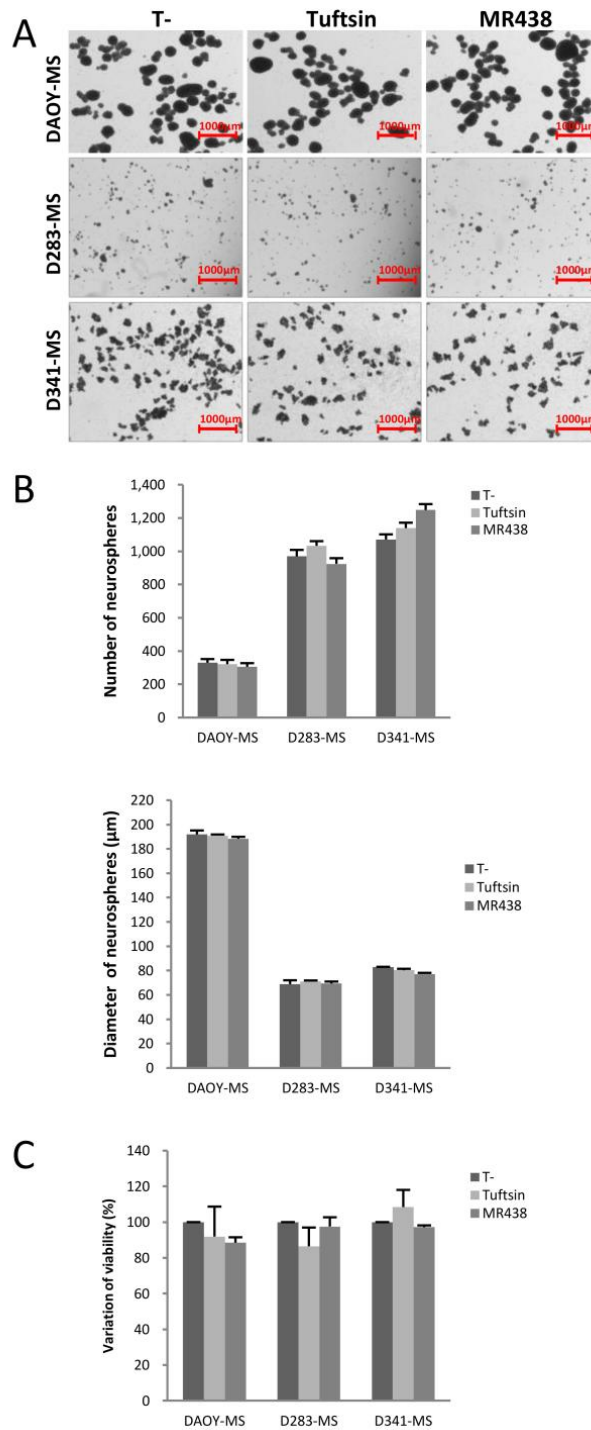


Figure 2. 5: Effects of MR438 or Tuftsin on cytotoxicity and on spheres formation for MB stem cell models of DAOY, D283-Med and D341-Med.

(A) Representative images of medullospheres from the different cell lines exposed to MR438 and Tuftsin evaluating the sphere formation ability (Bars:1000µm). (B) Effect of MR438 and Tuftsin on number and diameter of medullospheres. (C) Viability of cells contained in the medullospheres treated by MR438 and Tuftsin after 72 hours of exposition for three cell lines. MS: Medullosphere, $p > 0.05$, $n=6$.

Effect of peptidomimetic MR438 on self-renewal capacity

Self-renewal is the process by which stem cells divide to make more stem cells, perpetuating the stem cell pool throughout life. Self-renewal is division with maintenance of the undifferentiated state. Self-renewal programs involve networks that balance proto-oncogenes (promoting self-renewal), gate-keeping tumor suppressors (limiting self-renewal), and care-taking tumor suppressors (maintaining genomic integrity). The effect of MR438 on self-renewal capacity was assessed by using forming colonies assay (Figure 2.6). The number of MB stem cells (colony forming units) was statistically significantly decreased after adding NRP-1 targeting compounds for 72h, especially after exposition to MR438 peptidomimetic. We observed a reduction of about 25% for the colonies of DAOY stem cells and approximately 20 % of colonies of D283 and D341 stem cells. The colonies were divided into three groups according to their diameters: smaller than 75 μm (small clone), from 75 to 150 μm (normal clone) and higher than 150 μm (wide clone) for colonies of DAOY-MS and less than 50 μm , 50-100 μm and more than 100 μm for colonies of D283-MS and D341-MS (Figure 4 C). MR438 effects were mainly observed for wide colonies, especially for the DAOY cells, describing a mean reduction of 60% after MR438 exposition.

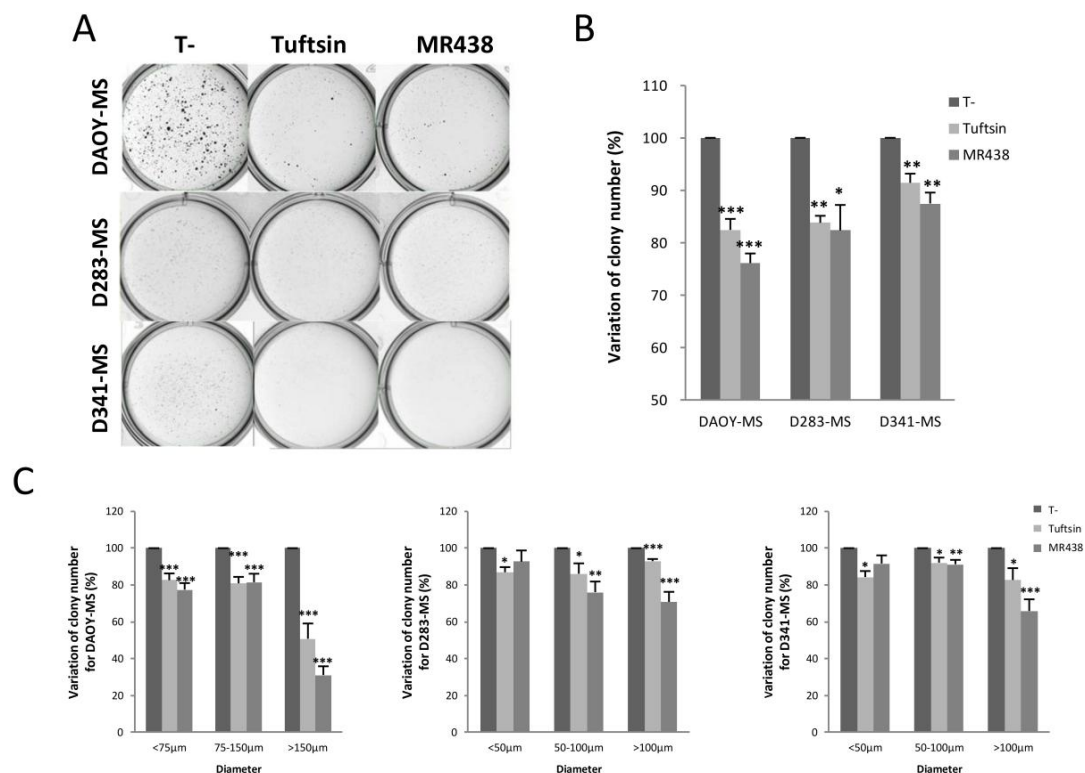


Figure 2. 6: Effects of MR438 or Tuftsin on self-renewal ability by clonogenic assay for DAOY, D283 and D341 stem cells.

(A) Representative images of medullospheres treated with MR438 or Tuftsin by clonogenic assay using methylcellulose culture medium for three cell lines: 2*10⁴ cells /well for DAOY-MS and 5*10⁴cells /well for D283-MS and D341-MS. (B) Ratio of colony number compared to control group. (C) Ratio of colony number compared to control group depending on different ranges of diameter for DAOY-MS, D283-MS and D341-MS. MS: Medullosphere, *p<0.05, ** p<0.01, ***p<0.001, n=6.

Effect of peptidomimetic MR438 on expression of neuropilins and phenotypic markers by western blot and qRT-PCR

After 72h of exposition to MR438, a statistically significant decrease of NRP-1 protein expression was observed for the 3 MB stem cell models (Figure 2.7, confirmed also by flow cytometry, see Figure 2.8). However, this compound did not

modify the protein expression level of NRP-2 (Figure 2.7 A and C). Otherwise, the influence of the compound on the expression of the phenotypic markers CD133 and CD15 and NF-M was measured by western blot analysis, demonstrating that MR438 reduced the expression of CD15 for the three cell lines (Figure 2.7), and decreased the expression of CD133 for D283-MS and D341-MS (Figure 2.7 D and E). Results of flow cytometry confirmed the decrease of CD15 expression after exposure with MR438 for all cell lines and related the same trend of NRP-1 (Figure 2.8).

Since CD133 protein was undetectable for DAOY-MS of the SHH subgroup MB, we used another stem cell phenotypic marker Sox2 (Becher and Holland, 2014) which showed an enrichment of Sox2⁺ cells and a decrease of Sox2 expression after exposure to MR438 by western blot (Figure 2.3). On the contrary, there was an increase in NF-M expression for DAOY-MS and D283-MS after exposure to MR438 (Figure 2.7 A and F). These results were confirmed by qRT-PCR. We observed that the mRNA expression of CD15 and CD133 decreased significantly for the 3 cell lines after treatment with MR438 except for CD133 mRNA of D283-MS cell line (Figure 2.7 G). Transcription factors Sox2, Oct4 and Nanog were also detected to supplement the impact of peptidomimetic on MB stem cells, whereas only a significant decrease of Sox2 for the D283-MS cell line was detected after the exposure to MR438 (Figure 2.9).

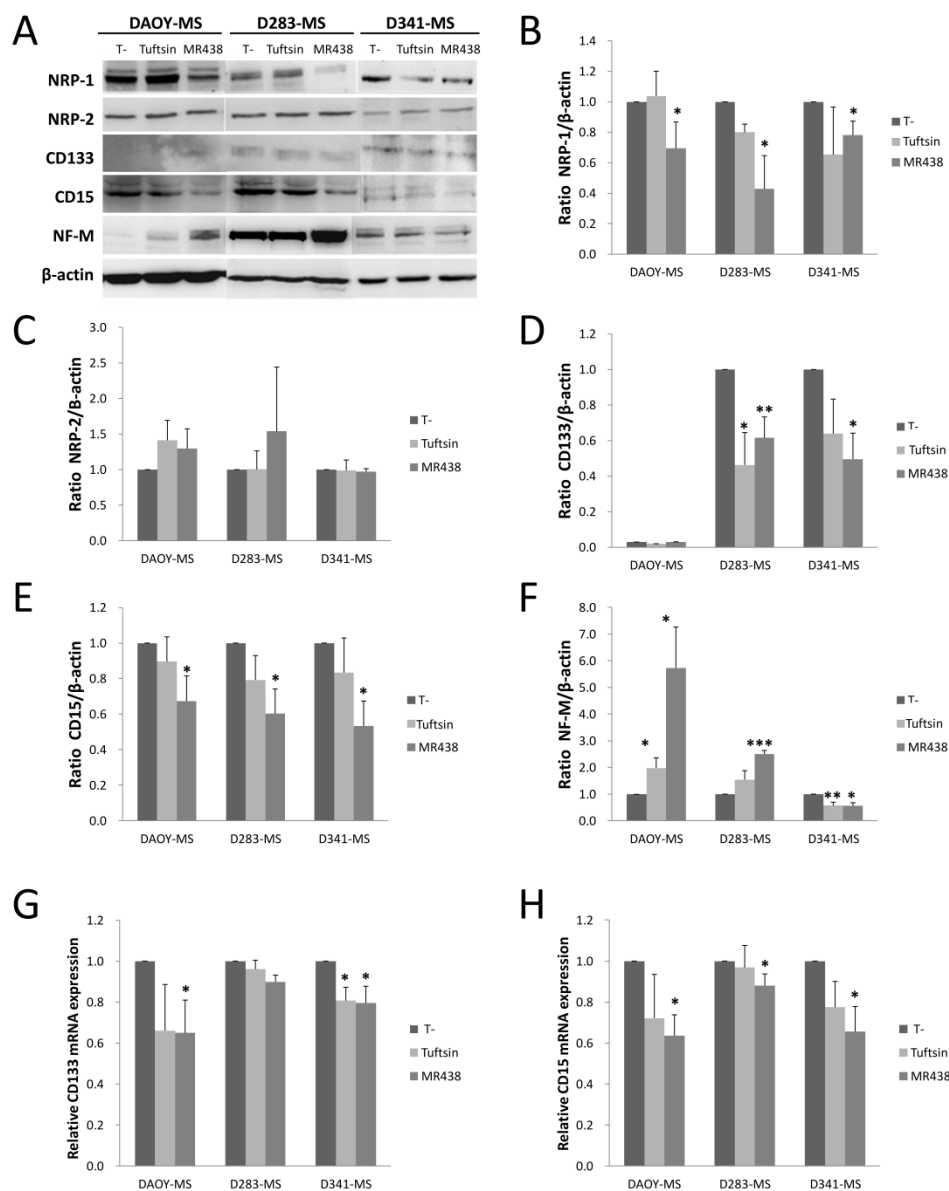


Figure 2. 7: Effects of MR438 or Tuftsin on proteins and transcripts expression of neuropilin receptors and stem cell markers.

(A) Representative blots of expression of neuropilins and phenotype markers for MB stem cells exposed to MR438 or Tuftsin by western blot. Ratio of NRP-1 (B), NRP-2 (C), CD133 (D), CD15 (E) and NF-M (F) protein expression normalized by β -actin expression for MB stem cells treated by MR438 or Tuftsin. Effects of compounds on mRNA expression of CD15 (G) and CD133 (H) for MB stem cells by qRT-PCR. *p<0.05, **p<0.01, ***p<0.001, n=3.

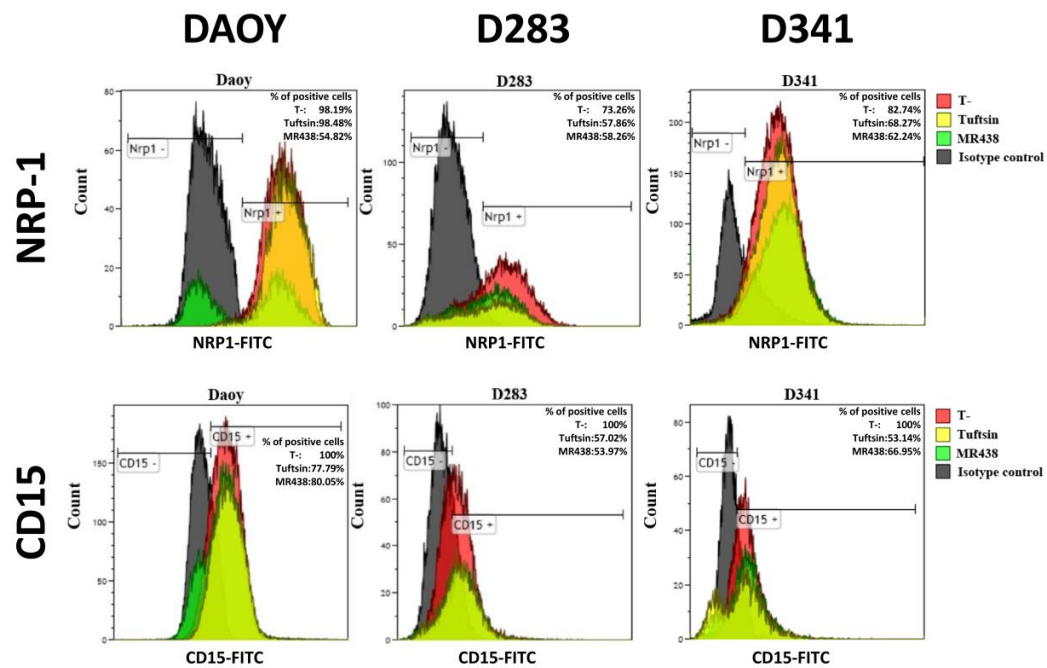


Figure 2. 8: Effect of MR438 or Tuftsin on expression of NRP-1 and CD15 by flow cytometry for the 3 MB stem cells models.

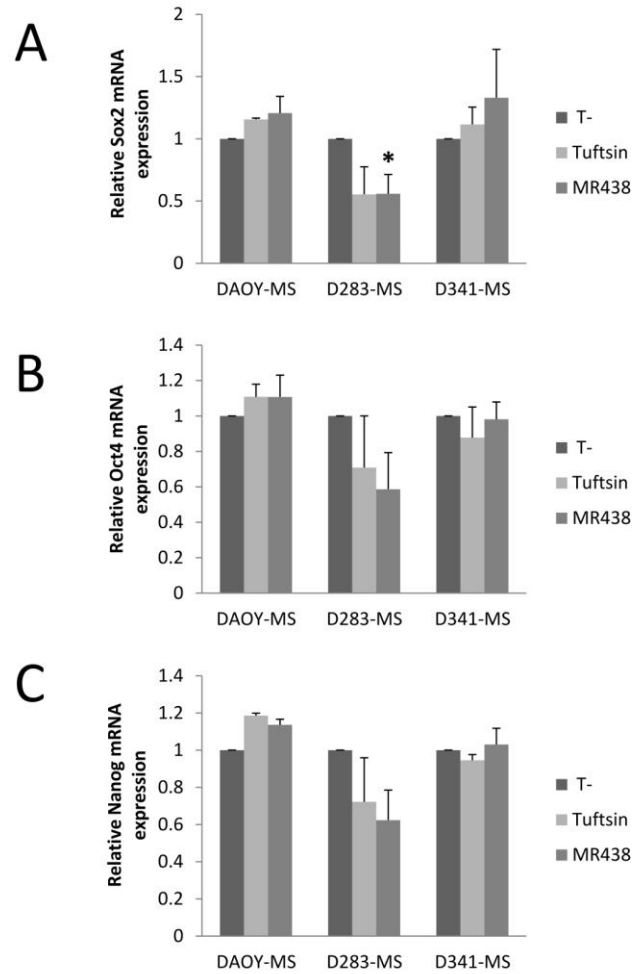


Figure 2.9: Effect of MR438 and Tuftsin on expression of transcripts by qRT-PCR: (A) Sox2 (B) Oct4 and (C) Nanog. * $p < 0.05$, $n = 3$.

Effect of peptidomimetic MR438 on invasive capacity of medullosphere cells

As NRP-1 is also involved in cell migration, we evaluated the effects of Tuftsin and MR438 on the invasive capacity of stem cells using the Boyden chamber model (Figure 2.10). MR438 induced a decrease in the capacity of invasion for MB stem cells derived from DAOY and D283 cell lines. Tuftsin is only able to inhibit invasion

for D283 cell line. It was not possible to perform the invasion assay for D341 cells due to the limitations of these cells to adhere to Matrigel® despite the use of chemoattractant factors in the bottom chamber (Figure 2.11).

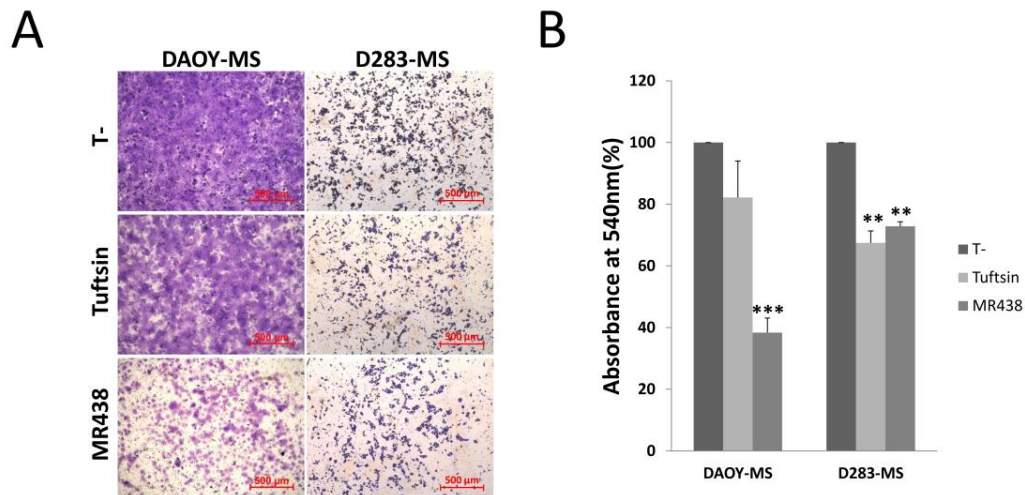


Figure 2. 9: Effects of MR438 or Tuftsin on invasive ability of MB stem cells derived from DAOY and D283 cell lines.

(A) Images of invasive cells exposed to MR438 or Tuftsin on the membrane surface of Boyden chamber (Bars: 500µm). (B) Ratio of invasive cells exposed to MR438 or Tuftsin compared with the no treated cells. ** $p < 0.01$, $n = 3$.

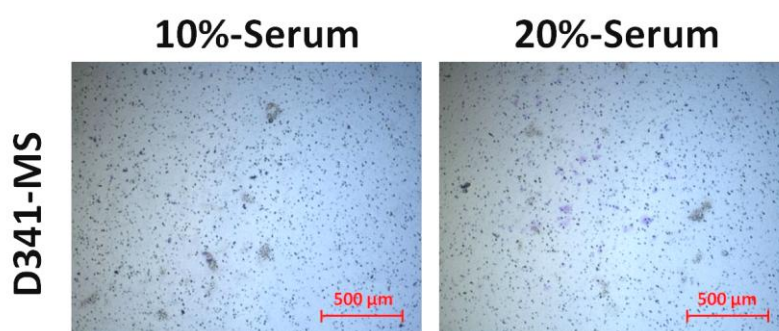


Figure 2. 10 : Invasive test for MB stem cells derived from D341 cell lines.

(A) Images of invasive cells culture with 10% and 20% serum to induce the cell invasive for D341-MS on the membrane surface of Boyden chamber (Bars: 500μm). Because of the suspension feature of this cell line, few cells could adhere to the membrane surface and detect the absorbance. n = 3.

Effect of peptidomimetic MR438 on the key proteins involved in the neuropilin pathways

The study of the main signaling pathways known to be regulated by NRP-1 was carried out by the analysis of the phosphorylation state of key proteins of each of the 3 signaling pathways PI3K/AKT, RAS/MAPK and SMAD (Figure 2.11). According to the activation state of the RAS/MAPK pathway, the expression of phospho-ERK1/2 showed a significant decrease for DAOY-MS cells after treatment with MR438 and Tuftsin compared to the untreated control (Figure 7AB). However, this difference in phosphorylation was not found for the 2 other models, probably because of a low level of expression of this protein (Figure 7A). Similarly, phosphorylated AKT expression also appeared to be significantly decreased for DAOY-MS cells after exposure to MR438 and Tuftsin, but no difference was observed for the two other cell

models (Figure 7AC). As for the signaling pathway of AKT and ERK, there was no difference in the expression of phospho-SMAD2/3 after treatment with Tuftsin or MR438 whatever the cell models. There is a trend of increase of phospho-SMAD2/3 expression after treatment with Tuftsin or MR438 for D341 cells (Figure 7AD).

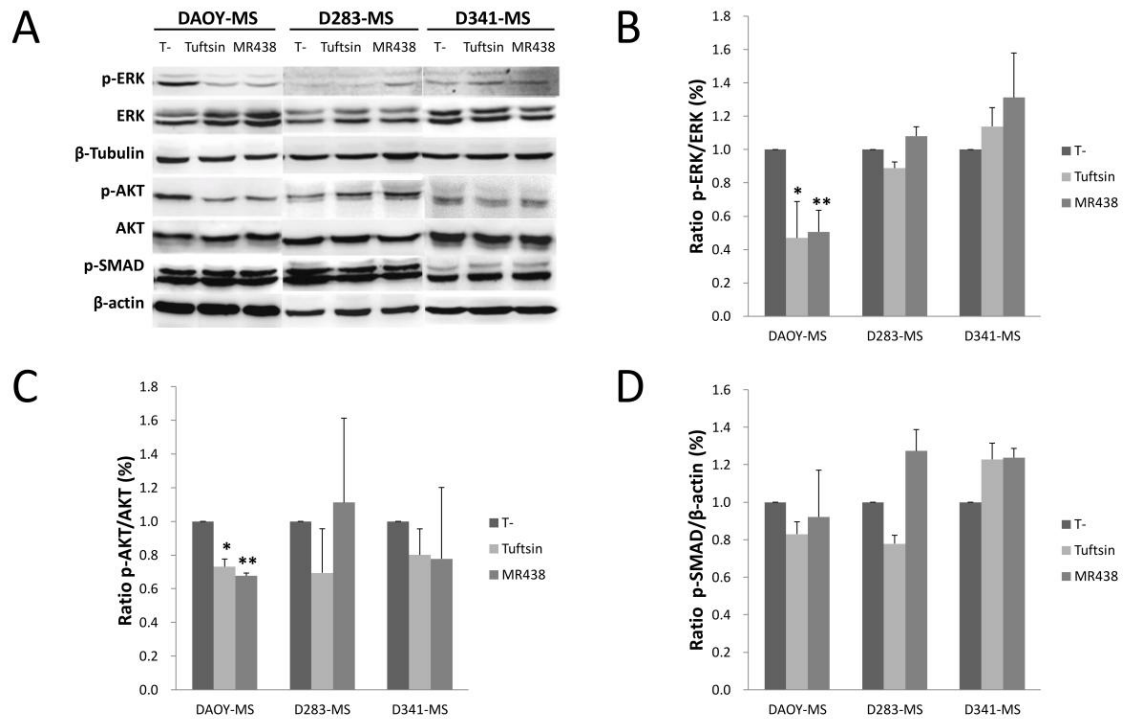


Figure 2.11: Effects of MR438 or Tuftsin on the key proteins involved in the neuropilin pathways. (A) Representative blots of p-ERK, ERK, p-AKT, AKT, p-SAMAD2/3, β-actin and β-tubulin by Western blot. (B) Ratio of p-ERK to ERK for MB stem cells treated by MR438 or Tuftsin. (C) Ratio of p-AKT to AKT for MB stem cells treated MR438 or Tuftsin. (D) Ratio of p-SMAD to β-actin protein for MB stem cells treated by MR438 or Tuftsin. *p<0.05, ** p<0.01, n=3.

Discussion and conclusion

A better understanding of the molecular characteristics involved in MB allowed to subdivide this pediatric brain tumor into four main molecular subgroups: WNT, SHH, Group 3 and Group 4, with different molecular characteristics and clinical outcomes and thus to consider new therapeutic approaches (Becher and Holland, 2014). The WNT and SHH groups were thus named in connection with signaling pathways which appear to play important roles in the pathogenesis of these subgroups. Subgroup 3 and 4 MB are related to a high incidence of metastasis and lead to a poorer prognosis. Thus, it is important to study as much as possible the therapeutic efficacy of new treatments on all the molecular subgroups of MB for a better understanding of this disease. Therefore, in our study, we analyzed the three most frequent used cell lines of MB: DAOY, D283-Med and D341-Med, corresponding to the subgroup SHH, subgroup 4 and subgroup 3, respectively (Snuderl *et al.*, 2013, Xu *et al.*, 2015).

NRP-1 is a single-pass transmembrane glycoprotein, which acts as a co-receptor by complexing with many transmembrane receptors such as VEGFR and Semaphorin receptor, or with TGF- β 1 receptor, as it has been more recently demonstrated (Wild *et al.*, 2012). NRP-1 is involved in cell survival and proliferation and has been reported to be over-expressed in various cancers and has been correlated with poor prognosis (Osada *et al.*, 2004, Jubb *et al.*, 2012, Chu *et al.*, 2014, Peng *et al.*, 2014). More recently, Snuderl *et al* found that MB patients with high NRP-1 expression level have a decrease of 50 % in survival. Moreover, targeting placental growth factor (PlGF)/NRP1 with monoclonal antibodies induced a direct antitumor effect in MB,

resulting in tumor regression, decrease of metastasis and increase of survival of mouse models . In the context of a peptide based approach, Tuftsin, a natural peptide produced by enzymatic cleavage of the Fc domain of the immunoglobulin G heavy chain, was found to bind specifically to NRP-1(Von Wronski *et al.*, 2006). However, Tuftsin is not an ideal agent for use in clinical practice because of several limiting points including size, stability (susceptible to degradation by peptidases), lack of effective methods for delivery, low oral bioavailability, rapid excretion and poor transport properties through biologic membranes (Vagner *et al.*, 2008, Recio *et al.*, 2016). Thus, we developed a novel peptidomimetic named MR438 which has been built by molecular modeling based on well-known A7R peptide (Bechet *et al.*, 2010, Richard *et al.*, 2016).

Recent studies report that CSCs are considered to be the origin of tumor proliferation and involved in the tumor recurrence because of their resistance to radiotherapy and chemotherapy (Eyler and Rich, 2008). CD133 is the most commonly used stem cell marker for the identification of brain CSCs (Singh *et al.*, 2004, Singh *et al.*, 2003), but it was also shown that CD15+ MB cells could recur and lead to poor prognosis in mouse models (Read *et al.*, 2009). Indeed, CD15 is a carbohydrate antigen that is expressed on both progenitors and stem cells in the embryonic and adult central nervous system and was recently considered as a marker of brain CSCs especially for Sonic hedgehog (SHH) MB subgroup cells (Read *et al.*, 2009, Ward *et al.*, 2009). As expected, our MB stem cells obtained in serum free conditions are characterized by overexpression of stem cell markers, in particular CD15 for DAOY stem cells (SHH subgroup) and CD133 for D283 cells (subgroup 4) compared to cell

lines cultured under classic conditions. Interestingly, *in vitro* enrichment of CSCs induced a NRP-1 overexpression for all cell lines, which is encouraging in a targeting strategy perspective applicable to different MB subgroups.

Nevertheless, the role of NRP-1 in the progression of MB is not clear, particularly in the behavior of MB stem cells. The dissemination of MB stem cells in hemato-meningeal space is a real clinical problem leading to metastasis occurrence and tumor recurrence (Garg *et al.*, 2017). Indeed, MBs are poorly differentiated tumors containing a large proportion of CSCs, so acting on their differentiation could also play an assisting role in the therapeutic management of MBs (Burger *et al.*, 1987). In our study, we have not observed early effects of NRP-1 targeting on cell viability nor on the ability of cells to form medullospheres. However, we observed a decrease in self-renewal capacity in the presence of MR438 and to a lesser extent in presence of Tuftsin indicating that CSCs probably enter in a differentiation way. This seems more efficient for SHH sub-group cells. Cao *et al* found that NRP-1 helps in maintaining an undifferentiated phenotype in renal cell carcinoma. The same authors showed that the knockdown of NRP-1 by short hairpin RNA reduced migration and invasion of renal carcinoma cells (Cao *et al.*, 2008) which was also found in our results with a decrease of invasion ability of MB stem cells after exposure to MR438. In the same way, it was recently shown that MiR-148a, a MiRNA which decreased NRP-1 expression, also inhibited invasion and tumorigenic potential of MB cells in the WNT subgroup (Yogi *et al.*, 2015).

Subsequently, we have endeavored to understand which signaling pathways of NRP-1 are preferably involved in the differentiation of MB stem cells. The precise

signaling pathways of NRP-1 action are still unclear as they interact with many cancer associated molecules. It has been demonstrated that overexpression of NRP-1 in cancer cells promotes tumor angiogenesis and stimulates cancer stem cell feature that depends on the complex NRP-1 / VEGFR-2 for the CD133(+) human glioma stem-like cells (GSCs) (Hamerlik *et al.*, 2012, Beck *et al.*, 2011). VEGFR and other VEGFR co-receptors of NRP-1 are involved in neoangiogenesis, tumor progression and differentiation by activating signaling pathways like PI3K / AKT, MAPK and SMAD. Thus, the most marked effect of MR438 as well as Tuftsin was the inactivation of PI3K / AKT and MAPK pathways for the SHH subgroup cells (DAOY). Frasson *et al* have also recently proposed that the most important pathway involved in cell differentiation of MB stem cells is the PI3K/AKT/mTOR pathway (Frasson *et al.*, 2015). Although TGF-beta-dependent SMAD signaling pathway did not appear to be disrupted in our study, Nissen *et al* reported that Tuftsin promotes Smad3 phosphorylation and reduces phosphorylation AKT by TGF-beta-dependent signaling pathway (Nissen *et al.*, 2013). In addition, we did not observe the effect of MR438 on the expression of SHH, although the expression of NRP-1 is known to activate the SHH signaling pathway (Hillman *et al.*, 2011). Other functions or roles of NRP-1 that are still unknown could explain the decrease in self-renewal capacity observed for the subgroups 3 and 4.

Essentially, by using models of MB stem cells, we found that inhibition of NRP-1 via the peptidomimetic MR438 seems to stimulate stem cell differentiation for different subgroups of MB, which can ultimately reduce the progression of MB, with an implication of the PI3K / AKT and MAPK signaling pathways for subgroup SHH.

The use of NRP-1 targeting molecules seems relevant to target MB stem cells, notably by promoting their differentiation. Further molecular studies could help us understand the involved mechanisms and we will confirm these results in the future in *in vivo* MB xenograft models.

Chapter 3:

**MR438 increases radiopotentialization
of medulloblastoma cells *in vitro* and *in vivo*
(Heterotopic xenografts models)**

Introduction

Radiotherapy (RT) is one of the most important effective therapies for MB, usually combined with surgical excision and chemotherapy (Siegel *et al.*, 2006). But they are mainly non-specific and aggressive to cause severe damage to the developing brain, especially for young patients, and there are still approximately one-third of patients died due to tumor recurrence (Smoll *et al.*, 2012). Strategies have therefore been proposed to try to reduce these sequelae by reducing the doses of RT combined with chemotherapy, by delaying the date of RT as much as possible or by reducing the irradiation fields in young children.

As the progresses of MB subgroup molecules, the potential for targeted therapy has provided a better understanding of tumor development. The role of targeted therapies is booming and the new treatments under study focus on the targeting of signaling pathways related to the main 4 molecular subgroups. WNT and SHH pathways were better studied (Remke *et al.*, 2013), while regarding to the poor prognosis and high risk recurrence in subgroup 3 and 4, it is also urgent to find new therapies especially in patients with high level of MYC amplifications related with the prognosis of MB. Some molecular inhibitors of MYC have been proposed, some of which are in early clinical trials (Lin *et al.*, 2010). Inhibition of effectors downstream of MYC corresponds to potential therapeutics, and it has recently been shown that BET specific inhibition of MYCN is effective in preclinical models of neuroblast (Puissant *et al.*, 2013). But other study found that c-MYC expression has no impact

on response in primary MB patients between samples of responders and non-responders with treatment (Von Bueren *et al.*, 2011).

Except the invasive and metastatic nature of MB to give rise to recurrence, tumor heterogeneity is recently considered as the important prognostic factor, which indicates that a small special cell population exists which could survive after radio-chemotherapy and due to recurrence. Recently, it has been suggested that the cancer stem-like cells (CSCs) are probably the origin of the tumorigenesis and may be involved with resistance to therapy and recurrence (Bao *et al.*, 2006). In MB CSCs, Blazek *et al.* found the same results that CD133+ MB cells were more radioresistant compared with CD133- cells (Blazek *et al.*, 2007). The identification of new molecular target specific for MB stem cells is a major challenge to improve the management of this pathology.

Our previous work in chapter 2 showed NRP-1 was related with the undifferentiated statut of MB and a novel NRP-1 inhibitor (MR438) stimulated the differentiation of MB stem-like cells. As the CSCs are related with radio-resistance, the differentiation induced effect might enhance the effective of RT with MR438 as the radiosensitizer, in order to decrease the tumor growth and control recurrence with a lower dose of RT. In this chapter, we test the effect of this peptidomimetic MR438 with RT *in vitro* to treat the 3 subgroup MB stem-like cells (DAOY, D283-Med and D341-Med) and confirm the results *in vivo* with heterotopic xenografts nude mice.

Materials and methods

Cell culture and drug solutions

The same MB cell lines of DAOY, D283-Med and D341-Med (Described in the chapter 2) were used in this chapter. MB stem like cells cultures were maintained in DMEM/F12 medium (GibcoUK) containing the same conditions of B27, N2, EGF, β FGF, heparin and insulin. After a 3-days culture in hydrophobic flasks at 37 °C with 5% CO₂ in a humidifier atmosphere, spheres were obtained. MB stem like cells were dissociated from spheres using Accumax (Gibco, Life Technologies Corporation, UK) and seeded in 25 cm² flasks depending on the experiment (Figure 3.1).

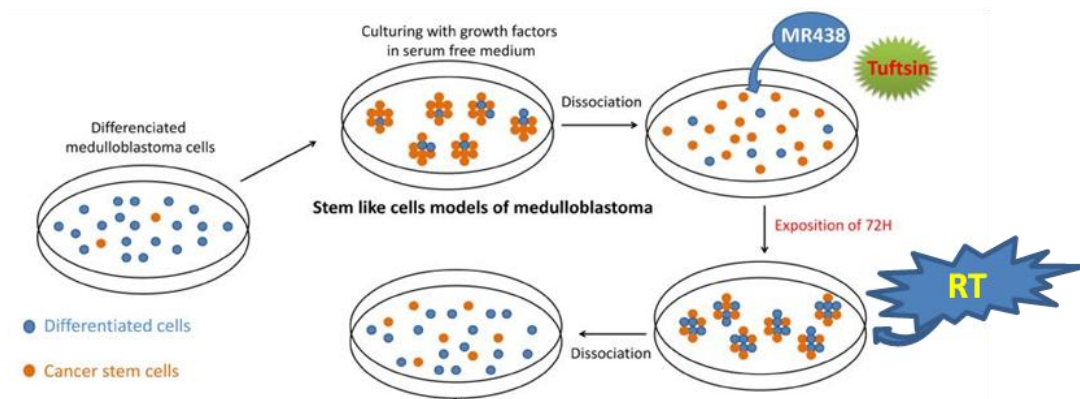


Figure 3. 1 :Scheme of experimental procedures to evaluate the irradiation effects on MB stem like cells models *in vitro*.

The same cells were used in this part and were exposed to MR438 and Tuftsin during 72H before irradiation, then clonogenic survival assays were realized 1 hour after RT.

For *in vitro* experiments, the stem like cells were exposed to MR438 (Molecular weight: 527.20 g/mol, supplied by the L2CM-UMR 7053 in powder form) and Tuftsin (Molecular weight: 500.60 g / mol, BACHEM, Switzerland) at 25 μ mol/L during 72h. MR438 and Tuftsin were each dissolved in PBS and stored in aliquots at -20 °C. For *in vivo* experiments, nude mice flank xenografts were treated with MR438 and Tuftsin (10mg/kg; D1 and D3; 2h pre-RT), and/or radiation (RT; 2 Gy/fraction; D1–D5) for one cycle as illustrated in the figure 3.3.

Tolerance assays *in vivo*

MR438 has no cytotoxic effect *in vitro* as described above in chapter 2, but should be also tested *in vivo* to confirm that. The compound was diluted in a physiologic serum (NaCl 0.9%, Virbac, France) to administrate the dose of 1 mg/kg or 10 mg/kg to act on the healthy nude mice. The mice were injected with MR438 at D1 and D3 (Figure 3.2), and followed by collecting blood sample 2 hours post injection by mandibular vein (200 – 250 μ l of blood). For all blood samples, we extracted the serum by collecting the blood within 15 μ L heparinized solution (0.5 UI/ μ L). Serum was extracted by centrifugation and kept at -70 °C for the detection of MR438 molecule by HPLC analysis. The injected animals were followed for 14 days post-injection by applying an observation score and weight measurement as mentioned in animal preparation section (Table 3.1). After sacrifice by Pentobarbital overdose administration, we dissected the animals to recover the vital organs (brain,

heart, liver, spleen, gut, kidneys, adrenal glands and lung) for macroscopic and microscopic observations.

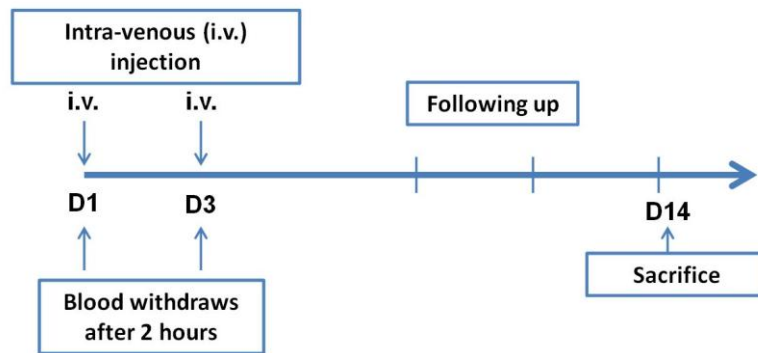


Figure 3. 2: Timeline of the MR438 tolerance assay.

Intra-venous (i.v.) injection at D1 and D3 and blood withdraws after 2 hours. D1:Day1;
D2:Day2

Table 3. 1: Evaluation score* followed up for tolerance assay

Observations	Distinctive signs	Pain score
Apparence	Vocalization	1
	Excess porphyrin (eyes and muzzle)	2
	Eyes and hollow abdomen	2
	Irritation back with slight flow	3
	Self harm	3
	Round or arched back	4
Respiration	Coughing, sneezing, runny nose	3
	Altered breathing a little jerky	3
	Difficult breathing (apnea and dyspnea)	5
	Convulsion	6
Behavior	Isolation / low displacement	2
	Absence of curiosity	2
	Altered behavior: jumps, goes around in circles constantly	3
	Tremor / Myoclonus	3
	Immobility and prostration in a corner of a cage	4
	Limb claudication	6
Thinness	Thin animal in weight loss	2
	Very thin animal / prominent bones	4
	Anorexic animal / no adipose tissue + prominent bones	6
Tumor size	Growth of a mass: Abscess / cyst / tumor <5mm	4
	Abscess / cyst / tumor > 5mm	6

*Score <5: Carefully monitor the evolution of symptoms on the animal, isolate it as needed.

Score 5~10: Undertake an action to relieve the animal, immediate analgesic medication.

Score > 10: Immediately consult the person responsible for the animal welfare structure to make a quick decision on the future of the animal.

Score > 15: The complications are too important, the last limit point is reached. Put the animal to death immediately to stop the suffering.

Animal models

Heterotopic xenograft models of MB stem like cells in immunodeficient mice (NMRI-nu, Janvier Labs, France) were used in this study within the agreement of the

French Minister of Research (agreement n° APAFiS #8731 MR438 evaluation). The stem like cells of DAOY, D283-Med and D341-Med were re-suspended in PBS, mixed 1:1 with Matrigel (BD Biosciences). The cells (2×10^6 cells/200 μ L) in 50% Matrigel were injected subcutaneously into the right and left flanks of 6 week old female nude mice. When tumors reached a volume of 1000 mm³, the tumors were divided into small pieces of 2-3 mm³ and re-planted subcutaneously in the inguinal region near the femoral vessel of mice. When palpable tumors reached a volume of 250 mm³, the mice were subjected to radiation as described below. Tumor size was monitored every 2 days by measuring two dimensions and the volume was calculated by calculating $(\text{length} \times \text{width}^2)/2$ and tumor growth was normalized by taking tumor volume at the start of treatment as a reference. The mice were followed at least 60 days or the tumor size reached approximatively 1500 mm³ (end point), and mice were euthanized and the tumors were harvested for the other experiments.

Irradiation

RT was performed using a Xrad 320 Irradiator (Precision X Ray, USA). For RT *in vitro*, cells located in the flask were exposed in 15x15cm² radiation field with the dose of 0, 2, 4, 6, 10 Gy at room temperature. Cells of each dose were given treatment of MR438 and Tuftsin (25 μ M) during 72 hour before RT. Following irradiation, all samples were returned to a 5% CO₂ incubator and maintained 1h for colony formation assay. For tumor RT *in vivo*, animals were anesthetized with a mix of xylazin / ketamin (90 et 8 mg/kg, respectively) and positioned such that the apex of each flank tumor was at the center of a 3x3cm² radiation field, with the rest of the

mice shielded from radiation by using the protecting baffle (Figure 3.3). Tumors were exposed with RT at the dose of 2 Gy by fraction during 5 days (D1–D5) with/without MR438 or Tuftsin administration. Molecular treatments carried out 2 hours before RT with 2 I.V. administrations at D1 and D3 (10mg/kg).

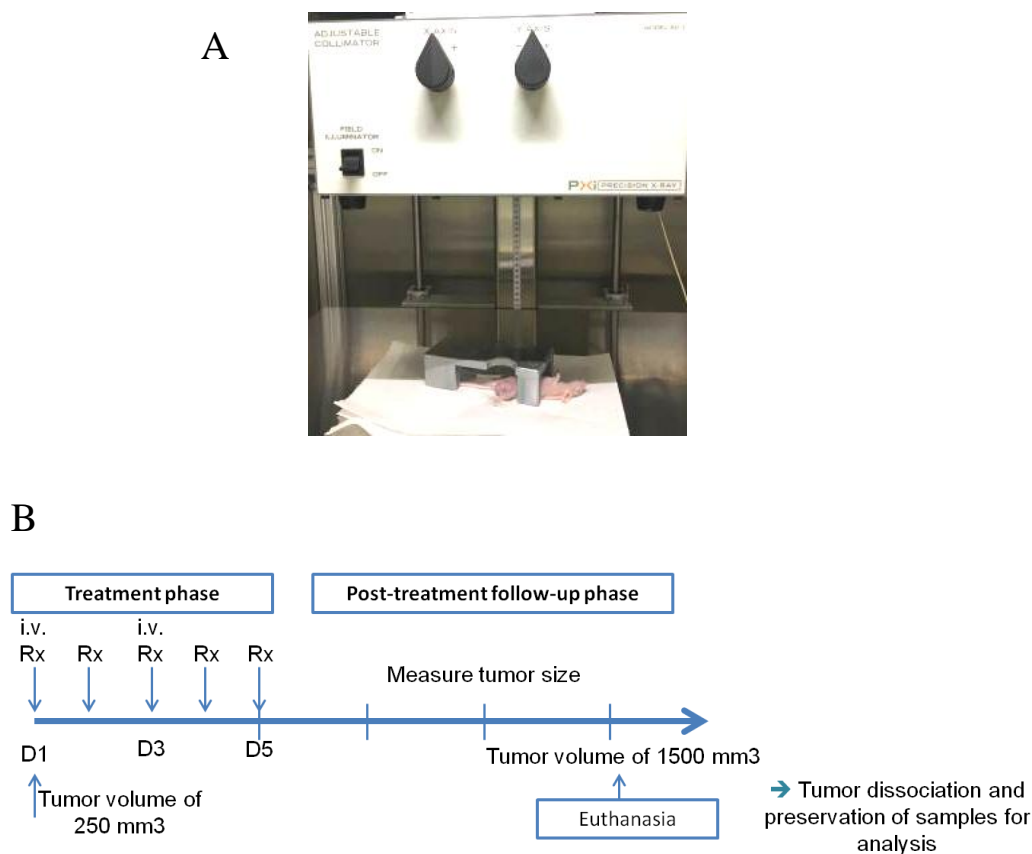


Figure 3. 3: Irradiation schedule for heterotopic xenograft nude mice.
(A) Irradiation position in irradiator and (B) treatment schedule for heterotopic xenograft nude mice.

Tumor dissociation

When the tumor volume reached 1500mm^3 , mice was sacrificed and tumors were harvested for dissociation. A part of tumor was separated into $1\text{-}2\text{ mm}^3$ small pieces, and digested 75mins in 7.65 ml dissociation buffer including HBSS (6mL, Hank's Balanced Salt Solution , Sigma, USA), collagenase type IV (0.6 WU / mL, Gibco, USA), Dispase II (1mg/mL, Sigma, USA), DNase I (200 U / mL, Roche, Germany), CaCl_2 ($75\mu\text{M}$) and MgCl_2 ($125\mu\text{M}$). Buffer DNase I (200 U/ mL) was then used to remove DNA interference with other living cells so that the cells do not aggregate easily. Cells were re-suspended in HBSS after eliminate the red blood cells by lysis buffer of NH_4Cl (0.15M), KHCO_3 (10 mM), EDTA ($100\text{ }\mu\text{M}$). Cell suspension then rapidly stained with the same volume of 0.4 % trypan-blue solution and deposited in counting chamber slides (TC20, Biorad). The number of surviving cells was counted twice before the cells seeding for the experimentations of WST-1 and clonogenic assay.

Clonogenic assay

After exposure of MB cells to MR438 or Tuftsin with or without RT, cells *in vitro* were re-suspended and tumors *in vivo* were harvested for dissociation. Clonogenic formation assay using 1% methylcellulose was done. Briefly, MB cells (*in vitro*: 20 000 cells / well for DAOY-MS and 50 000 cells / well for D283-MS and D341-MS; *in vivo*: 100 000 cells / well for DAOY-MS and 200 000 cells / well for D283-MS and D341-MS) were suspended in 2 ml of DMEM/F12 containing 1%

methylcellulose (SIGMA, USA). The cell suspension was then plated onto 6 well-plates and allowed to grow for 8-12 days. Colonies were incubated with 0.5% MTT solution (Thiazolyl blue tetrazolium bromide, 98%, Acros Organics™) and colonies larger than 30 µm in diameter were quantified using GelCount™ (Oxford Optronix, UK). Each experiment was repeated 6 times with 3 independent wells.

Sphere formation and Stem cell survival assay

After dissociation of the tumors, cells were seeded in 6 wells plates at a density of 100 000 cells/mL for DAOY-MS and D341-MS and D283-MS. The number of neurospheres larger than 30 µm was quantified using GelCount™ (Oxford Optronix, UK) to count the number of spheres and to evaluate the efficacy of medullosphere formation. Each experiment was repeated each time according to the number of mice with 3 independent wells. Cells after different treatments were plated at same concentration with 200 µL of suspended cells in 96-well plates. Cells were cultured for 72 h and then cell viability was measured by WST-1 (Roche, Germany) assay according to the recommended protocol. Absorbance at 450 nm of the solution was read by using a spectrophotometer (France). Each test was performed with 6 repeats. The viability of MB stem like cells was evaluated by automated cell counter TC20 (Biorad, France) using the trypan blue exclusion assay at the same condition of cell density like sphere formation assay. Cell suspension then rapidly stained with the same volume of 0.4 % trypan-blue solution and deposited in counting chamber slides

(TC20, Biorad). The percentage of surviving cells was counted twice and experiment was repeated 6 times.

Histological analysis

All vital organs and tumors have been collected and kept within the 4% formaldehyde solution for 48 hours (one week for brains). Then samples were transferred into inclusion cassette within 70% alcohol solution. The cassettes were transferred to an automated dehydration machine (HISTO-PRO 300) over night for paraffin inclusion. Microtome (LEICA RM 2135) was used to cut the paraffin blocks in 5 μ m thick slices. Then, the sections were fixed over the slides for staining step. Staining step was achieved either by a manual procedure or an automated machine with fixed protocol. H&E staining was used for microscopic observations. About the immunohistological assays, samples were incubated with primary antibody Vimentin (Abcam, monoclonal V9, IgG1, dilution of 1/16000) and NRP-1 (Abcam, ab81321, dilution of 1/400) to detect the presence of human cancerous cells of MB. Nikon Eclipse E600 equipped with a camera microscope (Nikon-DS Fi1) was used to take pictures and Nis – Elements AR 3.2 software used to analysis the histological samples slides.

Statistical analysis

All results were given as mean \pm standard error of the mean (SEM). Nonparametric test was employed to determine the statistical significance using SPSS

Statistics 5 (SPSS Statistics 19.0, USA) with a minimum of 3 repetitions. For all figures, $p < 0.05$ (marked by *) was considered significant and $p < 0.01$ and $p < 0.001$ were marked by ** and ***, respectively. For *in vivo* experimentations, the time growth of tumors to reach 1500mm^3 (set end point) served to build the Kaplan-Meier curves.

Results

Effect of MR438 *in vitro* on radiosensitivity of cancer stem like cells

The effect of MR438 on radiosensitivity was assessed by using colony formation assay (Figure 3.4). *In vitro* experimentations, cells were treated by Tuftsin and MR438 during 72 hours before RT. After irradiation with 0, 2, 4, 6, 10 Gy for different groups, spheres were dissociated to process for clonogenic survival. For the cells of DAOY-MS, the number of colonies was significant decreased after adding the NRP-1 targeting compounds at 2 Gy, especially after exposition to MR438 peptidomimetic (Figure 3.4 A C). D283-MS cells are more sensitive to radiation than the DAOY-MS cells. They could benefit the improvement of radiosensitivity at 2 Gy and 4 Gy after exposition to Tuftsin and MR438. D341 cells were the most sensitive to irradiation than the other 2 cell types, but MR438 still have an increase of D341 radiosensitivity at 2 Gy. As 2 Gy is the clinical wide used fraction dose, it is interesting to observe a reduction of about 25% of DMF2 (Dose modified factor at 2 Gy) for DAOY and approximately 10 % for D283 and D341 stem cells (Figure 3.4 B).

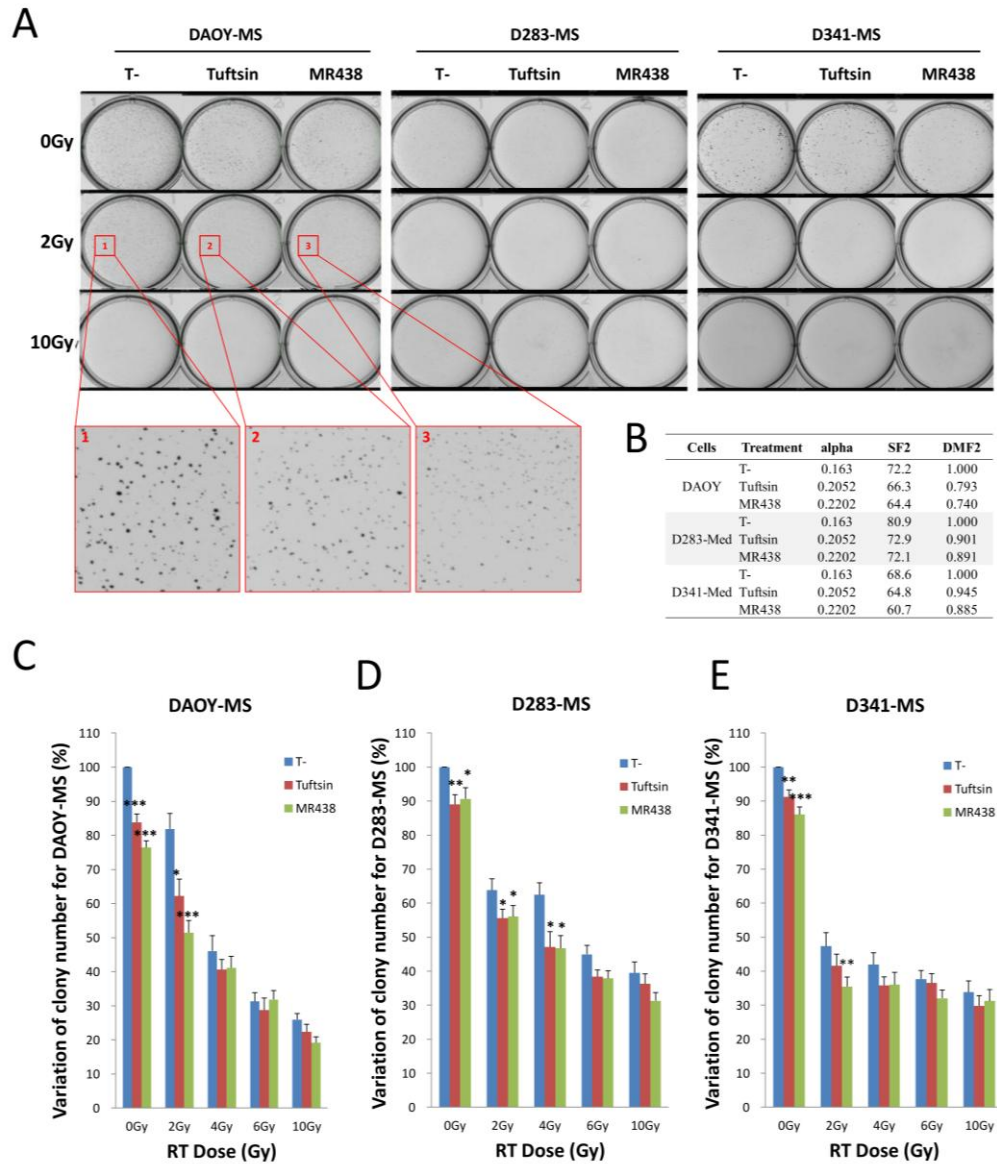


Figure 3. 4 : Effect of MR438 on tumor radiosensitization for cancer stem like cells of MB *in vitro*.

(A) Representative images of colony formation assay using methylcellulose was done for the 3 cell lines treated with Tuftsin and MR438 at 0, 2 and 10 Gy (1×10^5 cells /well for DAOY-MS and 2×10^5 cells /well for D283-MS and D341-MS). (B) Tumor radiosensitivity factors of SF2 and DMF2 changed after exposition to peptidomimetics. (C, D, E) Ratio of colony number compared to control group. MS: Medullosphere, SF2: Surviving fraction at 2 Gy, DMF2: Dose modified factor at 2 Gy, * $p < 0.05$, ** $p < 0.01$, *** $p < 0.001$, $n = 6$.

Tolerance and blood levels assays of MR438

Animals were divided into two concentration groups: 1 mg/kg and 10 mg/kg (Table 3.2). The MR438 was injected two times at Day 1 (D1) and Day 3 (D3) as represented by the timeline presented previously at Figure 3. 2. None of the mice within different groups developed a severe adverse effect during our follow up observation. Only one animal (ID:17S077) had a weight loss at the end point of approximately 10% probably due to a large hematoma after the blood collection procedure. There are no abnormalities represented by our macroscopic and microscopic observation of dissected organs after sacrifice (Figure 3.5 and Figure 3.6).

Table 3. 2 : Animals tested with two doses of MR438: 1 mg/kg and 10 mg/kg.

<i>Mice ID</i>	<i>Dose</i>	<i>1st injection weight(D1) (g)</i>	<i>2nd injection weight(D3) (g)</i>	<i>Intermediate weight(D7) (g)</i>	<i>Sacrifice weight (g)</i>	<i>Difference of weight(g) (g)</i>	<i>Follow up score</i>
17S076	1mg / kg	29,3	30	28,30	27,6	-1,7	0
17S077	1mg / kg	28	29	25,50	24,4	-3,6	0
17S078	1mg / kg	31,7	32,5	31,30	31,2	-0,5	0
17S098	10mg / kg	30	30	30,10	30,1	0,1	0
17S099	10mg / kg	29	29	29,90	31	2	0
17S100	10mg / kg	30	29	30,90	31,2	1,2	0

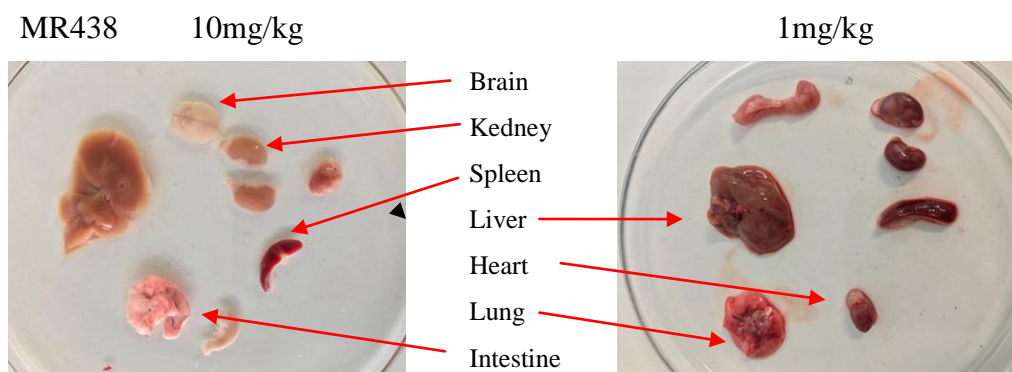


Figure 3. 5: Macroscopic view of dissected organs from a mouse of 10mg/kg group and 1mg/kg group: brain, liver, kidneys, adrenals, heart, spleen, lung and gut.

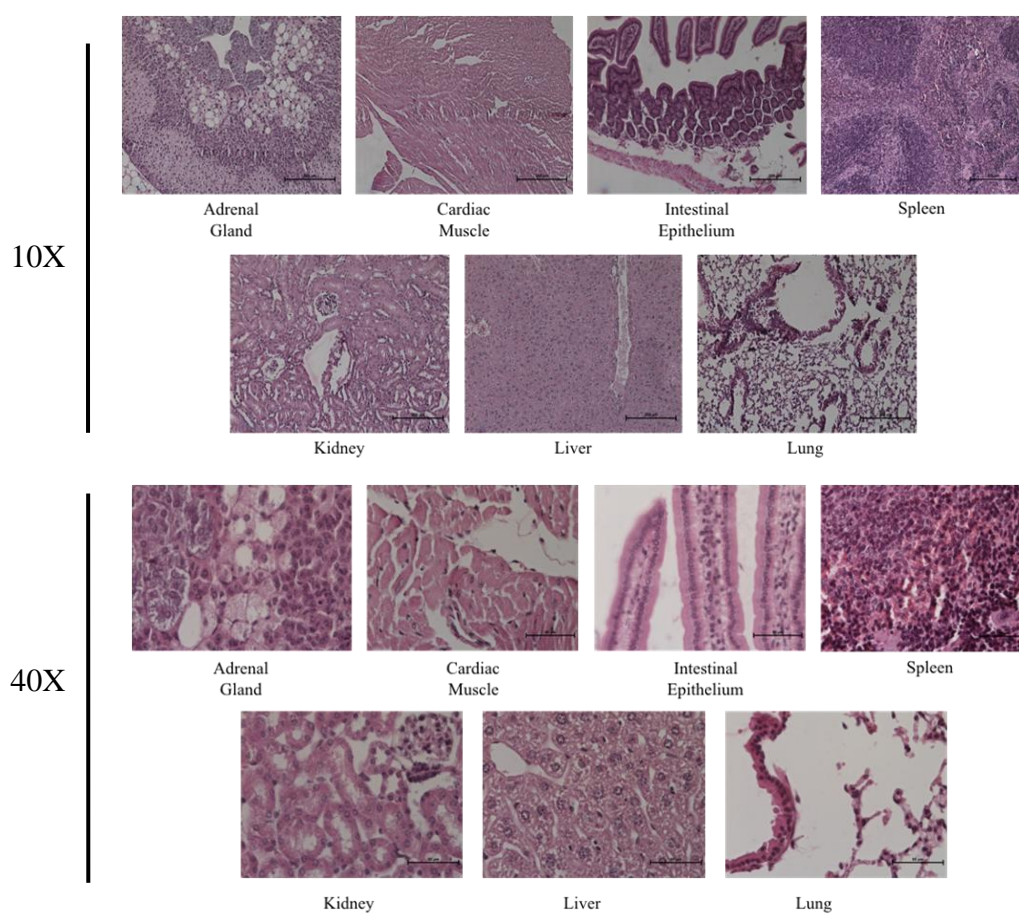


Figure 3. 6 : Microscopic views of different organs from mice treated with MR438.
Dose of 10 mg/kg was used for this group, slides stained by H&E stain at x40 (Image scale: 200 μ m) and x40 (Image scale: 50 μ m) were showed.

Despite detectable signals for concentrations of MR438 from 1 μ M until 500 μ M in plasma controls, MR438 blood level 2 hours post injection at the dose of 1 and 10 mg/kg (corresponding approximatively to 25 and 250 μ M in blood volume) was not detectable by High-Performance Liquid Chromatography (HPLC) (Figure 3.7).

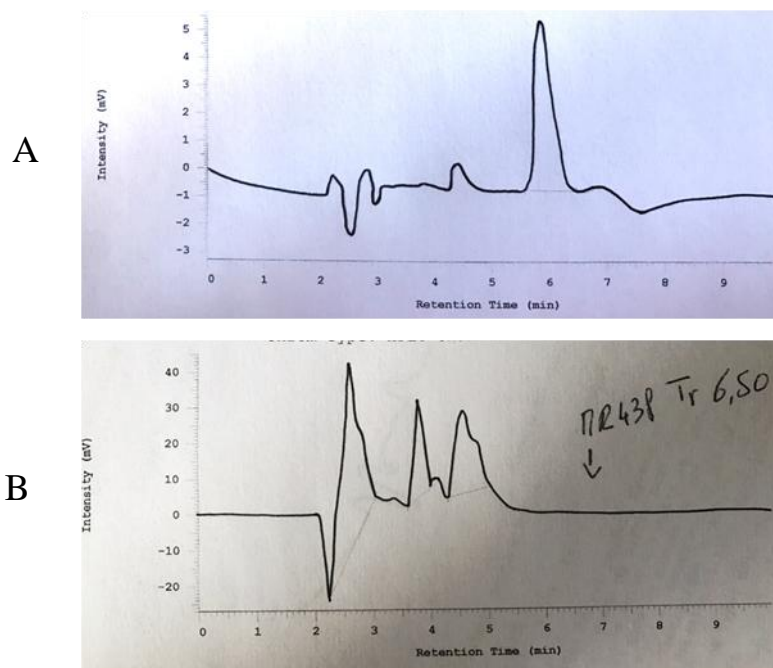


Figure 3. 7: High-performance liquid chromatography (HPLC) reading graphs for detecting the presence of MR438 molecule in the serum 2 hours post injection at the dose 10 mg/kg.

(A) Positive control graph where the signal of MR438 appears between 5,5 and 6,5 min. (B) The graph for the experimental analysis

Effect of MR438 on tumor growth following irradiation *in vivo*

Based on the results of our previous work (Gong *et al.*, 2018) and of radiotherapy *in vitro*, heterotopic xenograft models of immunodeficient mice were used to confirm whether the MR438 could also improve the radiosensitivity of MB *in vivo*. After at least 60 days of follow-up (Figure 3.8), we found that MR438 and Tuftsin alone have no significant effect on tumor growth for the DAOY and D341-Med tumors, but it seems to have a slight delay of growth with Tuftsin or MR438 for

D238 tumors. When combined with RT, MR438 decreased the tumor growth of DAOY model compared to the RT alone or RT+Tuftsin (Figure 3.8, $P < 0.05$). The ratio of radiopotentialization calculated with this data is 1.857 for MR438+RT. The average times of tumors achieved the endpoint volume (1500 mm^3) for DAOY were 27, 29, 27, 55, 60, 79 days for the groups of control, Tuftsin, MR438, RT, RT+Tuftsin and RT+MR438, respectively (Figure 3.9). Mice with tumor of DAOY benefited 24 days delay of endpoint volume ($P < 0.05$) when RT associated with MR438. Tumors of D283 and D341 are more sensitive to fractionned irradiation at the beginning of treatment as expected by *in vitro* results, combination of RT with MR438 seems to have less improvement of radiosensibility with the results of survival analysis. However, for tumor of D283, MR438 alone played a signifitive decrease of tumor growth.

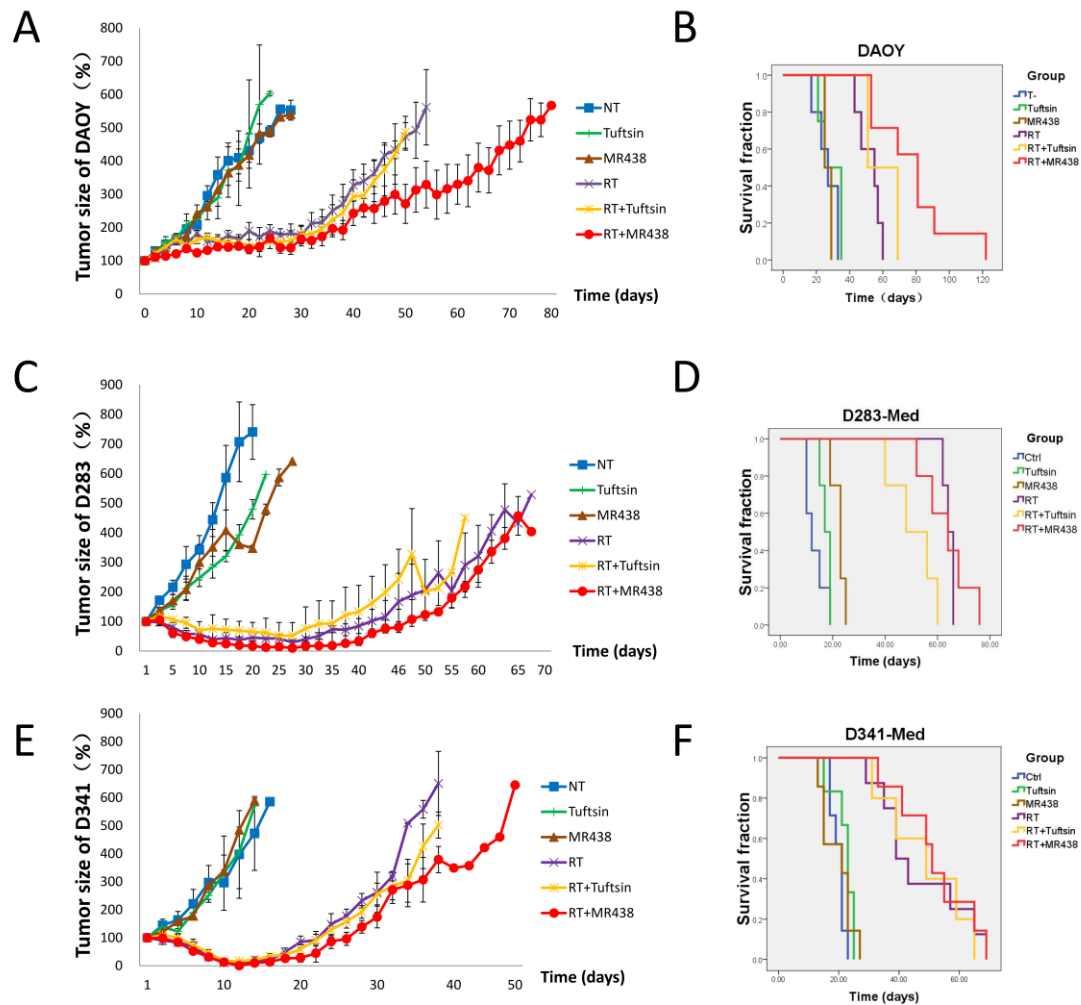


Figure 3. 8 : Effect of MR438 on tumor growth following irradiation with xenograft nude mice *in vivo*.

(A) Tumor growth of DAOY after radiation with or without MR438 and Tuftsin, the survival fraction was showed in (B), RT+MR438 decreased the tumor growth of DAOY compared to the RT alone or RT+Tuftsin. Tumor growth of D283(C) and of D341(E) and their survival fraction (D, F) seemed have less effect with MR438. n=6.

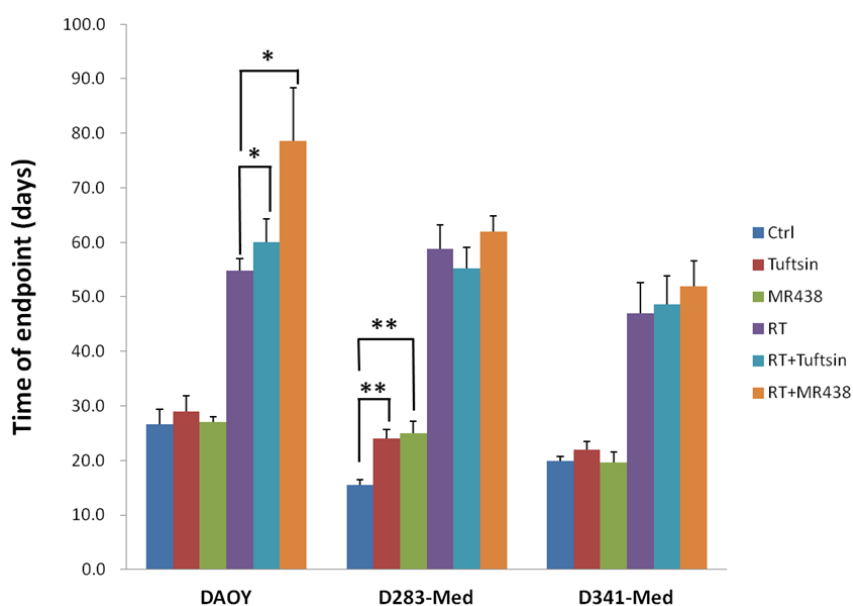


Figure 3. 9: Endpoint time for mice with three subtype MB tumor.
The endpoint of tumor size for mice is set to a volume of 1500mm^3 , representing about five fold change of tumor volume at initiation of treatment.

Effect of MR438 on cell viability and colony formation assay after tumor dissociation

In order to detect the effects of the compounds on the modification of phenotype, we evaluated the self-renewal ability by colony formation assay as well as the cell viability in serum free culture condition (Figure 3.10). MR438 alone had no influence the cell viability for the 3 types of tumors (Figure 3.10 A), but when combined with RT, there is a reduction of cell viability for RT+MR438 group compared to RT alone for the tumor of DAOY and D341. In an interesting way, the self-renewal ability evaluated by the colony formation assay gave the same types of responses with a

decrease observed with MR438 +RT (Figure 3.10 B). Beyond that, MR438 or Tuftsin alone could also reduce cell self-renewal ability for DAOY and D283.

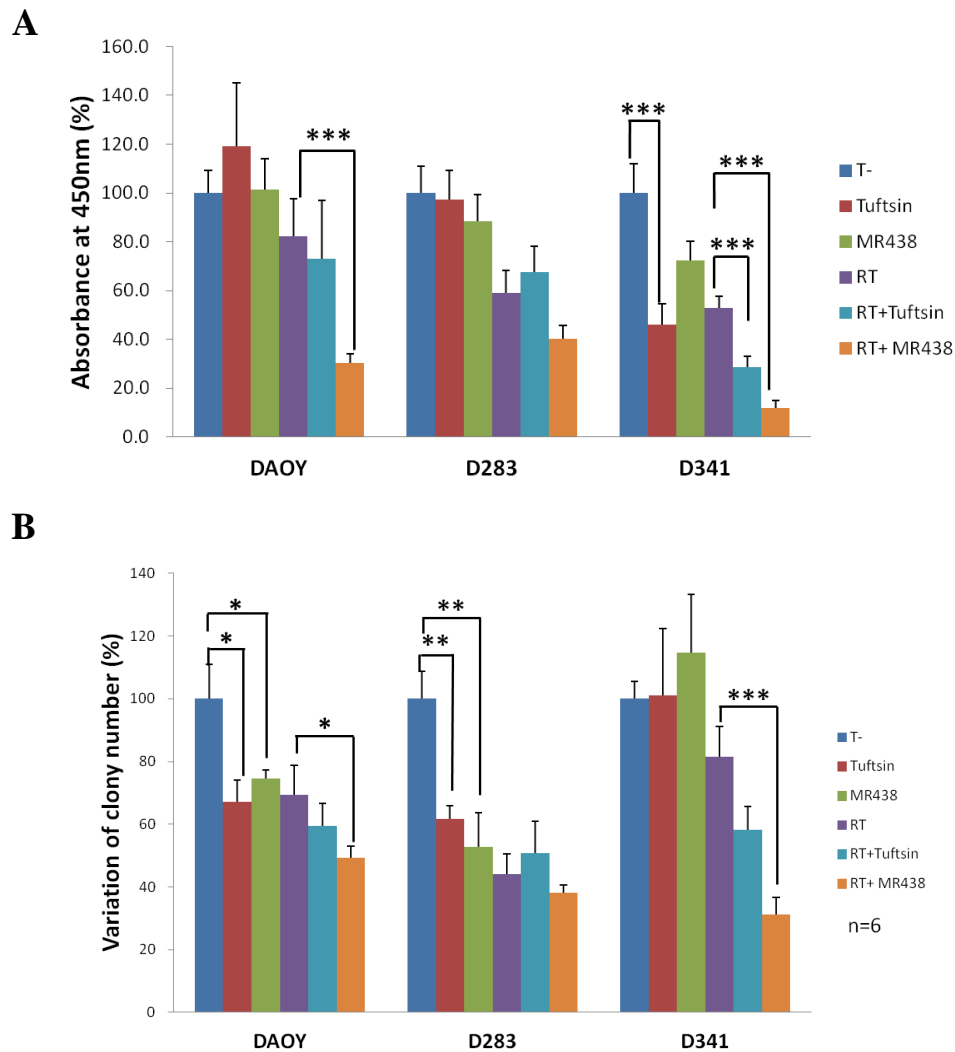


Figure 3. 10 : Effect of MR438 on cell viability and colony formation assay after tumor dissociation.

Results of colony formation to evaluate CSCs cell renewal capacity were demonstrated for DAOY, D283 and D341 (B), compared with the results of WST-1 (A). n=6.

Histological analysis of MB animal models treated by MR438

Animals were sacrificed at endpoint of a maximum volume 1500mm³ or insupportable tumor symptoms appeared and then all tumors were collected for histological analysis. Macroscopically, DAOY tumors were typical homogeneous solid tumors with less neovascularization, they have nearly round shape, smooth and clear boundary. D283 were more invasive with polygonal form and abundant neovascularization, gray fleshy masses beneath and less homogeneity than DAOY. D341 cells were highly invasive for surrounding tissue and incorporated striated muscle fibers with undifferentiated neoplasm. Macroscopically, tumor texture and vascularization are between DAOY and D283 with polygonal form (Figure 3.11) and the different treatments seemed to not induce the changes of tumor morphology.

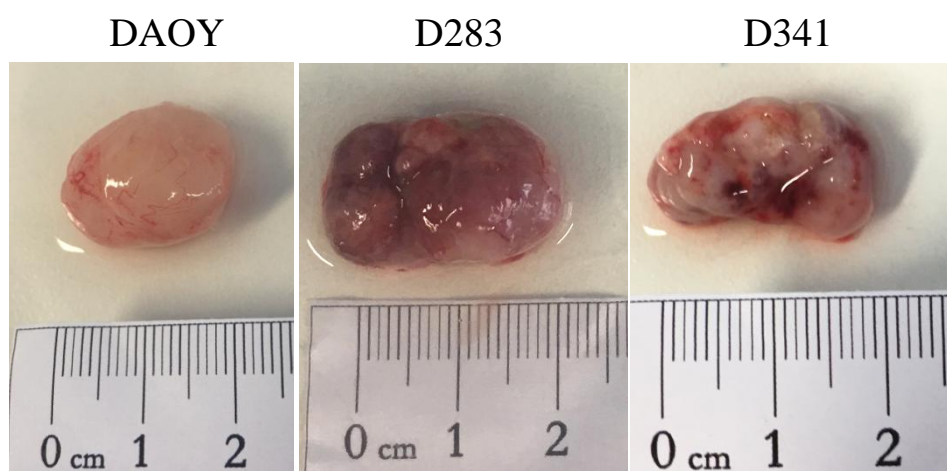


Figure 3. 11: Representative images of macroscopic view for 3 subgroup tumors: DAOY, D283 and D341 ctrl groups showed the different form, homogeneity and vascularization.

H&E staining showed DAOY cells were polygonal and elongated cells with small hyperchromatic nuclei and abundant cytoplasm, arranged more closely and larger than other 2 subgroups. D283 performed the smallest cells with scant cytoplasm, there were plenty of mitoses and high tumor heterogeneity. Characteristics of D341 cells seemed between D283 and DAOY, but they have many undifferentiated cells with abundant mitosis. Proportions of nucleus/cytoplasm from high to low were D283, D341 and DAOY, respectively. When treated with MR438 or Tuftsin only, the 2 compounds seemed to increase the differentiated cells and induce more necrosis of DAOY and D283, but had no effect for D341. RT decreased the tumor vascularization and increased the necrosis and apoptosis compared with control for the 3 type of cells, when associated with MR438, these effects seemed to be strengthened (Figure 3.12).

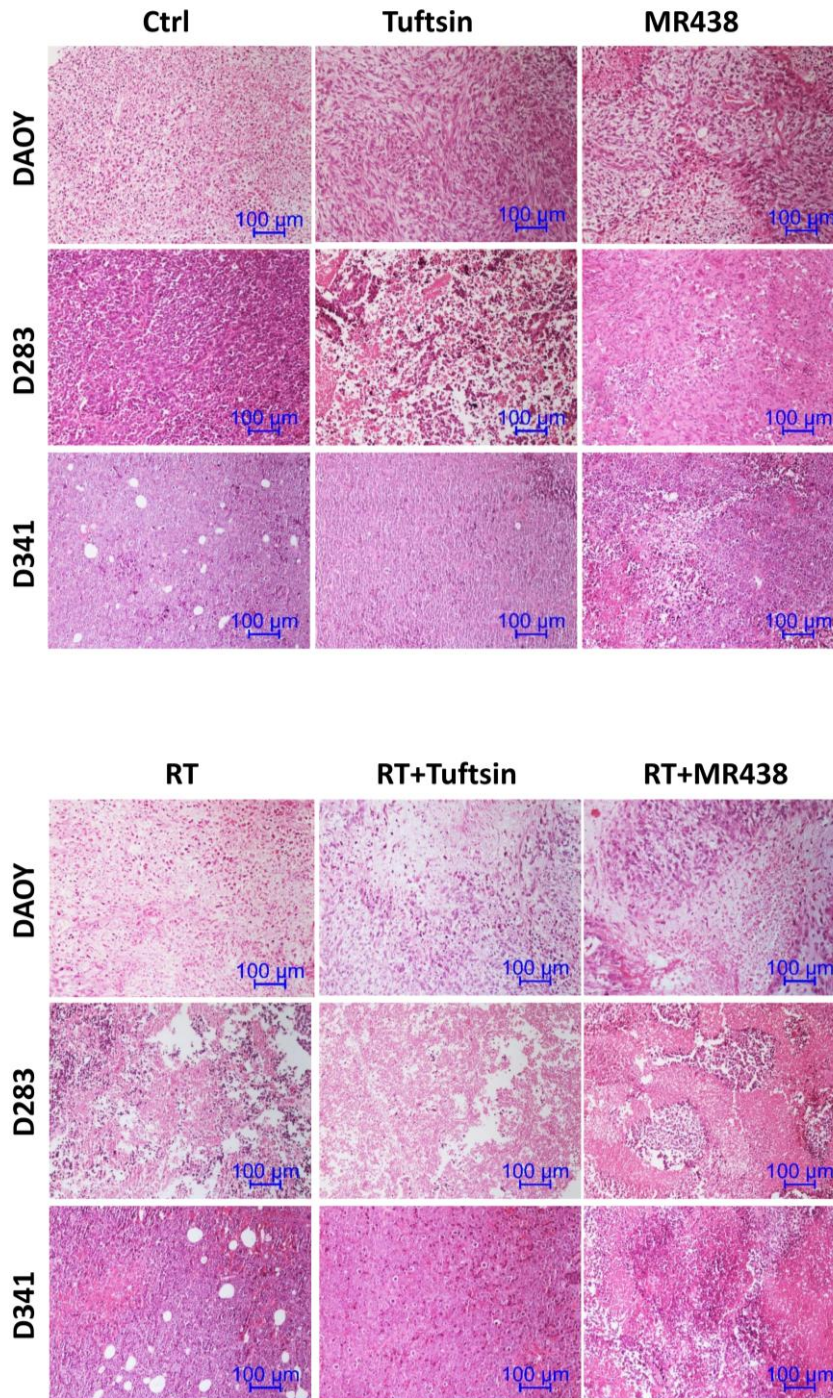


Figure 3. 12 : Microscopic views of MB tumors by HE staining.

Effect of MR438 or Tuftsia on tumor *in vivo* showed that MR438 seemed to induce necrosis for DAOY and D283 tumors, while combination with RT, MR438 increased necrosis and apoptosis lesion of MB tumor for DAOY, D283 and D341 tumors. MB: Medulloblastoma; RT: Radiotherapy; Image scale: 100 μ m.

According to immunohistological analysis, samples were incubated with primary antibody NRP-1 to detect the expression of NRP-1. For DAOY, there was an increase of NRP-1 expression after exposition to MR438 or Tuftsin, this augmentation is also observed when exposed to RT. But a decrease of NRP-1 expression was observed when MR438 or Tuftsin are associated with irradiation. For D283, NRP-1 expression was strong decreased by MR438 compared with control group. When associated with RT, results showed a similar trend. NRP-1 is less expressed by D341 tumors, it seems to be also a decrease for the RT+MR438 group vs RT (Figure 3.13).

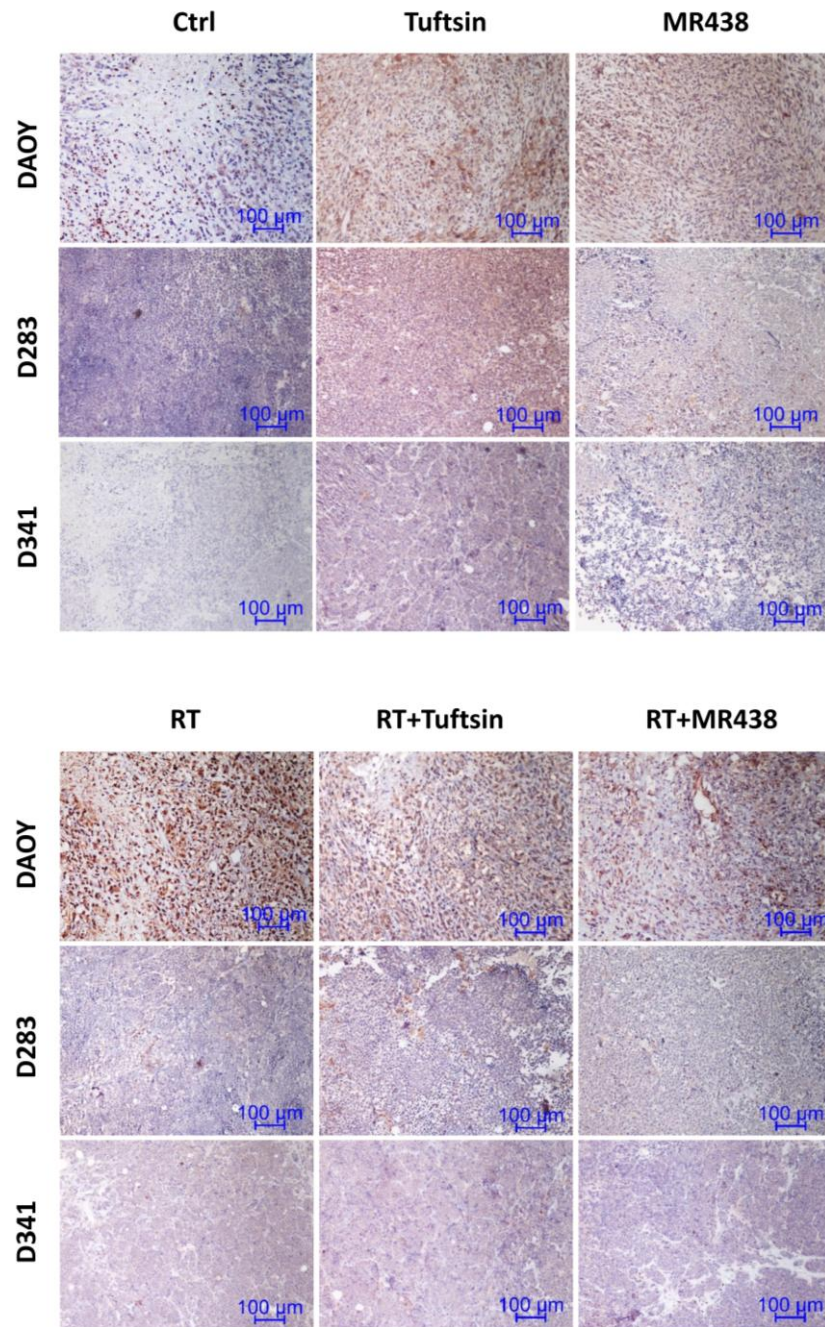


Figure 3. 13 : Effect of MR438 on NRP-1 expression in xenografted MB tumor by immunohistochemistry.

For DAOY, there was an increase of NRP-1 expression after exposed with MR438 or Tuftsia, this augmentation is combined with the augmentation of NRP-1 by RT therapy. But a decrease was observed when associated with irradiation therapy. For D283, NRP-1 expression was strong decreased by MR438 compared with control group. When associated with RT, results showed the similar trend. NRP-1 is less expressed by D341 tumor, there was also a decrease for the RT+MR438 group vs RT. MB: Medulloblastoma ; RT : Radiotherapy; Image scale: 100 μ m.

CD15 is recognized as the CSCs marker for MB, according to the observations of DAOY tumors, there were only few CD15+ positive cells, it seemed to have a decrease of CD15 expression for the RT+MR438 group compared with RT+Tuftsin group and RT. Regarding to D283 tumors, CD15 expression was strong increased by irradiation alone compared with tumors without treatment, when combined RT with tuftsin or MR438, this augmentation was decreased. RT+MR438 reduced the CD15+ cells for MB compared with RT group. For D341 tumors, CD15 seemed homogeneous expressed by D341 cells of control group, it seemed to have a weak decrease for the RT+MR438 group vs RT group (Figure 3.14).

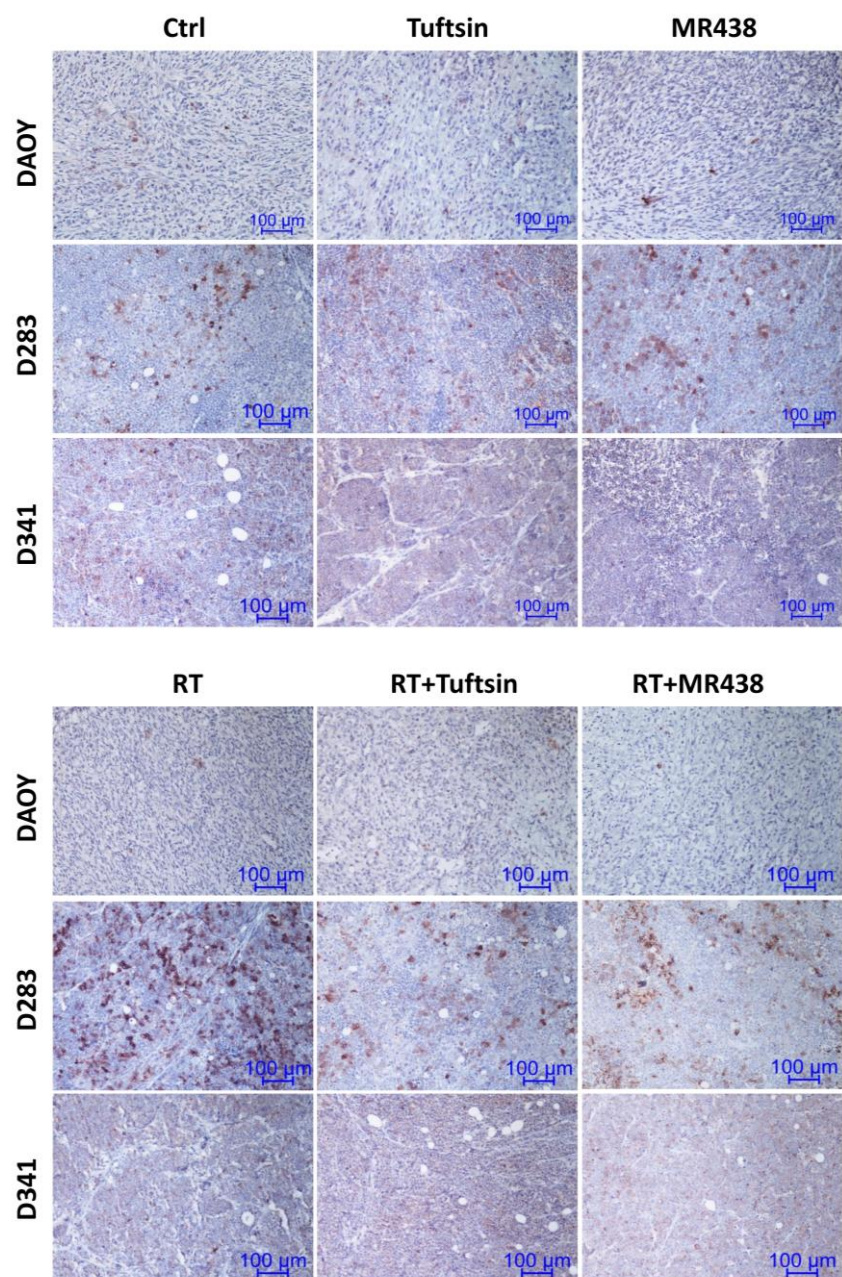


Figure 3. 14 : Effect of MR438 and Tuftsin on CD15 expression in xenografted MB tumor by immunohistochemistry.

According to DAOY, there were only a few CD15+ positive cells, it seemed to have a decrease of CD15 expression for the RT+MR438 group compared with RT+Tuftsin group and RT. Regarding to D283, CD15 expression was strong increased by irradiation alone in comparison with the control group, when RT combined with tuftsin and MR438, this augmentation was decreased. CD15 was homogeneous expressed by D341 tumor of control group, there was a weak decrease for the RT+MR438 group vs RT. MB: Medulloblastoma ; RT : Radiotherapy; Image scale: 100 µm.

Discussion and conclusion

Radiation therapy (RT) is commonly accepted as being one of the most essential treatments for MB. RT can improve survival and reduce recurrence, but remains aggressive with cognitive and sensory long term side effects, especially for young patients. So, it is necessary to develop new therapeutic modalities more adapted to the biological nature of this tumor in order to improve not only the outcomes but also the quality of life of young patients. Recent studies concentrate on targeted therapies mainly related to signaling pathways of the main 4 molecular subgroups: WNT, SHH, Group3 and Group4 (Taylor *et al.*, 2012). WNT and SHH pathways are better understanding (Remke *et al.*, 2013), while regarding to the poor prognosis and high risk recurrence in subgroup 3 and 4, it is even more urgent to find new therapies for these two subgroups. That is why we choose to envisage a strategy that can be applicable to the different subgroups by targeting specifically MB stem cells.

Recently, it has been suggested that the cancer stem-like cells (CSCs) are involved with resistance to radiotherapy and recurrence (Bao *et al.*, 2006). We have previously shown that our MB CSCs models over-expressed NRP-1 *in vitro* in relationship with the expression of CSC makers, and inhibition of NRP-1 induced a differentiated status of MB CSCs (Gong *et al.*, 2018). The over-expression of NRP-1 was correlated with tumor growth and proliferation, which is also related with the effect of radiotherapy (Battaglia *et al.*, 2008). Knockdown of NRP-1 showed a significant decrease of proliferation and an increase of radio-sensitivity of human non-small-cell lung cancer cells (NSCLC), not only *in vitro*, but also *in vivo*, via maybe the VEGF-PI3K-NF-kappa β pathway (Dong *et al.*, 2015). When using MR438

targeting NRP-1 in combination with RT, results showed that inhibition of NRP-1 could reduce about 25% of the dose of RT at 2Gy for SHH subgroup cells, while only approximately 10 % of decrease for cells of subgroup 3 or 4. It was shown that CD133+ MB cells were more radioresistant than compared to CD133- cells (Blazek *et al.*, 2007). In taken account our *in vitro* results discussed in chapter 2, DAOY model seems to be more sensitive to MR438 for the induction of differentiation with a 25 % of reduction of CSC and approximatively 20% for D283 and D341 model. Consequently, it seems difficult to predict a radiosensitivity effect solely by taken into account the *in vitro* ability of coumponds such as MR438 or Tuftsin to differentiate CSC.

We have also evaluated the tolerance of MR438 in mice before to envisage its therapeutic efficiency. The lethal dose of tuftsin is known to be of 2,4 g/kg in mice (Catane *et al* 1983). Our previous results *in vitro* showed that MR438 had no toxic effect on cells such as MB cells or endothelial cells (Richard *et al* 2016), and there are no side effects for all injected mice with an excellent tolerance. Just one animal from the 1mg/kg/dose group had a weight loss of more than 10%. But this observation was not found in the 10 mg/kg group. This weight loss could be explained by a feeding difficulty caused by blood withdraw from mandibular vein. Strangely, MR438 was not detectable in the serum level two hours post injection by our HPLC technique. Maybe explained first by the delay of blood sampling was long which means its elimination is too fast. Second, the possibility of transformation of this molecule to another form that is not detectable by our method. It's possible also that this molecule is able to bind to another molecule like serum proteins. Some studies have on the

biodistribution of similar compounds (Caveliers *et al.*, 2001, Chung *et al.*, 2015), but we still need to realize more investigations in order to determine the bioavailability of this molecule.

Despite the absence of MR438 in serum, we choose to test the efficiency in models with heterotopic tumors xenografted in nude mice in association with RT. All tumors types respond to RT, while combined with MR438, a decrease of tumor growth with a increase of mice survival were observed for DAOY and D341 tumors. This delay of tumor growth is clearly observed for SHH model tumors. Self-renewal ability of MB stem cells after MR438 + RT could explain the results obtained for tumor growth, however the cancer stem cell numbers for all tumor types have been reduced with combined treatments and more particularly for D341 tumors that are the non-responsive tumors to MR438. Moreover, D283 tumor cells seem expressed strongly CD15 and MR438 seems decrease the CD15 positive cells in this tumor. In the same way, it is difficult to connect our in vivo results with NRP-1 or CD15 expression knowing that the D341 tumors that expressed the least NRP1 and CD15 can have a delay of tumor growth intermediate between DAOY and D283. Several responses mechanisms can take place and it will be interesting to explore mechanism recently proposed via NRP-1 inhibition that appeared to regulate RAD51 expression through the VEGFR2-independent ABL-1 pathway and then increased radiation sensitivity (Hu *et al.*, 2018). Perhaps a different irradiation schedule with a longer irradiation time could improve the MR438 effect for D283 and D341 tumors.

TP53 mutations on RT for MB are subgroup dependent. SHH subgroup of MB are divided into TP53-mutant and TP53-wildtype in 2016 WHO classification. TP53

mutations as the high risk prognostic factors are associated with the majority of treatment failures in SHH MB (Ramaswamy *et al.*, 2016), a potential explanation for the local recurrence in TP53-mutated SHH subgroup is related with radiation resistance (Ramaswamy *et al.*, 2013). On the contrary, TP53 mutations are also frequently associated with CTNNB1 mutation in WNT subgroup but related with the best prognosis and more sensitive with irradiation. It is explained that accumulation of β -catenin protein is down-regulated by activated p53 (Levina *et al.*, 2004). However, p53-associated proteins in group 3 and 4 MB for the prognosis, progression and initiation remain still unclear. In our study, cell line DAOY is p53-mutant while D283 and D341 are p53-wildtype. TP53 Wild type of group 3 and 4 MB might be related the poor prognosis and radio-resistance. Our results *in vitro* and *in vivo* showed that the p53 wild-type D283 and D341 are more sensitive to RT than the p53 mutated DAOY cells at the beginning of treatment, but MR438 seems to increase the radiosensitivity of DAOY and lead to a better prognosis of SHH subgroup. The similar effect of RT for DAOY and D283 was observed by other authors that suggested an alternative p53-independent mechanism for the different molecular subgroups (Salaroli *et al.*, 2008).

In conclusion, inhibition of NRP-1 via MR438 increased *in vitro* radiosensitivity of CSC models especially at the dose of 2 Gy. In heterotopic models, a significant improvement of tumors radiosensitivity was also observed in the MR438 + RT group by comparing RT for DAOY and D341. In an interesting way, the self-renewal capacity for CSCs after tumor dissociation was also decreased significantly when tumors were treated by MR438 + RT versus RT. This work showed the interest of

targeting NRP-1 in association with radiotherapy to limit MB progression in decreasing the stem cells number in these tumors. Moreover, our *in vivo* experiments provide the possibility to use MR438 peptidomimetic as a radiosensitizing agent for treatment of MB. Further directions should confirm our results in orthotopic models and better understand the molecular mechanism of NRP-1 in MB progression.

Chapter 4:

**Elaboration of orthotopic models of
medulloblastoma obtained from cell lines
DAOY, D283-Med and D341-Med**

Introduction

Medulloblastoma (MB) is the most common malignant brain tumor in childhood with particularly poor prognosis and high tumor heterogeneity (Orbach *et al.*, 2012). The four mainly molecular subgroups WNT (Wingless), SHH (Sonic Hedgehog), Group 3 and Group 4 are different not only with molecular features but also with clinical characteristics (Taylor *et al.*, 2012, Northcott *et al.*, 2011). Recent discoveries in molecular biology of this tumor give an insight for targeted therapy and adapted therapy according to the molecular subgroups. Also the MB cell lines or animal models should be now classified into different molecular subgroups to test advanced therapies in a preclinical way. Compared to cell lines, animal models are more representative of the original MB in experimentations. These models especially orthotopic models represent biological and clinical nature of MB for our transitional experiments toward the application for the patients (Pei *et al.*, 2012, Kawauchi *et al.*, 2017).

More and more recent studies suggest the hypothesis of cancer stem cells (CSCs) existence in MBs, considered also as tumor-initiating cells (TICs) which can generate different cell types to arise tumor. These special cells are present in low number in brain tumors especially in MB (Vescovi *et al.*, 2006, Singh *et al.*, 2003, Hemmati *et al.*, 2003, Singh *et al.*, 2004). This cell population generates tumors through the stem cell patterns of self-renewal and differentiation into multiple tumor cell types. Moreover, these cells have better DNA repair capability contributing to tumor resistance during radiation and chemotherapy. BTSCs can be characterized by expression of stem cell phenotypic markers such as CD133 or CD15 (Singh *et al.*,

2003, Read *et al.*, 2009) and has a peculiar interest in understanding the progression of MB (Vescovi *et al.*, 2006).

The conventional therapies could kill differentiated tumor cells, but this small population of BTSCs survives and causes tumor proliferation, which seems to be a major cause for tumor aggressiveness and recurrence because of their resistance to radiotherapy or chemotherapy (Singh *et al.*, 2004, Vescovi *et al.*, 2006, Bao *et al.*, 2006). Therefore studying CSCs could be a reasonable and promising approach to establish the animal models and to better understand the tumor pathogenesis, and for the evaluation of new therapies.

Our previous work has already characterized the MB stem cell models with an increase of NRP-1 expression and stem cell markers and tested different treatments on three MB cell lines (DAOY, D283-Med and Med-D341) *in vitro* and their heterotopic animal models *in vivo*. As the high stability of subgroup molecular features for MB, the identified subgroup could not be changed at the time of recurrence or metastatic cases (Ramaswamy *et al.*, 2013, Wang *et al.*, 2015). In this chapter, we would like to establish the orthotopic models from injection of MB stem cells obtained by *in vitro* enrichment to better understanding the biological characteristics of CSCs and furthermore for the evaluation of new therapies.

Materials and methods

Cell culture and cancer stem cell preparation

The same cell lines were used in this part of my work and cultivated in the same conditions with MEM (Gibco, Life Technologies Corporation, UK) including 10 % fetal bovine serum (FBS, SIGMA,USA) for DAOY and D283, 20 % FBS for D341-Med, 1% L-glutamine (SIGMA,UK), 1 % non-essential amino acids (Gibco, UK), 1% penicillin/streptomycin (Gibco, UK) and 1 % Sodium pyruvate (GibcoUK) at 37 °C and 5 % CO₂. While MB stem like cells cultures were maintained in DMEM/F12 medium (GibcoUK) containing B27 and N2 supplement (Gibco, Life Technologies Corporation, USA), 20 ng/mL of human recombinant epidermal growth factor (EGF) and basic fibroblast growth factor (bFGF) (EGF and FGF from Miltenyi Biotec, Germany). After a 3 days culture in hydrophobic flasks coated with polyHema at 37 °C with 5% CO₂ in a humidifier atmosphere, spheres were obtained. MB stem like cells were dissociated from spheres using Accumax (Gibco, Life Technologies Corporation, UK). After cell counting, a concentration of 1×10^5 cells/ μ L of MB stem like cells in HBSS was prepared for injection and conserved on ice.

Orthotopic xenografts of medulloblastoma stem cells

Orthotopic xenograft models in nude mice (NMRI-nu, Janvier Labs, France) were used in this study within the agreement of the French Minister of Research (agreement n°APAFiS #4037) (Figure 4.1). Mice were anesthetized by injecting 5 μ L/g of weight of solution mixture of xylazin / ketamin (90 and 8 mg/kg, respectively)

in the intra peritoneal cavity. The stereotaxic instrument (KOPF®) (Figure 4.2 A) has been used to fix the mice for the orthotopic transplantation procedure. After making a scalp vertical incision, we defined the site of orthotopic transplantation (Figure 4.2 B), 2 mm right and bottom to the lambda suture. MB stem like cells was prepared in HBSS (cell suspension: 1×10^5 cells/ μL) for injection by using HAMILTON Syringe 2 mm in the deep of the cerebellar cortex. All the mice should be followed up at least 3 weeks post injection or when neurologic symptoms appeared (experimental endpoints). The sacrifice method is by Pentobarbital overdose. At experimental endpoints, resection of the complete brains (cerebral hemispheres and cerebellum) were performed. The brain samples were fixed by the 4% formaldehyde solution (Diapath, Italy) for a week.

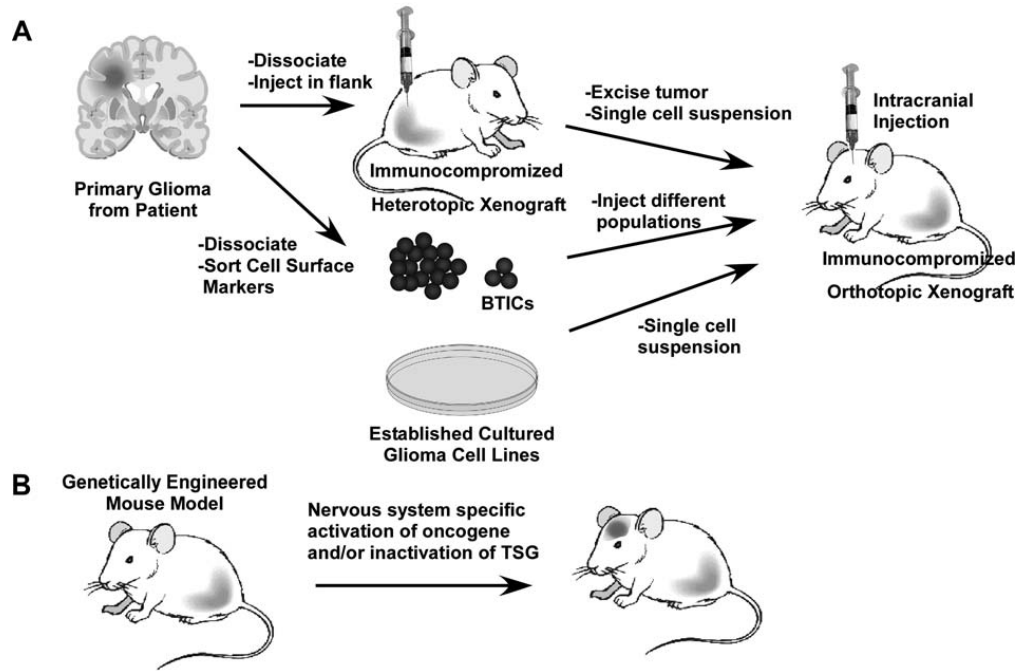


Figure 4. 1: Nervous System Tumor Models.

(A) Xenograft models are created from patients' tumors or from established glioma cell lines injected into immunocompromised mice. Brain tumor-initiating cells (BTICs) are isolated from freshly dissociated tumors and sorted based on cell surface markers. (B) GEM models are designed to produce tumors de novo by activating oncogenic mutations and/or inactivating tumor suppressor genes (TSGs) in a cell-type specific manner. (Gutmann et al., 2011)

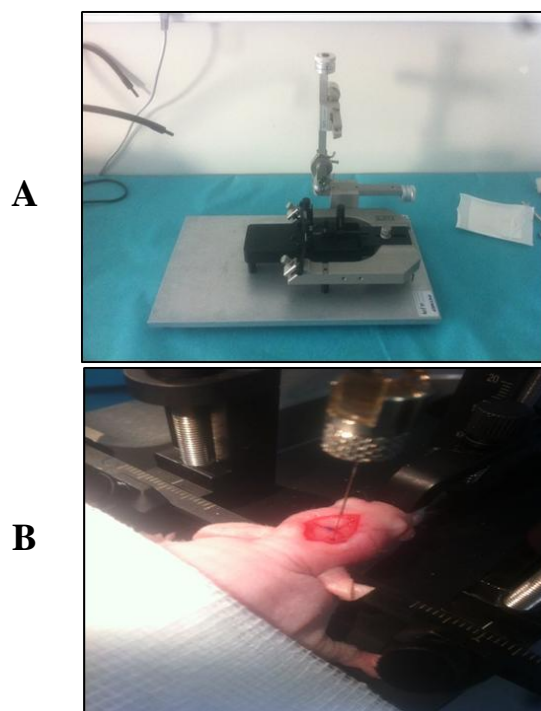


Figure 4. 2 : Orthotopic transplantation with Stereotaxic Instrument.
 (A) Stereotaxic instrument to fix the mouse through the transplantation procedure. (B) Injection by HAMILTON syringe into brain.

Histological preparation of H&E tumor sections

The mice brains have been withdrawn and kept within the 4% formaldehyde solution for 7 days. Then samples were transferred into inclusion cassette within 70% alcohol solution. The cassettes were transferred to an automated dehydration machine (HISTO-PRO 300) over night for paraffin inclusion. Microtome tool (LEICA RM 2135) was used to cut the paraffin blocks in 5 μ m thick slices. Then, the slices were fixed over the slides for staining step. Staining step was achieved either by a manual procedure or an automated machine with fixed protocol. H&E staining was used for microscopic observations with the following experimental procedure:

Haematoxylin	6 min
Distilled water	4 min
Hydrochloric acid	3 sec
Distilled water	3 min
Distilled water	3 min
Eosin	5 min
Distilled water	3 min
Ethanol 96 %	3 min
Ethanol 100 %	3 min
Ethanol 100 %	5 min
Lighten by toluene	3 min
Coverslide mounted.	

Immunohistochemistry of tumor sections

The expression of Vimentin and NRP-1 were examined by immunohistochemistry with the same paraffin blocks of H&E staining sample. 5 μ m thick slice of sample was fixed on the polysine slides (VWR, Leuven) for the immunohistological assays. The deparaffinized slides should be pretreated in citrate buffer (pH 6.1) by autoclave. Samples were then incubated overnight at 4 °C with primary antibody Vimentin (dilution of 1/8000, [V9], ab8069, Abcam) and NRP-1 (dilution of 1/800, ab81321, Abcam). After washing with PBS, secondary antibody was incubated for 1h and 6% hydrogen peroxide was used for 20 min at room temperature to inhibit EGPO (Endogenous peroxidase). Kit Vector Novared substrate (#14328, Abcys) was used to develop the peroxidase activity of sections which were counterstained with hematoxylin. After dehydration with three 100% alcohol baths

(30 ", 30 ", 1 ') and mounting in Eukitt, the samples were performed to analysis by the software (Nis – Elements AR 3.2) with a camera microscope (Nikon–DS Fi1). Primary antibody of Vimentin or NRP-1 was replaced by PBS during incubation for negative control.

***In vitro* transfection of Luciferase-RFP in MB cells**

In order to follow up the brain tumor *in vivo* without sacrifice the mice, we need to marker the MB cells with fluorescent marker or by bioluminescence to indicate the tumor growth within the brain. The Luciferase-RFP-Puro lentivirus (CMV-Luciferase-2A-RPF-Puro, Amsbio, UK) was used to transfect the 3 MB cell lines. Before transfection, 6 concentrations of puromycin (0, 2, 4, 6, 8, 10µg/mL) were tested and 2µg/mL of puromycin was selected to contribute a 100% mortality of DAOY, D283-Med and D341-Med. We added 65 µL of lentivirus into 50%~70% confluent cells into each well of 6 well plates. After 72 h of transduction, 2µg/mL of puromycin was added into cell culture to select the fluorescent cells and then transduction rate was checked by fluorescence microscopy (AZ100 Nikon, France).

Results

Animal models of orthotopic transplantation experiments

Each group of MB cell lines (DAOY, D283-Med and D341-Med) included 6 mice represented in Table 4.1. After a follow up of 20 to 31 days, mice weight changed only a little before and after injection. During the follow up, all mice had a good tolerance to the brain injection, except one mice of the D283 group which died after anesthesia. There was no death during the follow up. Only one animal (17S040) of D341 had clear neurological symptoms at the end of the followup (ataxia, unilateral muscle weakness) because of tumor progression.

Concerning the presence of tumor, results showed that 76.5% (13/17) of mice developed a tumor from injected MB stem like cells, 5/6 for DAOY, 3/5 for D283 and 5/6 for D341. The patterns of tumor progress and tumor size varied between different subgroups. The average tumor volume of the DAOY group was 0,19 mm³, 3.3 mm³ for D283, and 20.7 mm³ for D341. The largest tumor volume was 101,37 mm³, developed from D341Med cell line which is the most invasive subgroup, and the smallest is 0,002 mm³ developed from DAOY cell line which has the best prognosis.

Table 4. 1 : Orthotopic transplantation experimental data of 3 MB cell lines.

P: present, N: non-present.

Cell line	ID	Follow up period (days)	Injection Weight (g)	Sacrifice Weight (g)	Difference weight (g)	Tumor presence (P/N)	Tumor size (mm3)
DAOY-MS	16S169	20	33	31,2	-1,8	P	0,076
	16S031	31	28,3	28,7	0,4	P	0,50
	16S032	22	28	28,2	0,2	P	0,002
	16S242	21	33.5	33	0.5	P	0.08
	16S017	21	32	32.4	0.4	P	0.3
	16S241	23	33.4	32.5	-0.9	N	-
D283-MS	17S020	20	28,7	29,2	0,5	P	0,82
	17S024	23	27	27,7	0,7	P	14,93
	17S025	23	28,3	29,9	1,6	N	0
	16S173	Died					-
	17S039	27	33,8	34,7	0.9	P	0.6
	17S072	20	29.7	30	0.3	N	-
D341-MS	17S026	23	31	30,7	-0,3	P	0,85
	16S172	21	29	29,3	0,3	P	0,88
	17S040	27	27,9	27,75	-0,15	P	101,37
	16S170	20	33	30.1	-2.9	P	0.4
	17S023	23	27.5	27	-0.5	N	-
	17S021	20	29.78	30	0.2	P	-

To confirm the presence of tumor in mice injected with DAOY, D283 and D341 CSCs (N = 6 for each cell line), animals were sacrificed at 3 weeks of surveillance or endpoint of insupportable tumor symptoms. After the mice sacrifice, tumors were collected and fixed in formaldehyde, then, histologic analysis was done (Figure 4.3). Images showed the presence of MB cells with different cell cycle stages, necrotic cells at the middle of the large volume tumors and vascular vessels frequently at peripheral areas. Most of the tumors from different lines showed a round to oval shape tumors with demarcated area from the adjacent tissues. Among the D341-Med group, tumor developed by an invasive manner from the space between cerebellar

folds to the interior of cerebellum tissue (Figure 4.4). The immuno-histology confirms the presence of MB cells DAOY by positive reaction with human Vimentin antibodies (Figure 4.5).

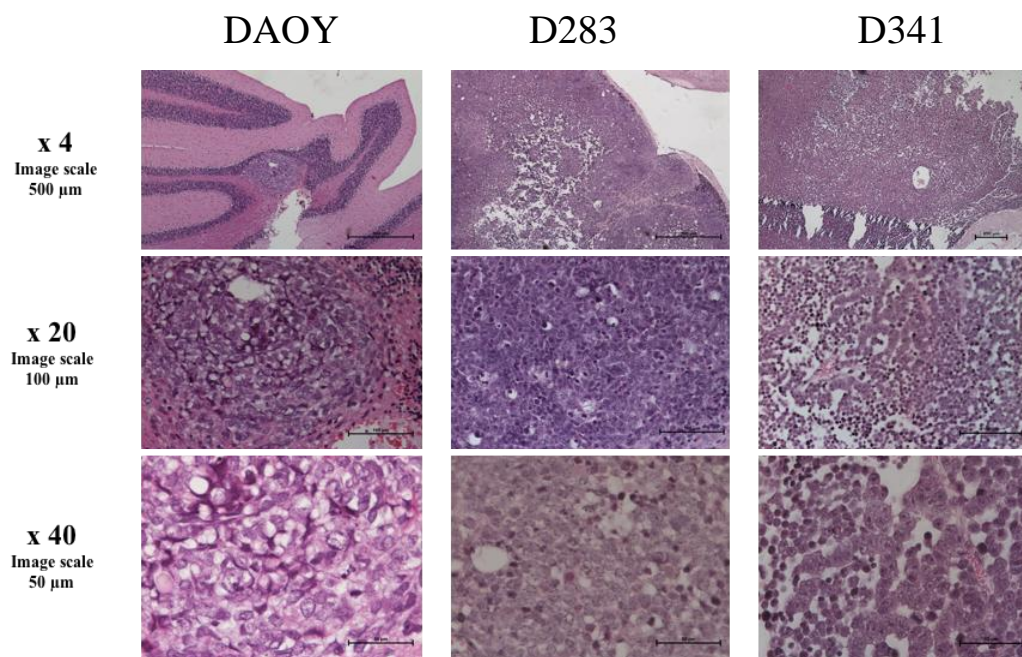


Figure 4. 3 : Histological presentation of tumors *in vivo* from different cell lines.

This figure is demonstrating the histological appearance of different cell lines tumors H&E slides at different microscopic powers. DAOY: x4 a round shape tumor with in cerebellar tissue, x20 transitional outer layer from adjacent cerebellar tissue. x40 different mitotic stages. D283: x4 large tumor with distinct outer layer and edematous central area, x20 number of necrotic cells, x40 cancerous cells at different mitotic stages. D341: x4 large tumor detached from granular layer of cerebellum and central vessel inside the tumor. x20 transversal vessels inside tumor surrounded by edematous area. x40 cancerous cells at different mitotic stages and condensed chromatin nucleus.

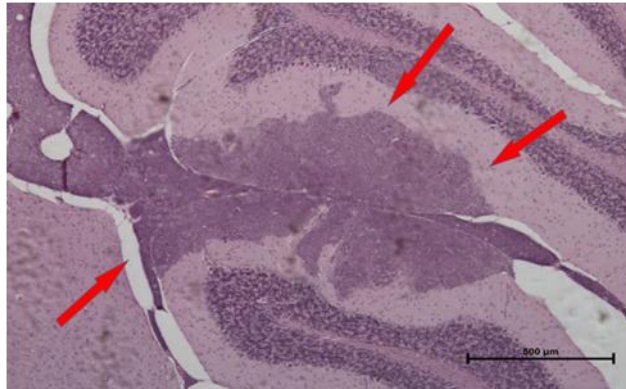


Figure 4. 4 : An invasive tumor of D341Med cell line.

H&E histology slide showed invasive tumor inside cerebellar tissue (arrows at the right) from a tumor developed outside (arrow at the left).

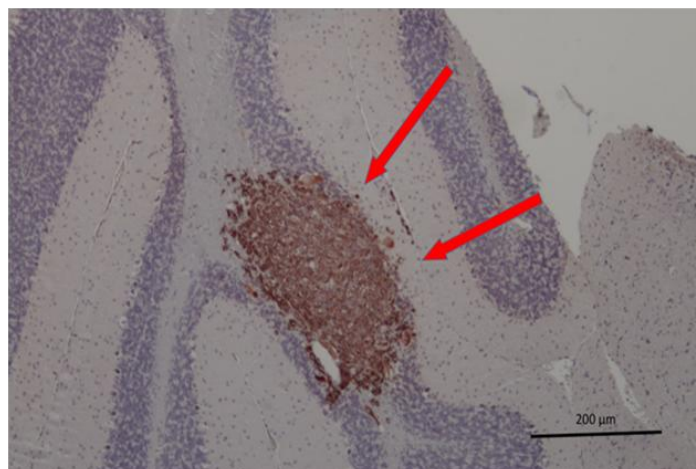


Figure 4. 5: Immunohistochemistry of vimentin human antibody in DAOY tumor.

Arrows are indicating the cancerous cells of DAOY cell line tumor with in cerebellar tissue of nude mouse injected by MB CSCs.

RFP /Luciferase models of MB cell lines

After testing 6 concentrations of puromycin (0, 2, 4, 6, 8, 10µg/mL) for the selection of positive DAOY, D283 and D341, 2 µg/mL of puromycin is chosen to select the cells which contributed a 100% mortality of DAOY in 24H and about 90% mortality of D283-Med and D341-Med in 48H (Figure 4.6 A and B). After 72H of transfection and selection by Puromycin, 3 cell lines seemed to have integrated the lentiviral sequence as observed by the red fluorescence of RFP, even if DAOY cells expressed less RFP than the cells of D283 and D341 (Figure 4.6 C).

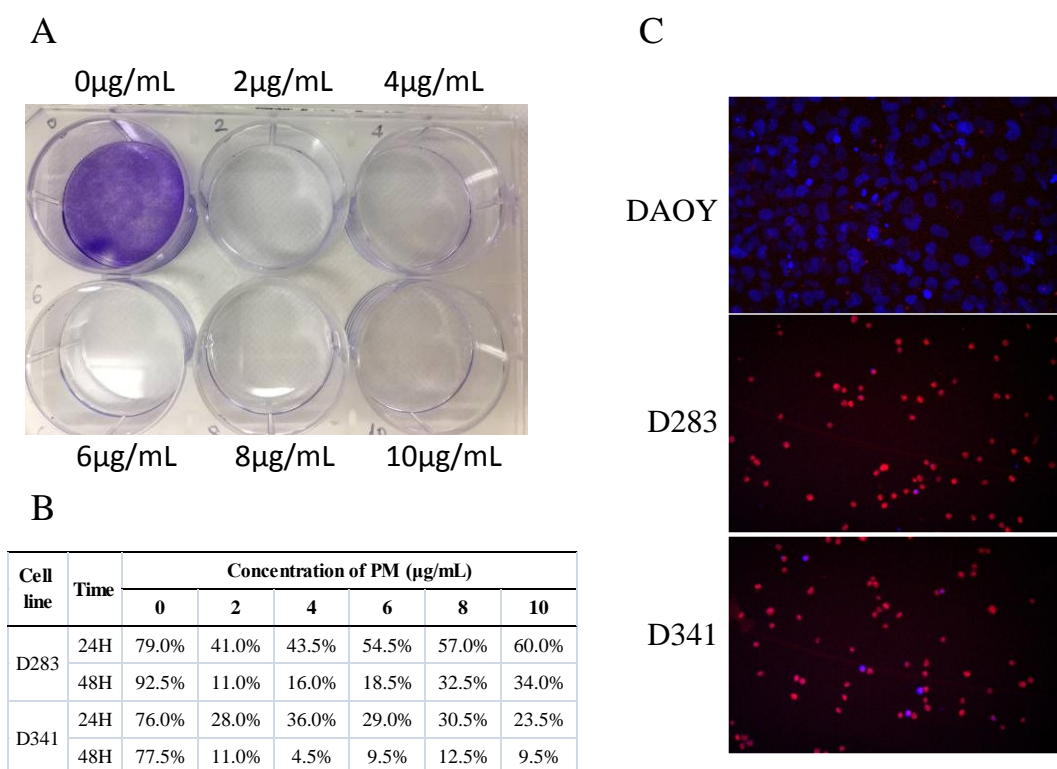


Figure 4. 6: Transduction of RFP for 3 cell lines

(A) Test for concentration of PM for the treatment of the cells DAOY, showed the concentration of 2µg/mL contributed 100% death rate of DAOY after 24H of exposition. (B) Table of cell average viability of D283 and D341 after treatment of different concentration of PM. (C) Confocal microscopy of autoimmunofluoresence for cells of DAOY, D283 and D341 after transduction of RFP (red), nucleus marked with DAPI (blue). PM: Puromycin

Discussion and conclusion

The cell lines of DAOY and D283 were used to establish the animal models first in 1985 (Jacobsen *et al.*, 1985, Friedman *et al.*, 1985), while cell line D341 was characterized in 1988 (Friedman *et al.*, 1988). All our models of MBs generate tumors within 3 weeks, with an overall 76.5% success of tumor appearance (13/17). Tumor progressions from CSCs of DAOY-MS, D283-MS and D341-MS are 2, 3 and 1 weeks faster than results published by Friedman *et al.* with the differentiated cells, respectively (Table 4.1). These results indicated that the CSCs seem to relate with the MB progression. CSCs have better DNA repair capability contributing to resistance of radiation and chemotherapy (Bao *et al.*, 2006, Hussein *et al.*, 2010). So the CSCs targeted therapy maybe a useful approach to control tumor progression. CD133 is the most common cancer stem cell phenotypic marker for CSCs, while CD15 can be also considered as the tumor progenitor cell marker in MB (Singh *et al.*, 2003, Read *et al.*, 2009). For animal models, except classical characteristics of subgroup and the expression of CSCs markers, the cancer stem cell characteristics include neurosphere formation, multilineage differentiation, high ALDH-activity and high tumorigenicity (Dietl *et al.*, 2016). Mice with one copy of the *Ptch1* gene knocked out (*Ptch1* +/-) develop the MB tumor of SHH subgroup spontaneously which are very radiosensitive and have some CSCs characteristics (Goodrich *et al.*, 1997, Hahn *et al.*, 1998). MBs with overexpression of MYC oncogene (c-MYC) are related with poor prognosis, cerebellar stem cells expressing *Myc* and mutant *Trp53* (p53) generate aggressive tumors after orthotopic transplantation which is another animal model that can be

used to test therapies for this devastating disease (Pei *et al.*, 2012), and furthermore it can be classified in subgroup 3 (Kawauchi *et al.*, 2017).

Table 4. 1 : Time of tumor apparition after cell transplantation following different cell culture method and amount of transplanted cells.

	Cells	Injection cells	Appearance tumor time
CSCs enrichment by medullosphere culture*	DAOY-MS	5×10^5 cells/5 μ L	< 3 weeks
	D283-MS	5×10^5 cells/5 μ L	< 3 weeks
	D341-MS	5×10^5 cells/5 μ L	< 3 weeks
Classical culture of differentiated cells**	DAOY	5×10^5 cells/50 μ L	5 weeks
	D283	5×10^6 cells/30 μ L	5-6 weeks
	D341	2.3×10^7 or 2.1×10^5 cells/30 μ L	4 weeks

*Our orthotopic models with MB cancer stem like cells(CSCs).**Results obtained from references: Jacobsen *et al.*, 1985, Friedman *et al.*, 1985 and Friedman *et al.*, 1988

Numerous mouse models of MB were proposed to be classified with the molecular subgroup to better study the MB biology. The identified molecules of MB subgroups are stable at the time of recurrence or even in metastatic cases (Ramaswamy *et al.*, 2013, Wang *et al.*, 2015), and it is crucial to match preclinical models to molecular subgroups in order to choose the appropriate model for preclinical studies on MB (Poschl *et al.*, 2014). Global gene expression profiling

helps to classify the molecular subgroup for more approximate models, using the 4 genes SFRP1, WIF1, NPR3, and KCNA1 to classify with a high fidelity the subgroup SHH, WNT, Group 3 and Group 4, respectively for xenograft mouse models and cell lines of MB (Zhao *et al.*, 2012). Lagerweij *et al* used the same genes to classify the cell lines that showed the most used cell line DAOY belong to subgroup SHH and the cell line D283-Med to the subgroup 3 (Lagerweij *et al.*, 2016). However, the molecular subgrouping has not been completely studied for all cell lines and sometimes showed the different results. The classification of D283-Med above has been confirmed by some authors to be assigned in Group 3 (Sengupta *et al.*, 2014), but also seems to have the characteristics of Group 4 by others (Snuderl *et al.*, 2013), as well as the cell line UW228. Most of the cells in culture maintain the mutation and hold the stability of subgroups like in tissue samples whereas the MED6 cell line reverted to wild type and changed WNT mutation into Group 3 (Othman *et al.*, 2014). The culture and environmental conditions could interact with the phenotypic type to active or silence some mutation and signaling pathways. In our study, we analyzed the three most frequent used cell lines of MB: DAOY, D283-Med and D341-Med, corresponding to the subgroup SHH, subgroup 4 or 3 and subgroup 3, respectively (Xu *et al.*, 2015, Snuderl *et al.*, 2013).

Tumors do not have the same growth rate over time depending on the cell lines. Also, the aggressiveness of developed tumors correlates with the clinical nature of isolated tumor. The invasive features observed were not changed, D341 classified in most invasive subgroup, developed the maximum tumor volume and tumor invaded the cerebellar tissue from outside to inside. Moreover, neurologic symptoms were

observed with the MBS D341-Med cells from the Group 3 which is known as the most aggressive subgroup. DAOY cells developed the smallest tumors circumscribed at the site of injection in the relationship with the SHH group, and their prognosis is more favorable than Group 3 tumors. For tumor size follow up, MRI (magnetic resonance imaging) is one of tumor growth surveillance method for brain tumors. Nevertheless, this technique lacks of sensitivity for small or disseminated tumors. In preclinical context, fluorescent or bioluminescent imaging allows to detect tumor cells without sacrifice animals, by transfecting cells with a reporter gene as luciferase or RFP (Choi *et al.*, 2016). We have transfected our cells by lentiviral particle containing RFP and Luciferase genes. We must characterize the *in vitro* behavior of our cell lines transfected with Luciferase and RFP especially in term of cell growth before envisaging their transplantations *in vivo*.

In this preliminary study we established 3 orthotopic xenograft animal models by using MB stem cells for our prospective assays. These developed tumors need additional histological analysis in order to determine their behavior in particular concerning their dissemination ability. For our prospective experiments, novel therapies could be tested with our orthotopic models to better understand their biological effects.

Chapter 5:

General Discussion

Advances in the classification of MB molecular biology, allow current researches to focus on the targets involved in the molecular subgroup related signaling pathways (Taylor *et al.*, 2012, Northcott *et al.*, 2011). It is clear that the classical histological classification and even the four mainly molecular subgroups of WNT, SHH, Group 3 and Group 4 are not enough for the clinical practice, thus abundant mutations should be considered as prognostic factors, such as TP53. So the 2016 WHO classification of brain tumors added these molecular modifications, including WNT-activated, SHH-activated, TP53-mutant or TP53-wildtype, non-WNT/non-SHH Group 3 and Group 4 (Louis *et al.*, 2016). More recently, additional age and risk factor features to molecular subgroups within childhood MB helped to divide MB into seven novel, clinically significant subgroups: WNT, SHH-Child (>4.3 years) and MBSHH-Infant (<4.3 years), MBGrp3-HR, MBGrp4-HR, MBGrp3-LR and MBGrp4-LR, these disease risk-stratifications assist to better understand the prognosis and make reasonable treatment decisions of MB (Schwalbe *et al.*, 2017). In patients, the identified mutations on signaling pathways of MB subgroups remain stable at the time of recurrence or even in metastatic cases (Ramaswamy *et al.*, 2013) (Wang *et al.*, 2015), but some are contested, especially in experimental models (Poschl *et al.*, 2014). Global gene expression profiling helps to classify the molecular subgroup for more approximate models, using the 4 genes SFRP1, WIF1, NPR3, and KCNA1 to classify the subgroup features with more widely samples (Zhao *et al.*, 2012). In our study, we analyzed the three most frequent used cell lines of MB: DAOY, D283-Med and D341-Med, corresponding to the subgroup SHH, subgroup 4 or 3 and subgroup 3, respectively (Xu *et al.*, 2015, Snuderl *et al.*, 2013).

NRP-1 expression has been reported to be over-expressed in various cancers, which is related with the CSCs biological behaviors, involved in cell survival and renewal abilities (Osada *et al.*, 2004, Jubb *et al.*, 2012, Chu *et al.*, 2014, Peng *et al.*, 2014). CSCs are also considered to be involved in the tumor recurrence and resistance to radio-chemotherapy (Eyler and Rich, 2008). Moreover, targeting placental growth factor (PIGF)/NRP1 with monoclonal antibodies induced a direct antitumor effect in MB, resulting in tumor regression, decrease of metastasis and increase of survival of mouse models (Snuderl *et al.*, 2013). NRP-1 seems to be a useful target to control CSCs proliferation. In the context of a peptide based approach, Tuftsin is a natural peptide to bind specifically to NRP-1 (Von Wronski *et al.*, 2006). However, it isn't an ideal agent for use in clinical practice because of several limiting points including size, stability (susceptible to degradation by peptidases), lack of effective methods for delivery, low oral bioavailability, rapid excretion and poor transport properties through biologic membranes. Thus, we developed several novel peptidomimetics, and found one named MR438, which has a good biological activity to NRP-1 (Richard *et al.*, 2016). In chapter 2, we found that the compound MR438 had no direct cytotoxicity but could stimulate the differentiated status of MB CSCs *in vitro*.

However, the effects of compounds may have different results *in vitro* and *in vivo* experiments because of the complicated internal environment. Models with heterotopic tumors xenografted in nude mice were performed to confirm the effects of MR438, but only the D283 group had a decreased tumor growth after exposed with MR438, accompanied by a diminution of cell renewal ability. Interestingly, when associated with RT, a high decrease of tumor growth and an increase of mice survival

times were observed for DAOY tumors. To a lesser extent, D341 tumors seemed also to have an inhibition of tumor progression. Self-renewal ability of MB stem cells *in vitro* and *in vivo* for MR438 + RT were decreased when compared with the RT group, which could explain the results of decreased tumor growth. Perhaps different irradiation schedule with a longer irradiation time could improve the MR438 effect for D283 and D341 tumors. For the moment, it's not clear for us to propose a relation between NRP-1 expression and CSC status from our *in vivo* experimentations. The significant improvement of radiosensitivity for SHH subgroup indicated that CSCs regulate probably through NRP-1 with the SHH signaling pathway. As the specific signaling pathways remain still unclear for the non SHH/WNT subgroup MB. Bmi1 and Gli1 may be two essential possible regulatory effectors in the more aggressive subgroups (Leung *et al.*, 2004). Bmi1 is implicated in CSCs features, related with SHH pathway. Gli1 is also one of the downstream reactors of SHH, which can be preferentially binded to the Bmi1 promoter and influence the Gli1 expression. In fact, SHH and Bmi1 are 2 indispensable signaling pathways in MB stem cell maintenance but also be related with each other (Wang *et al.*, 2012).

The precise signaling pathways of NRP-1 action are still unclear as they interact as co-receptors with many cancers associated molecules. Subsequently, we have endeavored to understand the signaling pathways of NRP-1 involved in the differentiation of MB stem cells and thus contributed to improve the radiosensitivity. Overexpression of NRP-1 in cancer cells promoted cancer stem cell features that depended on the complex NRP-1 / VEGFR-2 for the CD133(+) human glioma stem-like cells (GSCs) (Hamerlik *et al.*, 2012, Beck *et al.*, 2011). VEGFR and other

VEGFR co-receptors of NRP-1 are involved in neoangiogenesis, tumor progression and differentiation by activating signaling pathways like PI3K / AKT, MAPK and SMAD. We found that inhibition of NRP-1 led to a decrease of phosphorylation AKT and ERK interacting in inactivation of PI3K / AKT and MAPK pathways for at least the MB SHH subgroup. Frasson *et al* have also recently proposed similar results indicating that the most important pathway involved in cell differentiation of MB stem cells is the PI3K/AKT/mTOR pathway (Frasson *et al.*, 2015). Although TGF-beta-dependent SMAD signaling pathway did not appear to be disrupted in our study, Nissen *et al* reported that Tuftsin promotes SMAD3 phosphorylation and reduces the phosphorylation of AKT by the TGF-beta-dependent signaling pathway (Nissen *et al.*, 2013). The involving of MR438 in cancer stem cells signaling pathways should also be confirmed by *in vivo* experimentations.

Cells transplanted in the subcutaneous heterotopic xenograft nude mice reduce *in vitro* culture steps, lead to approach clinical tumor cell morphology and molecular biology characteristics, thereby better mimicking human tumors and predicting clinical efficacy. But most human solid tumors do not represent the same biological behaviour and the expression of receptors and target proteins may also be changed because of the original microenvironment of human tumors. So the orthotopic transplanted tumor model is proposed to mimic the same microenvironment of tumor tissue *in vivo* and its origin has relatively higher clinical relevance to relative ectopic transplantation and reduces the incidence of false positives (Hasselbach *et al.*, 2014, Irtenkauf *et al.*, 2017). The establishments of MB orthotopic models were important to evaluate in the future our compound *in vivo*. In chapter 4, we have succeed to

obtain the 3 subgroup MB models of SHH, group3 and group4 with MB CSCs. However, there are still many points to be optimized. For tumor size follow up, MRI (magnetic resonance imaging) is one of tumor growth surveillance method for brain tumors but is limited for small tumors. Fluorescent or bioluminescent methods can solve this limitation and tumor cells could be also detectable without sacrifice of animals. Cells can be transfected with a reporter gene such as luciferase (Choi *et al.*, 2016). We have consequently transfected our MB cells by lentiviral particle containing RFP and luciferase genes. These cells transfected with Luciferase and RFP must be characterized for their properties for *in vivo* imaging as well as tumor growth.

In conclusion, concerning our *in vitro* models of MB stem cells, we found that inhibition of NRP-1 via the peptidomimetic MR438 seems to stimulate stem cell differentiation for different subgroups of MB, which can ultimately reduce the progression of MB, with an implication of the PI3K / AKT and MAPK signaling pathways for subgroup SHH. In addition, inhibition of NRP-1 via MR438 increased *in vitro* radiosensitivity of CSC models especially at the dose of 2 Gy. In heterotopic models, MR438 increased significantly radiosensitivity of SHH subgroup tumors. In an interesting way, the self-renewal capacity for CSCs after tumor dissociation was also decreased significantly when tumors were treated by MR438 + RT versus RT alone, not only for the SHH subgroup but also for group 3 and 4. This work showed the interest of targeting NRP-1 in association with radiotherapy to limit MB progression in decreasing the stem cells number in these tumors. Moreover, our *in vivo* experiments proved the possibility to use MR438 peptidomimetic as a

radiosensitizing agent for treatment of MB. Orthotopic xenograft animal models by using MB stem cells were established for our prospective study.

References:

References:

- ADESINA A M., NALBANTOGLU J.,CAVENEE W K.
p53 gene mutation and mdm2 gene amplification are uncommon in medulloblastoma.
Cancer Res., 1994, 54(21): 5649-51.
- BAO S., WU Q., MCLENDON R E., HAO Y., SHI Q., HJELMELAND A B.,
DEWHIRST M W., BIGNER D D.,RICH J N.
Glioma stem cells promote radioresistance by preferential activation of the DNA
damage response.
Nature., 2006, 444(7120): 756-60.
- BATTAGLIA A., BUZZONETTI A., MONEGO G., PERI L., FERRANDINA G.,
FANFANI F., SCAMBIA G.,FATTOROSS I A.
Neuropilin-1 expression identifies a subset of regulatory T cells in human lymph
nodes that is modulated by preoperative chemoradiation therapy in cervical cancer.
Immunology., 2008, 123(1): 129-38.
- BECHER O J.,HOLLAND E C.
Sox2, a marker for stem-like tumor cells in skin squamous cell carcinoma and
hedgehog subgroup medulloblastoma.
EMBO J., 2014, 33(18): 1984-6.
- BECHET D., TIRAND L., FAIVRE B., PLENAT F., BONNET C., BASTOGNE T.,
FROCHOT C., GUILLEMIN F.,BARBERI-HEYOB M.
Neuropilin-1 targeting photosensitization-induced early stages of thrombosis via
tissue factor release.
Pharm Res., 2010, 27(3): 468-79.
- BECK B., DRIESSENS G., GOOSSENS S., YOUSSEF K K., KUCHNIO A.,
CAAUWE A., SOTIROPOULOU P A., LOGES S., LAPOUGE G., CANDI A.,
MASCRE G., DROGAT B., DEKONINCK S., HAIGH J J., CARMELIET
P.,BLANPAIN C.
A vascular niche and a VEGF-Nrp1 loop regulate the initiation and stemness of skin
tumours.
Nature., 2011, 478(7369): 399-403
- BENACHOUR H., SEVE A., BASTOGNE T., FROCHOT C., VANDERESSE R.,
JASNIEWSKI J., MILADI I., BILLOTEY C., TILLEMENT O., LUX F.,BARBERI-
HEYOB M.
Multifunctional Peptide-conjugated hybrid silica nanoparticles for photodynamic
therapy and MRI.
Theranostics., 2012, 2(9): 889-904.

- BEN-SHUSHAN E., FELDMAN E., REUBINOFF B E.
Notch signaling regulates motor neuron differentiation of human embryonic stem cells.
Stem Cells., 2015, 33(2): 403-15.
- BIEGEL J A., BURK C D., BARR F G., EMANUEL B S.
Evidence for a 17p tumor related locus distinct from p53 in pediatric primitive neuroectodermal tumors.
Cancer Res., 1992, 52(12): 3391-5.
- BLAZEK E R., FOUTCH J L., MAKI G.
Daoy medulloblastoma cells that express CD133 are radioresistant relative to CD133-cells, and the CD133+ sector is enlarged by hypoxia.
Int J Radiat Oncol Biol Phys., 2007, 67(1): 1-5.
- BLOBE G C., SCHIEMANN W P., LODISH H F.
Role of transforming growth factor beta in human disease.
N Engl J Med., 2000, 342(18): 1350-8.
- BOURDEAUT F., MIQUEL C., ALAPETITE C., ROUJEAU T., DOZ F.
Medulloblastomas: update on a heterogeneous disease.
Curr Opin Oncol., 2011, 23(6): 630-7.
- BRUGIERES L., PIERRON G., CHOMPRET A., PAILLERETS B B., Di ROCCO F., VARLET P., PIERRE-KAHN A., CARON O., GRILL J., DELATTRE O.
Incomplete penetrance of the predisposition to medulloblastoma associated with germ-line SUFU mutations.
J Med Genet., 2010, 47(2): 142-4.
- BURGER P C., GRAHMANN F C., BLIESTLE A., KLEIHUES P.
Differentiation in the medulloblastoma. A histological and immunohistochemical study.
Acta Neuropathol., 1987, 73(2): 115-23.
- CAO Y., WANG L., NANDY D., ZHANG Y., BASU A., RADISKY D., MUKHOPADHYAY D.
Neuropilin-1 upholds dedifferentiation and propagation phenotypes of renal cell carcinoma cells by activating Akt and sonic hedgehog axes.
Cancer Res., 2008, 68(21): 8667-72.
- CAVELIERS V., GOODBODY A E., TRAN L L., PEERS S H., THORNBACK J R., BOSSUYT A.
Evaluation of ^{99m}Tc-RP128 as a potential inflammation imaging agent: human dosimetry and first clinical results.
J Nucl Med., 2001, 42(1): 154-61.

CHEN J K., TAIPALE J., YOUNG K E., MAITI T., BEACHY P A.
Small molecule modulation of Smoothened activity.
Proc Natl Acad Sci U S A., 2002, 99(22): 14071-6.

CHO Y J., TSHERNIAK A., TAMAYO P., SANTAGATA S., LIGON A.,
GREULICH H., BERHOUKIM R., AMANI V., GOUMNEROVA L., EBERHART
C G., LAU C C., OLSON J M., GILBERTSON R J., GAJJAR A., DELATTRE O.,
KOOL M., LIGON K., MEYERSON M., MESIROV J P., POMEROY S L.
Integrative genomic analysis of medulloblastoma identifies a molecular subgroup that
drives poor clinical outcome.
J Clin Oncol., 2011, 29(11): 1424-30.

CHOI S A., KWAK P A., KIM S K., PARK S H., LEE J Y., WANG K C., OH H J.,
KIM K., LEE D S., HWANG D W., PHI J H.
In vivo bioluminescence imaging for leptomeningeal dissemination of
medulloblastoma in mouse models.
BMC Cancer., 2016, 16(1): 723.

CHU W., SONG X., YANG X., MA L., ZHU J., HE M., WANG Z., WU Y.
Neuropilin-1 promotes epithelial-to-mesenchymal transition by stimulating nuclear
factor-kappa B and is associated with poor prognosis in human oral squamous cell
carcinoma.
PLoS One., 2014, 9(7): e101931.

CHUNG E J., MLINAR L B., SUGIMOTO M J., NORD K., ROMAN B
B., TIRRELL M.
In vivo biodistribution and clearance of peptide amphiphile micelles.
Nanomedicine., 2015, 11(2): 479-87.

CRAVEIRO R B., EHRHARDT M., HOLST M I., PIETSCH T., DILLOO D.
In comparative analysis of multi-kinase inhibitors for targeted medulloblastoma
therapy pazopanib exhibits promising in vitro and in vivo efficacy.
Oncotarget., 2014, 5(16): 7149-61.

CRAWFORD J R., MACDONALD T J., PACKER R J.
Medulloblastoma in childhood: new biological advances.
Lancet Neurol., 2007, 6(12): 1073-85.

CRAWFORD J R., ROOD B R., ROSSI C T., VEZINA G.
Medulloblastoma associated with novel PTCH mutation as primary manifestation of
Gorlin syndrome.
Neurology., 2009, 72(18): 1618.

DE LA POMPA J L., WAKEHAM A., CORREIA K M., SAMPER E., BROWN S.,
AGUILERA R J., NAKANO T., HONJO T., MAK T W., ROSSANT J., CONLON R
A.
Conservation of the Notch signalling pathway in mammalian neurogenesis.

Development., 1997, 124(6): 1139-48.

De JESUS-ACOSTA, A., LAHERU, D., MAITRA, A., ARCAROLI, J., RUDEK, M. A., DASARI, A., BLATCHFORD, P. J., QUACKENBUSH, K. & MESSERSMITH, W. (2014),

A phase II study of the gamma secretase inhibitor RO4929097 in patients with previously treated metastatic pancreatic adenocarcinoma.

Invest New Drugs, 2014, 32(4):739-45.

DIAZ-PADILLA, I., WILSON, M. K., CLARKE, B. A., HIRTE, H. W., WELCH, S. A., MACKAY, H. J., BIAGI, J. J., REEDIJK, M., WEBERPALS, J. I., FLEMING, G. F., WANG, L., LIU, G., ZHOU, C., BLATTNER, C., IVY, S. P. & OZA, A. M.

A phase II study of single-agent RO4929097, a gamma-secretase inhibitor of Notch signaling, in patients with recurrent platinum-resistant epithelial ovarian cancer: A study of the Princess Margaret, Chicago and California phase II consortia.

Gynecol Oncol, 2015, 137(2):216-22.

DIETL S., SCHWINN S., DIETL S., RIEDEL S., DEINLEIN F., RUTKOWSKI S., von BUEREN A O., KRAUSS J., SCHWEITZER T., VINCE G H., PICARD D., EYRICH M., ROSENWALD A., RAMASWAMY V., TAYLOR M D., REMKE M., MONORANU C M., BEILHACK A., SCHLEGEL P G., WOLFL M.

MB3W1 is an orthotopic xenograft model for anaplastic medulloblastoma displaying cancer stem cell- and Group 3-properties.

BMC Cancer., 2016, 16:115.

DONG J C., GAO H., ZUO S Y., ZHANG H Q., ZHAO G., SUN S L., HAN H L., JIN L L., SHAO L H., WEI W., JIN S Z.

Neuropilin 1 expression correlates with the Radio-resistance of human non-small-cell lung cancer cells.

J Cell Mol Med., 2015, 19(9): 2286-95.

DRAY N., TESSMAR-RAIBLE K., Le GOUAR M., VIBERT L., CHRISTODOULOU F., SCHIPANY K., GUILLOU A., ZANTKE J., SNYMAN H., BEHAGUE J., VERVOORT M., ARENDT D., BALAVOINE G.

Hedgehog signaling regulates segment formation in the annelid *Platynereis*.

Science., 2010, 329(5989): 339-42.

EHRHARDT M., CRAVEIRO R B., HOLST M I., PIETSCH T., DILLOO D.

The PI3K inhibitor GDC-0941 displays promising in vitro and in vivo efficacy for targeted medulloblastoma therapy.

Oncotarget., 2015, 6(2): 802-13.

EYLER C E., RICH J N.

Survival of the fittest: cancer stem cells in therapeutic resistance and angiogenesis.

J Clin Oncol., 2008, 26(17): 2839-45.

FISCHER A., GESSLER M.

Delta-Notch--and then? Protein interactions and proposed modes of repression by Hes and Hey bHLH factors.

Nucleic Acids Res., 2007, 35(14): 4583-96.

FRANGE P., ALAPETITE C., GABORIAUD G., BOURS D., ZUCKER J M., ZERAH M., BRISSE H., CHEVIGNARD M., MOSSERI V., BOUFFET E., DOZ F.

From childhood to adulthood: long-term outcome of medulloblastoma patients. The Institut Curie experience (1980-2000).

J Neurooncol., 2009, 95(2): 271-9.

FRASSON C., RAMPAZZO E., ACCORDI B., BEGGIO G., PISTOLLATO F., BASSO G., PERSANO L.

Inhibition of PI3K Signalling Selectively Affects Medulloblastoma Cancer Stem Cells.

Biomed Res Int., 2015, 2015: 973912.

FRIEDMAN H S., BURGER P C., BIGNER S H., TROJANOWSKI J Q., BRODEUR G M., HE X M., WIKSTRAND C J., KURTZBERG J., BERENS M E., HALPERIN E C., ET A.

Phenotypic and genotypic analysis of a human medulloblastoma cell line and transplantable xenograft (D341 Med) demonstrating amplification of c-myc.

Am J Pathol., 1988, 130(3): 472-84.

FRIEDMAN H S., BURGER P C., BIGNER S H., TROJANOWSKI J Q., WIKSTRAND C J., HALPERIN E C., BIGNER D D.

Establishment and characterization of the human medulloblastoma cell line and transplantable xenograft D283 Med.

J Neuropathol Exp Neurol., 1985, 44(6): 592-605.

FOULADI, M., STEWART, C. F., OLSON, J., WAGNER, L. M., ONAR-THOMAS, A., KOCAK, M., PACKER, R. J., GOLDMAN, S., GURURANGAN, S., GAJJAR, A., DEMUTH, T., KUN, L. E., BOYETT, J. M. & GILBERTSON, R. J.

Phase I trial of MK-0752 in children with refractory CNS malignancies: a pediatric brain tumor consortium study.

J Clin Oncol., 2011, 29(26):3529-3534.

GARG N., BAKHSHINYAN D., VENUGOPAL C., MAHENDRAM S., ROSA D A., VIJAYAKUMAR T., MANORANJAN B., HALLETT R., MCFARLANE N., DELANEY K H., KWIECIEN J M., ARPIN C C., LAI P S., GOMEZ-BIAGI R F., ALI A M., de ARAUJO E D., AJANI O A., HASSELL J A., GUNNING P T., SINGH S K.

CD133+ brain tumor-initiating cells are dependent on STAT3 signaling to drive medulloblastoma recurrence.

Oncogene., 2017, 36(5): 606-17.

GE X., MILENKOVIC L., SUYAMA K., HARTL T., PURZNER T., WINANS A., MEYER T., SCOTT M P.

Phosphodiesterase 4D acts downstream of Neuropilin to control Hedgehog signal transduction and the growth of medulloblastoma.
Elife., 2015, 4

GLINKA Y., STOILOVA S., MOHAMMED N., PRUD'HOMME G J.
Neuropilin-1 exerts co-receptor function for TGF-beta-1 on the membrane of cancer cells and enhances responses to both latent and active TGF-beta.
Carcinogenesis., 2011, 32(4): 613-21.

GONG C., VALDUGA J., CHATEAU A., RICHARD M., PELLEGRINI-MOISE N., BARBERI-HEYOB M., CHASTAGNER P., BOURA C.
Stimulation of medulloblastoma stem cells differentiation by a peptidomimetic targeting neuropilin-1.
Oncotarget., 2018, 9(20): 15312-25.

GOODRICH L V., MILENKOVIC L., HIGGINS K M., SCOTT M P.
Altered neural cell fates and medulloblastoma in mouse patched mutants.
Science., 1997, 277(5329): 1109-13.

GRAZIANI G., LACAL P M.
Neuropilin-1 as Therapeutic Target for Malignant Melanoma.
Front Oncol., 2015, 5: 125.

GRILL J., SAINTE-ROSE C., JOUVET A., GENTET J C., LEJARS O., FRAPPAZ D., DOZ F., RIALLAND X., PICHON F., BERTOZZI A I., CHASTAGNER P., COUANET D., HABRAND J L., RAQUIN M A., Le DELEY M C., KALIFA C.
Treatment of medulloblastoma with postoperative chemotherapy alone: an SFOP prospective trial in young children.
Lancet Oncol., 2005, 6(8): 573-80.

HAHN H., WOJNOWSKI L., ZIMMER A M., HALL J., MILLER G., ZIMMER A.
Rhabdomyosarcomas and radiation hypersensitivity in a mouse model of Gorlin syndrome.
Nat Med., 1998, 4(5): 619-22.

HAMERLIK P., LATHIA J D., RASMUSSEN R., WU Q., BARTKOVA J., LEE M., MOUDRY P., BARTEK J J., FISCHER W., LUKAS J., RICH J N., BARTEK J.
Autocrine VEGF-VEGFR2-Neuropilin-1 signaling promotes glioma stem-like cell viability and tumor growth.
J Exp Med., 2012, 209(3): 507-20.

HASSELBACH L A., IRTENKAUF S M., LEMKE N W., NELSON K K., BEREZOVSKY A D., CARLTON E T., TRANSOU A D., MIKKELSEN T., DECARVALHO A C.
Optimization of high grade glioma cell culture from surgical specimens for use in clinically relevant animal models and 3D immunochemistry.
J Vis Exp., 2014, 83: e51088.

HAYDEN G M., SU Y S., BANDARA S., TSAI F C., HONG J., CONLEY N., RAYBURN H., MILENKOVIC L., MEYER T.,SCOTT M P.

Neuropilin-2 contributes to tumorigenicity in a mouse model of Hedgehog pathway medulloblastoma.

J Neurooncol., 2013, 115(2): 161-8.

HE X., ZHANG L., CHEN Y., REMKE M., SHIH D., LU F., WANG H., DENG Y., YU Y., XIA Y., WU X., RAMASWAMY V., HU T., WANG F., ZHOU W., BURNS D K., KIM S H., KOOL M., PFISTER S M., WEINSTEIN L S., POMEROY S L., GILBERTSON R J., RUBIN J B., HOU Y., WECHSLER-REYA R., TAYLOR M D.,LU Q R.

The G protein alpha subunit Galphas is a tumor suppressor in Sonic hedgehog-driven medulloblastoma.

Nat Med., 2014, 20(9): 1035-42.

HEMMATI H D., NAKANO I., LAZAREFF J A., MASTERMAN-SMITH M., GESCHWIND D H., BRONNER-FRASER M.,KORNBLUM H I.

Cancerous stem cells can arise from pediatric brain tumors.

Proc Natl Acad Sci U S A., 2003, 100(25): 15178-83.

HILLMAN R T., FENG B Y., NI J., WOO W M., MILENKOVIC L., HAYDEN G M., TERUEL M N., ORO A E., CHEN J K.,SCOTT M P.

Neuropilins are positive regulators of Hedgehog signal transduction.

Genes Dev., 2011, 25(22): 2333-46.

HU C., ZHU P., XIA Y., HUI K., WANG M.,JIANG X.

Role of the NRP-1-mediated VEGFR2-independent pathway on radiation sensitivity of non-small cell lung cancer cells.

J Cancer Res Clin Oncol., 2018, 144(7):1329-37.

HUSSEIN D., PUNJARUK W., STORER L C D., SHAW L., OTHMAN R T., PEET A., MILLER S., BANDOPADHYAY G., HEATH R., KUMARI R., BOWMAN K J., BRAKER P., RAHMAN R., JONES G D D., WATSON S., LOWE J., KERR I D., GRUNDY R G.,COYLE B.

Pediatric brain tumor cancer stem cells: cell cycle dynamics, DNA repair, and etoposide extrusion.

Neuro-Oncology., 2010, 13(1): 70-83.

INGHAM P W., NAKANO Y.,SEGER C.

Mechanisms and functions of Hedgehog signalling across the metazoa.

Nat Rev Genet., 2011, 12(6): 393-406.

IRTENKAUF S M., SOBIECHOWSKI S., HASSELBACH L A., NELSON K K., TRANSOU A D., CARLTON E T., MIKKELSEN T.,DECARVALHO A C.

Optimization of Glioblastoma Mouse Orthotopic Xenograft Models for Translational Research.

Comp Med., 2017, 67(4): 300-14.

ISO T., KEDES L.,HAMAMORI Y.

HES and HERP families: multiple effectors of the Notch signaling pathway.

J Cell Physiol., 2003, 194(3): 237-55.

JACOBSEN P F., JENKYN D J.,PAPADIMITRIOU J M.

Establishment of a human medulloblastoma cell line and its heterotransplantation into nude mice.

J Neuropathol Exp Neurol., 1985, 44(5): 472-85.

JENKIN D., SHABANAH M A., SHAIL E A., GRAY A., HASSOUNAH M.,
KHAFAFA Y., KOFIDE A., MUSTAFA M.,SCHULTZ H.

Prognostic factors for medulloblastoma.

Int J Radiat Oncol Biol Phys., 2000, 47(3): 573-84.

JUBB A M., STRICKLAND L A., LIU S D., MAK J., SCHMIDT M.,KOEPPEN H.

Neuropilin-1 expression in cancer and development.

J Pathol., 2012, 226(1): 50-60.

KAWAUCHI D., OGG R J., LIU L., SHIH D., FINKELSTEIN D., MURPHY B L.,
REHG J E., KORSHUNOV A., CALABRESE C., ZINDY F., PHOENIX T.,
KAWAGUCHI Y., GRONYCH J., GILBERTSON R J., LICHTER P., GAJJAR A.,
KOOL M., NORTHCOTT P A., PFISTER S M.,ROUSSEL M F.

Novel MYC-driven medulloblastoma models from multiple embryonic cerebellar cells.

Oncogene., 2017, 36(37): 5231-42.

KIM E J., SAHAI V., ABEL E V., GRIFFITH K A., GREENSON J K., TAKEBE N.,
KHAN G N., BLAU J L., CRAIG R., BALIS U G., ZALUPSKI M M.,SIMEONE D M.

Pilot clinical trial of hedgehog pathway inhibitor GDC-0449 (vismodegib) in combination with gemcitabine in patients with metastatic pancreatic adenocarcinoma.

Clin Cancer Res., 2014, 20(23): 5937-45.

KIM W., SEOK K Y., SOO K J., SHIN N Y., HANKS S K.,SONG W K.

The integrin-coupled signaling adaptor p130Cas suppresses Smad3 function in transforming growth factor-beta signaling.

Mol Biol Cell., 2008, 19(5): 2135-46.

KLAGSBRUN M.,SHIMIZU A.

Semaphorin 3E, an exception to the rule.

J Clin Invest., 2010, 120(8): 2658-60.

KOOL M., KORSHUNOV A., REMKE M., JONES D T., SCHLANSTEIN M.,
NORTHCOTT P A., CHO Y J., KOSTER J., SCHOUTEN-VAN M A., van
VUURDEN D., CLIFFORD S C., PIETSCH T., von BUEREN A O., RUTKOWSKI

S., MCCABE M., COLLINS V P., BACKLUND M L., HABERLER C., BOURDEAUT F., DELATTRE O., DOZ F., ELLISON D W., GILBERTSON R J., POMEROY S L., TAYLOR M D., LICHTER P., PFISTER S M.

Molecular subgroups of medulloblastoma: an international meta-analysis of transcriptome, genetic aberrations, and clinical data of WNT, SHH, Group 3, and Group 4 medulloblastomas.

Acta Neuropathol., 2012, 123(4): 473-84.

KUMAR V., KUMAR V., MCGUIRE T., COULTER D W., SHARP J G., MAHATO R I.

Challenges and Recent Advances in Medulloblastoma Therapy.

Trends Pharmacol Sci., 2017, 38(12): 1061-84.

LAGERWEIJ T., HIDDINGH L., BIESMANS D., CROMMENTUIJN M H., CLOOS J., LI X N., KOGISO M., TANNOUS B A., VANDERTOP W P., NOSKE D P., KASPERS G J., WURDINGER T., HULLEMAN E.

A chemical screen for medulloblastoma identifies quercetin as a putative radiosensitizer.

Oncotarget., 2016, 7(24): 35776-88.

LEUNG C., LINGBEEK M., SHAKHOVA O., LIU J., TANGER E., SAREMASLANI P., Van LOHUIZEN M., MARINO S.

Bmi1 is essential for cerebellar development and is overexpressed in human medulloblastomas.

Nature., 2004, 428(6980): 337-41.

LEVINA E., OREN M., BEN-ZE'EV A.

Downregulation of beta-catenin by p53 involves changes in the rate of beta-catenin phosphorylation and Axin dynamics.

Oncogene., 2004, 23(25): 4444-53.

LIN C P., LIU C R., LEE C N., CHAN T S., LIU H E.

Targeting c-Myc as a novel approach for hepatocellular carcinoma.

World J Hepatol., 2010, 2(1): 16-20.

LOUIS D N., PERRY A., REIFENBERGER G., von DEIMLING A., FIGARELLA-BRANGER D., CAVENEE W K., OHGAKI H., WIESTLER O D., KLEIHUES P., ELLISON D W.

The 2016 World Health Organization Classification of Tumors of the Central Nervous System: a summary.

Acta Neuropathol., 2016, 131(6): 803-20.

MANORANJAN B., VENUGOPAL C., MCFARLANE N., DOBLE B W., DUNN S E., SCHEINEMANN K., SINGH S K.

Medulloblastoma stem cells: where development and cancer cross pathways.

Pediatr Res., 2012, 71(4 Pt 2): 516-22.

MASSAGUE J.,XI Q.

TGF-beta control of stem cell differentiation genes.

FEBS Lett., 2012, 586(14): 1953-8.

MINDE D P., RADLI M., FORNERIS F., MAURICE M M.,RUDIGER S G.

Large extent of disorder in Adenomatous Polyposis Coli offers a strategy to guard Wnt signalling against point mutations.

PLoS One., 2013, 8(10): e77257.

MORRISSY A S., GARZIA L., SHIH D J., ZUYDERDUYN S., HUANG X., SKOWRON P., REMKE M., CAVALLI F M., RAMASWAMY V., LINDSAY P E., JELVEH S., DONOVAN L K., WANG X., LUU B., ZAYNE K., LI Y., MAYOH C., THIESSEN N., MERCIER E., MUNGALL K L., MA Y., TSE K., ZENG T., SHUMANSKY K., ROTH A J., SHAH S., FAROOQ H., KIJIMA N., HOLGADO B L., LEE J J., MATAN-LITHWICK S., LIU J., MACK S C., MANNO A., MICHEALRAJ K A., NOR C., PEACOCK J., QIN L., REIMAND J., ROLIDER A., THOMPSON Y Y., WU X., PUGH T., ALLY A., BILENKY M., BUTTERFIELD Y S., CARLSEN R., CHENG Y., CHUAH E., CORBETT R D., DHALLA N., HE A., LEE D., LI H I., LONG W., MAYO M., PLETTNER P., QIAN J Q., SCHEIN J E., TAM A., WONG T., BIROL I., ZHAO Y., FARIA C C., PIMENTEL J., NUNES S., SHALABY T., GROTZER M., POLLACK I F., HAMILTON R L., LI X N., BENDEL A E., FULTS D W., WALTER A W., KUMABE T., TOMINAGA T., COLLINS V P., CHO Y J., HOFFMAN C., LYDEN D., WISOFF J H., GARVIN J J., STEARNS D S., MASSIMI L., SCHULLER U., STERBA J., ZITTERBART K., PUGET S., AYRAULT O., DUNN S E., TIRAPELLI D P., CARLOTTI C G., WHEELER H., HALLAHAN A R., INGRAM W., MACDONALD T J., OLSON J J., Van MEIR E G., LEE J Y.,WANG K C, *et al.*

Divergent clonal selection dominates medulloblastoma at recurrence.

Nature., 2016, 529(7586): 351-7.

NASSAR D.,BLANPAIN C.

Cancer Stem Cells: Basic Concepts and Therapeutic Implications.

Annu Rev Pathol., 2016, 11: 47-76.

NISSEN J C., SELWOOD D L.,TSIRKA S E.

Tuftsins signal through its receptor neuropilin-1 via the transforming growth factor beta pathway.

J Neurochem., 2013, 127(3): 394-402.

NORTHCOTT P A., KORSHUNOV A., WITT H., HIELSCHER T., EBERHART C G., MACK S., BOUFFET E., CLIFFORD S C., HAWKINS C E., FRENCH P., RUTKA J T., PFISTER S.,TAYLOR M D.

Medulloblastoma comprises four distinct molecular variants.

J Clin Oncol., 2011, 29(11): 1408-14.

NUSSE R.

Wnt signaling in disease and in development.

Cell Res., 2005, 15(1): 28-32.

ORBACH D., CHASTAGNER P., BOURDEAUT F., DOZ F.

[Medulloblastoma in childhood: an heterogeneous disease requiring treatment adjustments to known risk factors].

Rev Prat., 2012, 62(7): 989-90.

OSADA H., TOKUNAGA T., NISHI M., HATANAKA H., ABE Y., TSUGU A., KIJIMA H., YAMAZAKI H., UHEYAMA Y., NAKAMURA M.

Overexpression of the neuropilin 1 (NRP1) gene correlated with poor prognosis in human glioma.

Anticancer Res., 2004, 24(2B): 547-52.

OTHMAN R T., KIMISHI I., BRADSHAW T D., STORER L C., KORSHUNOV A., PFISTER S M., GRUNDY R G., KERR I D., COYLE B.

Overcoming multiple drug resistance mechanisms in medulloblastoma.

Acta Neuropathol Commun., 2014, 2: 57.

PEI Y., MOORE C E., WANG J., TEWARI A K., EROSHKIN A., CHO Y J., WITT H., KORSHUNOV A., READ T A., SUN J L., SCHMITT E M., MILLER C R., BUCKLEY A F., MCLENDON R E., WESTBROOK T F., NORTHCOTT P A., TAYLOR M D., PFISTER S M., FEBBO P G., WECHSLER-REYA R J.

An animal model of MYC-driven medulloblastoma.

Cancer Cell., 2012, 21(2): 155-67.

PENG Y., LIU Y M., LI L C., WANG L L., WU X L.

MicroRNA-338 inhibits growth, invasion and metastasis of gastric cancer by targeting NRP1 expression.

PLoS One., 2014, 9(4): e94422.

PERNOT M., VANDERESSE R., FROCHOT C., GUILLEMIN F., BARBERI-HEYOB M.

Stability of peptides and therapeutic success in cancer.

Expert Opin Drug Metab Toxicol., 2011, 7(7): 793-802.

PFAFF E., REMKE M., STURM D., BENNER A., WITT H., MILDE T., von BUEREN A O., WITTMANN A., SCHOTTLER A., JORCH N., GRAF N., KULOZIK A E., WITT O., SCHEURLIN W., von DEIMLING A., RUTKOWSKI S., TAYLOR M D., TABORI U., LICHTER P., KORSHUNOV A., PFISTER S M.

TP53 mutation is frequently associated with CTNNB1 mutation or MYCN amplification and is compatible with long-term survival in medulloblastoma.

J Clin Oncol., 2010, 28(35): 5188-96.

POSCHL J., STARK S., NEUMANN P., GROBNER S., KAWAUCHI D., JONES D T., NORTHCOTT P A., LICHTER P., PFISTER S M., KOOL M., SCHULLER U.

Genomic and transcriptomic analyses match medulloblastoma mouse models to their human counterparts.

Acta Neuropathol., 2014, 128(1): 123-36.

PRUD'HOMME G J., GLINKA Y.

Neuropilins are multifunctional coreceptors involved in tumor initiation, growth, metastasis and immunity.

Oncotarget., 2012, 3(9): 921-39.

PUISSANT A., FRUMM S M., ALEXE G., BASSIL C F., QI J., CHANTHERY Y H., NEKRITZ E A., ZEID R., GUSTAFSON W C., GRENINGER P., GARNETT M J., MCDERMOTT U., BENES C H., KUNG A L., WEISS W A., BRADNER J E., STEGMAIER K.

Targeting MYCN in neuroblastoma by BET bromodomain inhibition.

Cancer Discov., 2013, 3(3): 308-23.

RAMASWAMY V., REMKE M., ADAMSKI J., BARTELS U., TABORI U., WANG X., HUANG A., HAWKINS C., MABBOTT D., LAPERRIERE N., TAYLOR M D., BOUFFET E.

Medulloblastoma subgroup-specific outcomes in irradiated children: who are the true high-risk patients?

Neuro Oncol., 2016, 18(2): 291-7.

RAMASWAMY V., REMKE M., BOUFFET E., FARIA C C., PERREAULT S., CHO Y J., SHIH D J., LUU B., DUBUC A M., NORTHCOTT P A., SCHULLER U., GURURANGAN S., MCLENDON R., BIGNER D., FOULADI M., LIGON K L., POMEROY S L., DUNN S., TRISCOTT J., JABADO N., FONTEBASSO A., JONES D T., KOOL M., KARAJANNIS M A., GARDNER S L., ZAGZAG D., NUNES S., PIMENTEL J., MORA J., LIPP E., WALTER A W., RYZHOVA M., ZHELUDKOVA O., KUMIROVA E., ALSHAMI J., CROUL S E., RUTKA J T., HAWKINS C., TABORI U., CODISPOTI K E., PACKER R J., PFISTER S M., KORSHUNOV A., TAYLOR M D.

Recurrence patterns across medulloblastoma subgroups: an integrated clinical and molecular analysis.

Lancet Oncol., 2013, 14(12): 1200-7.

RAMASWAMY V., TAYLOR M D.

Medulloblastoma: From Myth to Molecular.

J Clin Oncol., 2017, 35(21): 2355-63.

READ T A., FOGARTY M P., MARKANT S L., MCLENDON R E., WEI Z., ELLISON D W., FEBBO P G., WECHSLER-REYA R J.

Identification of CD15 as a marker for tumor-propagating cells in a mouse model of medulloblastoma.

Cancer Cell., 2009, 15(2): 135-47.

RECIO C., MAIONE F., IQBAL A J., MASCOLO N., De FEO V.

The Potential Therapeutic Application of Peptides and Peptidomimetics in Cardiovascular Disease.

Front Pharmacol., 2016, 7: 526.

REMKE M., RAMASWAMY V., TAYLOR M D.

Medulloblastoma molecular dissection: the way toward targeted therapy.

Curr Opin Oncol., 2013, 25(6): 674-81.

RICHARD M., CHATEAU A., JELSCH C., DIDIERJEAN C., MANIVAL X., CHARRON C., MAIGRET B., BARBERI-HEYOB M., CHAPLEUR Y., BOURA C., PELLEGRINI-MOISE N.

Carbohydrate-based peptidomimetics targeting neuropilin-1: Synthesis, molecular docking study and in vitro biological activities.

Bioorg Med Chem., 2016, 24(21): 5315-25.

RODON J., TAWBI H A., THOMAS A L., STOLLER R G., TURTSCHI C P., BASELGA J., SARANTOPOULOS J., MAHALINGAM D., SHOU Y., MOLES M A., YANG L., GRANVIL C., HURH E., ROSE K L., AMAKYE D D., DUMMER R., MITA A C.

A phase I, multicenter, open-label, first-in-human, dose-escalation study of the oral smoothened inhibitor Sonidegib (LDE225) in patients with advanced solid tumors.

Clin Cancer Res., 2014, 20(7): 1900-9.

ROZHOK A I., DEGREGORI J.

Toward an evolutionary model of cancer: Considering the mechanisms that govern the fate of somatic mutations.

Proc Natl Acad Sci U S A., 2015, 112(29): 8914-21.

SALAROLI R., Di TOMASO T., RONCHI A., CECCARELLI C., CAMMELLI S., CAPPELLINI A., MARTINELLI G N., BARBIERI E., GIANCASPERO F., CENACCHI G.

Radiobiologic response of medulloblastoma cell lines: involvement of beta-catenin?

J Neurooncol., 2008, 90(3): 243-51.

SAMKARI A., WHITE J C., PACKER R J.

Medulloblastoma: Toward Biologically Based Management.

Semin Pediatr Neurol., 2015, 22(1): 6-13.

SARKAR S., MIRZAEI R., ZEMP F J., WU W., SENGHER D L., ROBBINS S M., YONG V W.

Activation of NOTCH signaling by tenascin-C promotes growth of human brain tumor-initiating cells.

Cancer Res., 2017, 77(12): 3231-3243

SCHROEDER K., GURURANGAN S.

Molecular variants and mutations in medulloblastoma.

Pharmgenomics Pers Med., 2014, 7: 43-51.

SCHWALBE E C., LINDSEY J C., NAKJANG S., CROSIER S., SMITH A J., HICKS D., RAFIEE G., HILL R M., ILIASOVA A., STONE T., PIZER B., MICHALSKI A., JOSHI A., WHARTON S B., JACQUES T S., BAILEY S., WILLIAMSON D., CLIFFORD S C.

Novel molecular subgroups for clinical classification and outcome prediction in childhood medulloblastoma: a cohort study.

The Lancet Oncology., 2017, 18(7): 958-71.

SENGUPTA S., WEERARATNE S D., SUN H., PHALLEN J., RALLAPALLI S K., TEIDER N., KOSARAS B., AMANI V., PIERRE-FRANCOIS J., TANG Y., NGUYEN B., YU F., SCHUBERT S., BALANSAY B., MATHIOS D., LECHPAMMER M., ARCHER T C., TRAN P., REIMER R J., COOK J M., LIM M., JENSEN F E., POMEROY S L., CHO Y J.

alpha5-GABAA receptors negatively regulate MYC-amplified medulloblastoma growth.

Acta Neuropathol., 2014, 127(4): 593-603.

SIEGEL M J., FINLAY J L., ZACHAROULIS S.

State of the art chemotherapeutic management of pediatric brain tumors.

Expert Rev Neurother., 2006, 6(5): 765-79.

SINGH S K., CLARKE I D., TERASAKI M., BONN V E., HAWKINS C., SQUIRE J., DIRKS P B.

Identification of a cancer stem cell in human brain tumors.

Cancer Res., 2003, 63(18): 5821-8.

SINGH S K., HAWKINS C., CLARKE I D., SQUIRE J A., BAYANI J., HIDE T., HENKELMAN R M., CUSIMANO M D., DIRKS P B.

Identification of human brain tumour initiating cells.

Nature., 2004, 432(7015): 396-401.

SMOLL N R.

Relative survival of childhood and adult medulloblastomas and primitive neuroectodermal tumors (PNETs).

Cancer., 2012, 118(5): 1313-22.

SMOLL N R., DRUMMOND K J.

The incidence of medulloblastomas and primitive neuroectodermal tumours in adults and children.

J Clin Neurosci., 2012, 19(11): 1541-4.

SNUDERL M., BATISTA A., KIRKPATRICK N D., RUIZ D A C., RIEDEMANN L., WALSH E C., ANOLIK R., HUANG Y., MARTIN J D., KAMOUN W., KNEVELS E., SCHMIDT T., FARRAR C T., VAKOC B J., MOHAN N., CHUNG E., ROBERGE S., PETERSON T., BAIS C., ZHELYAZKOVA B H., YIP S., HASSELBLATT M., ROSSIG C., NIEMEYER E., FERRARA N., KLAGSBRUN

- M., DUDA D G., FUKUMURA D., XU L., CARMELIET P., JAIN R K.
Targeting placental growth factor/neuropilin 1 pathway inhibits growth and spread of medulloblastoma.
Cell., 2013, 152(5): 1065-76.
- SOKER S., GOLLAMUDI-PAYNE S., FIDDER H., CHARMAHELLI H., KLAGSBRUN M.
Inhibition of vascular endothelial growth factor (VEGF)-induced endothelial cell proliferation by a peptide corresponding to the exon 7-encoded domain of VEGF165.
J Biol Chem., 1997, 272(50): 31582-8.
- STARZEC A., LADAM P., VASSY R., BADACHE S., BOUCHEMAL N., NAVAZA A., du PENHOAT C H., PERRET G Y.
Structure-function analysis of the antiangiogenic ATWLPPR peptide inhibiting VEGF(165) binding to neuropilin-1 and molecular dynamics simulations of the ATWLPPR/neuropilin-1 complex.
Peptides., 2007, 28(12): 2397-402.
- TAIPALE J., COOPER M K., MAITI T., BEACHY P A.
Patched acts catalytically to suppress the activity of Smoothened.
Nature., 2002, 418(6900): 892-7.
- TAYLOR M D., NORTHCOTT P A., KORSHUNOV A., REMKE M., CHO Y J., CLIFFORD S C., EBERHART C G., PARSONS D W., RUTKOWSKI S., GAJJAR A., ELLISON D W., LICHTER P., GILBERTSON R J., POMEROY S L., KOOL M., PFISTER S M.
Molecular subgroups of medulloblastoma: the current consensus.
Acta Neuropathol., 2012, 123(4): 465-72.
- TEODORCZYK M., SCHMIDT M H.
Notching on Cancer's Door: Notch Signaling in Brain Tumors.
Front Oncol., 2014, 4: 341.
- THOMPSON M C., FULLER C., HOGG T L., DALTON J., FINKELSTEIN D., LAU C C., CHINTAGUMPALA M., ADESINA A., ASHLEY D M., KELLIE S J., TAYLOR M D., CURRAN T., GAJJAR A., GILBERTSON R J.
Genomics identifies medulloblastoma subgroups that are enriched for specific genetic alterations.
J Clin Oncol., 2006, 24(12): 1924-31.
- VAGNER J., QU H., HRUBY V J.
Peptidomimetics, a synthetic tool of drug discovery.
Curr Opin Chem Biol., 2008, 12(3): 292-6.
- VANDER K C., JUSINO M A., PERMAN B., NEAU D B., BELLAMY H D., LEAHY D J.
Structural basis for ligand and heparin binding to neuropilin B domains.

Proc Natl Acad Sci U S A., 2007, 104(15): 6152-7.

VESCOVI A L., GALLI R., REYNOLDS B A.

Brain tumour stem cells.

Nat Rev Cancer., 2006, 6(6): 425-36.

VON BUEREN A O., OEHLER C., SHALABY T., von HOFF K., PRUSCHY M., SEIFERT B., GERBER N U., WARMUTH-METZ M., STEARNS D., EBERHART C G., KORTMANN R D., RUTKOWSKI S., GROTZER M A.

c-MYC expression sensitizes medulloblastoma cells to radio- and chemotherapy and has no impact on response in medulloblastoma patients.

BMC Cancer., 2011, 11:74.

VON WRONSKI M A., RAJU N., PILLAI R., BOGDAN N J., MARINELLI E R., NANJAPPAN P., RAMALINGAM K., ARUNACHALAM T., EATON S., LINDER K E., YAN F., POCHON S., TWEEDLE M F., NUNN A D.

Tuftsins bind neuropilin-1 through a sequence similar to that encoded by exon 8 of vascular endothelial growth factor.

J Biol Chem., 2006, 281(9): 5702-10.

WANG L., DUTTA S K., KOJIMA T., XU X., KHOSRAVI-FAR R., EKKER S C., MUKHOPADHYAY D.

Neuropilin-1 modulates p53/caspases axis to promote endothelial cell survival.

PLoS One., 2007, 2(11): e1161.

WANG X., DUBUC A M., RAMASWAMY V., MACK S., GENDOO D M., REMKE M., WU X., GARZIA L., LUU B., CAVALLI F., PEACOCK J., LOPEZ B., SKOWRON P., ZAGZAG D., LYDEN D., HOFFMAN C., CHO Y J., EBERHART C., MACDONALD T., LI X N., Van METER T., NORTHCOTT P A., HAIBEKAINS B., HAWKINS C., RUTKA J T., BOUFFET E., PFISTER S M., KORSHUNOV A., TAYLOR M D.

Medulloblastoma subgroups remain stable across primary and metastatic compartments.

Acta Neuropathol., 2015, 129(3): 449-57.

WANG X., VENUGOPAL C., MANORANJAN B., MCFARLANE N., O'FARRELL E., NOLTE S., GUNNARSSON T., HOLLENBERG R., KWIECIEN J., NORTHCOTT P., TAYLOR M D., HAWKINS C., SINGH S K.

Sonic hedgehog regulates Bmi1 in human medulloblastoma brain tumor-initiating cells.

Oncogene., 2012, 31(2): 187-99.

WARD R J., LEE L., GRAHAM K., SATKUNENDRAN T., YOSHIKAWA K., LING E., HARPER L., AUSTIN R., NIEUWENHUIS E., CLARKE I D., HUI C C., DIRKS P B.

Multipotent CD15+ cancer stem cells in patched-1-deficient mouse medulloblastoma.

Cancer Res., 2009, 69(11): 4682-90.

WEEKES C D., BEERAM M., TOLCHER A W., PAPADOPOULOS K P., GORE L., HEGDE P., XIN Y., YU R., SHIH L M., XIANG H., BRACHMANN R K.,PATNAIK A.

A phase I study of the human monoclonal anti-NRP1 antibody MNRP1685A in patients with advanced solid tumors.

Invest New Drugs., 2014, 32(4): 653-60.

WENDT M K., SMITH J A.,SCHIEMANN W P.

p130Cas is required for mammary tumor growth and transforming growth factor-beta-mediated metastasis through regulation of Smad2/3 activity.

J Biol Chem., 2009, 284(49): 34145-56.

WILD J R., STATON C A., CHAPPLE K.,CORFE B M.

Neuropilins: expression and roles in the epithelium.

Int J Exp Pathol., 2012, 93(2): 81-103.

XU J., MARGOL A., ASGHARZADEH S.,ERDREICH-EPSTEIN A.

Pediatric brain tumor cell lines.

J Cell Biochem., 2015, 116(2): 218-24.

YOGI K., SRIDHAR E., GOEL N., JALALI R., GOEL A., MOIYADI A., THORAT R., PANWALKAR P., KHIRA A., DASGUPTA A., SHETTY P.,SHIRSAT N V.

MiR-148a, a microRNA upregulated in the WNT subgroup tumors, inhibits invasion and tumorigenic potential of medulloblastoma cells by targeting Neuropilin 1.

Oncoscience., 2015, 2(4): 334-48.

YOSHIDA A., SHIMIZU A., ASANO H., KADONOSONO T., KONDOH S K., GERETTI E., MAMMOTO A., KLAGSBRUN M.,SEO M K.

VEGF-A/NRP1 stimulates GIPC1 and Syx complex formation to promote RhoA activation and proliferation in skin cancer cells.

Biol Open., 2015, 4(9): 1063-76.

ZHAO X., LIU Z., YU L., ZHANG Y., BAXTER P., VOICU H., GURUSIDDAPPA S., LUAN J., SU J M., LEUNG H C.,LI X N.

Global gene expression profiling confirms the molecular fidelity of primary tumor-based orthotopic xenograft mouse models of medulloblastoma.

Neuro Oncol., 2012, 14(5): 574-83.

Appendix:

Stimulation of medulloblastoma stem cells differentiation by a peptidomimetic targeting Neuropilin-1

Caifeng Gong¹, Julie Valduga^{1,2}, Alicia Chateau¹, Mylène Richard³, Nadia Pellgrini-Moïse³, Muriel Barberi-Heyob¹, Pascal Chastagner^{1,2} and Cédric Boura¹

¹Université de Lorraine, CNRS, CRAN, F-54000 Nancy, France

²Service d'Onco-Hématologie Pédiatrique, CHRU-Nancy, F-54000 Nancy, France

³Université de Lorraine, CNRS, L2CM, F-54000 Nancy, France

Correspondence to: Cédric Boura, email: cedric.boura@univ-lorraine.fr

Keywords: medulloblastoma; neuropilin-1; cancer stem cells; peptidomimetic; cell differentiation

Received: July 07, 2017

Accepted: February 10, 2018

Published: February 16, 2018

Copyright: Gong et al. This is an open-access article distributed under the terms of the Creative Commons Attribution License 3.0 (CC BY 3.0), which permits unrestricted use, distribution, and reproduction in any medium, provided the original author and source are credited.

ABSTRACT

Medulloblastoma (MB) is the most common malignant pediatric brain tumor. Despite the progress of new treatments, the risk of recurrence, morbidity, and death remains important. The neuropilin-1 (NRP-1) receptor has recently been implicated in tumor progression of MB, which seems to play an important role in the phenotype of cancer stem cells. Targeting this receptor appears as an interesting strategy to promote MB stem cells differentiation. Cancer stem-like cells of 3 MB cell lines (DAOY, D283-Med and D341-Med), classified in the more pejorative molecular subgroups, were obtained by *in vitro* enrichment. These models were characterized by an increase of NRP-1 and cancer stem cell markers (CD15, CD133 and Sox2), meanwhile a decrease of the differentiated cell marker Neurofilament-M (NF-M) was observed. Our previous work investigated potential innovative peptidomimetics that specifically target NRP-1 and showed that MR438 had a good affinity for NRP-1. This small molecule decreased the self-renewal capacity of MB stem cells for the 3 cell lines and reduced the invasive ability of DAOY and D283 stem cells while NRP-1 expression and cancer stem cell markers decreased at the same time. Possible molecular mechanisms were explored and showed that the activation of PI3K/AKT and MAPK pathways significantly decreased for DAOY cells after treatment. Finally, our results highlighted that targeting NRP-1 with MR438 could be a potential new strategy to differentiate MB stem cells and could limit medulloblastoma progression.

INTRODUCTION

Medulloblastoma (MB) is the most common malignant pediatric brain tumor and affects children at a median age of 9 years [1]. Despite the progress of radio- and chemotherapy, the risk of recurrence, frequent cognitive and endocrine sequelae and death after treatment remain important [2, 3]. Recent results showed that MB was composed of four molecular subgroups: WNT (Wingless), SHH (Sonic Hedgehog), Group 3 and Group 4, which correspond to different molecular

and clinical characteristics. Indeed, patients of groups 3 and 4, also called non-WNT and non-SHH groups, frequently present metastasis and have a poor prognosis [4, 5]. MB is classified as an embryonic tumor in which brain tumor stem cells (BTSCs) are present in very low proportion. BTSCs can be characterized by expression of stem cell phenotypic markers such as CD133 or CD15 [6, 7] and has a peculiar interest in understanding the progression of MB [8]. This cell population generates tumors through the stem cell patterns of self-renewal and differentiation into multiple tumor cell types. Moreover,

these cells have better DNA repair capability contributing to tumor resistance during radiation and chemotherapy. Conventional therapies could kill differentiated tumor cells, but the small population of BTSCs can survive and causes tumor recurrence [8–10].

Neuropilin-1 (NRP-1) is a single-pass transmembrane glycoprotein that plays a very important role in the development of neuronal and vascular systems, and shares about 44% homology with neuropilin-2 (NRP-2). It acts as a co-receptor by complexation with other transmembrane receptors such as VEGFR and plexin receptors, which are involved in neoangiogenesis and tumor progression by activating signaling pathways leading to cell survival, proliferation or migration [11]. Recently, Snuderl et al. demonstrated that PlGF acts through NRP-1 to promote MB cell survival but not through VEGFR1 [12]. Moreover, NRP-1 seems to favor an undifferentiated phenotype in cancer cells [13]. Targeting directly this receptor, especially in BTSCs, could thus provide interesting therapeutic value to change the fate of cancer stem cells to a differentiated state for improvement of survival and quality of life of medulloblastoma patients.

Our previous work focused on the development of peptides for targeting NRP-1 and we have proposed to use peptidomimetics for their theoretical stability [14, 15]. We have recently designed and assessed some new sugar-based peptidomimetics targeting NRP-1 and one of them named MR438 presented a relevant *in vitro* affinity for NRP-1 (IC_{50} of 88 μ M) [16]. Tuftsin (TKPR: Thr-Lys-Pro-Arg) is a natural ligand of NRP-1 with a IC_{50} of 25 μ M [17, 18] and it was used in our work as reference compound. Therefore, we investigated the exposition of these two compounds targeting NRP-1 on MB stem cells (obtained from 3 cell lines : DAOY, D283-Med and Med-D341) in order to assess their short-term effects as cytotoxicity and cell invasion or their long-term effects as self-renewing ability and the change of phenotypic status. We first characterized the 3 MB stem cell models which over-expressed NRP-1 and stem cell markers and found that inhibition of NRP1 decreased the self-renewing ability of MB stem cells by inducing their differentiation.

RESULTS

Phenotypic characteristics of MB stem cell models

Three cell lines of MB: DAOY, D283-Med and D341-Med were used *in vitro* to obtain medullospheres (MS) as MB stem cell models (Figure 1A). They correspond to the subgroup SHH, subgroup 4 and subgroup 3, respectively [5, 12, 19]. The medullospheres of DAOY were larger and more regular than the other two cell lines and reached a diameter of about 150 μ m after a 72 h culture period. These models were characterized by

protein expression of stem cell markers which showed, as expected, an increase in the expression of cancer stem cell markers: CD15 for all 3 models and CD133 for D283 and D341 compared to the differentiated cells (Figure 1B and 1C, Supplementary Table 1). A decrease of the neuronal differentiated phenotype marker, Neurofilament-M (NF-M), was also observed for the cells from medullospheres compared to the differentiated cells. Furthermore, because expressions of protein CD133 and NF-M for DAOY cells were very weak, we evaluated Sox2, another stem cell marker, which increased for the DAOY stem cells (Supplementary data, Supplementary Figure 1 and Table 2). These results confirmed by qRT-PCR and showed an increase of gene level expression of CD15 and Sox2 for all models of MB stem cell and of CD133 for DAOY and D341 compared to the differentiated cells (Figure 1D).

Protein expression of neuropilins by MB stem cell models

NRP-1 and NRP-2 play an important role in the development of neuronal and vascular systems. NRP-2 is a homologous protein that shares a sequence similarity of 44% in structural and biological properties with NRP-1 [20]. In our study, NRP-1 and NRP-2 were expressed by all cell lines of MB (Figure 2 and Supplementary Table 2). Meaningfully, there was a significant increase in the expression of NRP-1 protein (120 kDa) by MB stem cells compared to differentiated cells. A decrease of NRP-2 expression was observed for D283 and D341 stem cells compared to the differentiated cells.

Effect of peptidomimetic MR438 on spheres formation and cell viability

To detect the short-term effects of these compounds on medullospheres, we evaluated the ability of spheres formation (number and diameter of spheres) as well as the cell viability after 72 hours of treatment (Figure 3). DAOY rapidly formed numerous large spheres in serum free condition contrary to D283 and D341, but MR438 or Tuftsin were not able to influence the cell ability to form spheres for all cell lines (Figure 3A and 3B). In the same way, no significant difference was observed in cell viability for the different cell lines (DAOY-MS, D283-MS and D341-MS) (Figure 3C).

Effect of peptidomimetic MR438 on self-renewal capacity

Self-renewal is the process by which stem cells divide to make more stem cells, perpetuating the stem cell pool throughout life. Self-renewal is division with maintenance of the undifferentiated state. Self-renewal programs involve networks that balance proto-oncogenes (promoting self-renewal), gate-keeping tumor suppressors

(limiting self-renewal), and care-taking tumor suppressors (maintaining genomic integrity). The effect of MR438 on self-renewal capacity was assessed by using forming colonies assay (Figure 4). The number of MB stem cells (colony forming units) was statistically significantly decreased after adding NRP-1 targeting compounds for 72 h, especially after exposition to MR438. We observed

a reduction of about 25% of colonies of DAOY stem cells and approximately 20% of colonies of D283 and D341 stem cells. The colonies were divided into three groups according to their diameters: smaller than 75 μm (small clone), from 75 to 150 μm (normal clone) and higher than 150 μm (wide clone) for clones of DAOY-MS and less than 50 μm , 50–100 μm and more than 100 μm for

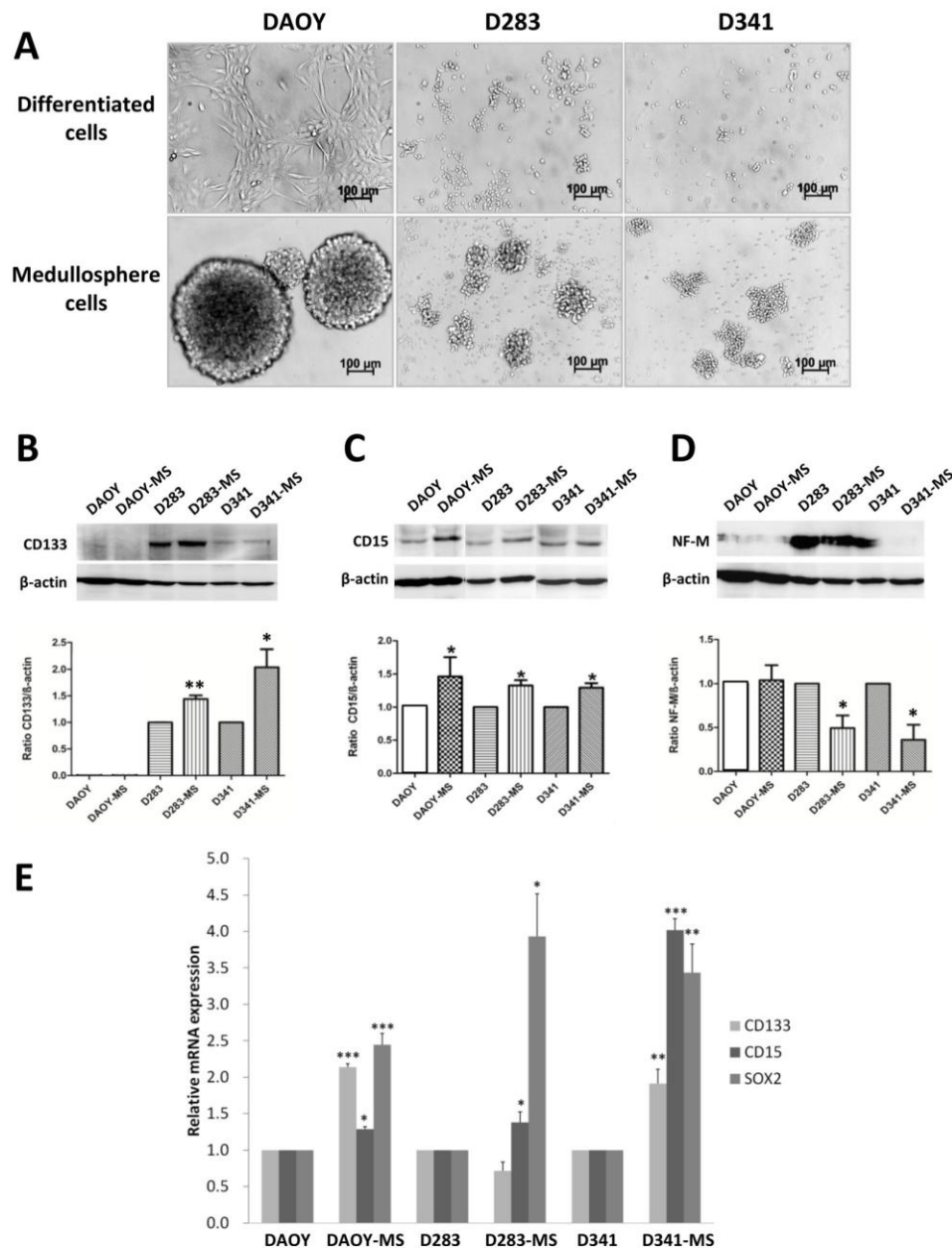


Figure 1: Phenotypic proteins and transcripts expression of MB stem cells models. (A) Images of medullospheres of MB stem cells from cell lines: DAOY, D283-Med and D341-Med ($\times 40$ magnification, Bars:100 μm). Expression of CD133 (B), CD15 (C) and NF-M (D) between differentiated cells and MB stem cells by Western blot normalized by β -actin expression. (E) Gene expression of phenotypic transcripts of CD133, CD15 and Sox2 of differentiated cells and MB stem cells normalized by RNA pol II expression. * $p < 0.05$, ** $p < 0.01$, *** $p < 0.001$, $n = 3$.

colonies of D283-MS and D341-MS (Figure 4C). MR438 effects were mainly observed for wide colonies, especially for the DAOY cells, describing a mean reduction of 60% after MR438 exposition.

Effect of peptidomimetic MR438 on expression of neuropilins and phenotypic markers by western blot and qRT-PCR

After 72 h of exposition to MR438, a statistically significant decrease of NRP-1 protein expression was observed for the 3 MB stem cell models (Figure 5A and 5B,

supplementary Table 3 and confirmed also by flow cytometry, see Supplementary Figure 2). However, this compound did not modify the protein expression level of NRP-2 (Figure 5A and 5C, Supplementary Table 3). Otherwise, the influence of the compound on the expression of the phenotypic markers CD133 and CD15 and NF-M was measured by western blot analysis, demonstrating that MR438 reduced the expression of CD15 for the three cell lines (confirmed also by flow cytometry, see Supplementary Figure 2), and decreased the expression of CD133 for D283-MS and D341-MS (Figure 5D and 5E, Supplementary Table 3). Since CD133 protein was undetectable for DAOY-MS of the SHH subgroup, we

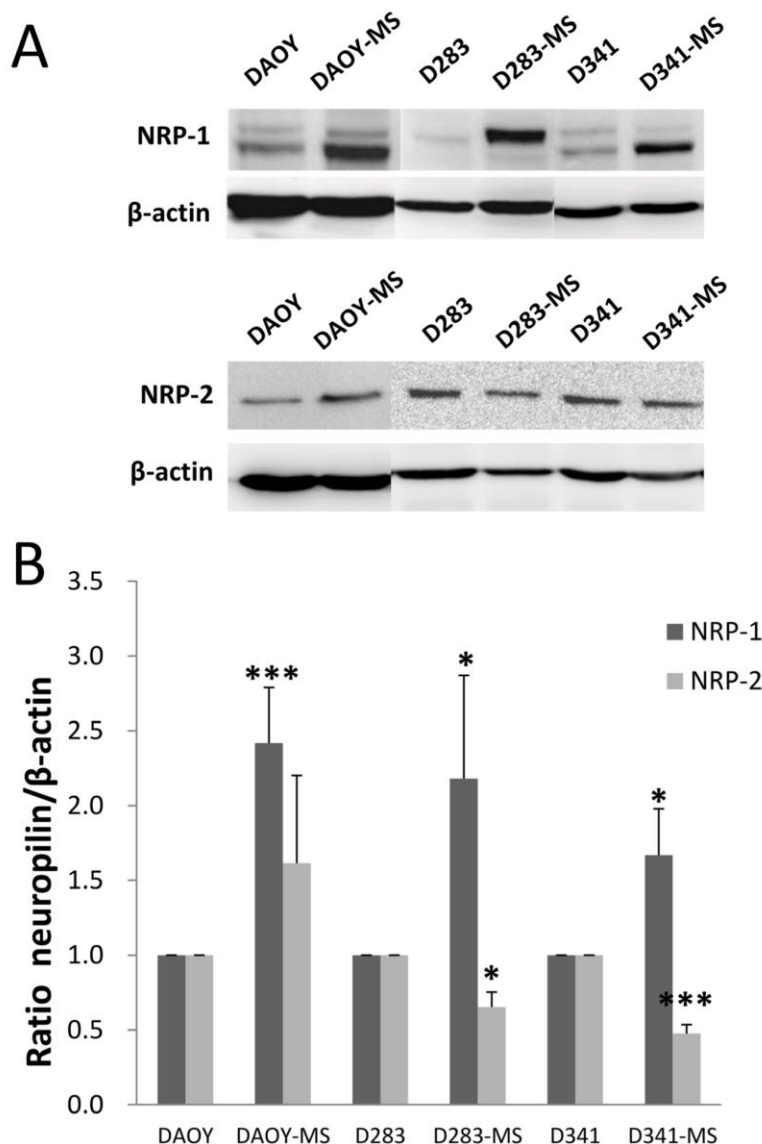


Figure 2: NRP-1 and NRP-2 proteins expression of MB stem cell models of DAOY, D283-Med and D341-Med by Western blot. (A) Representative results of expression of NRP-1 and NRP-2 for differentiated cells and MB stem cells. (B) Ratio of NRP-1 and NRP-2 expression to β-actin protein for differentiated cells and MB stem cells. * $p < 0.05$, *** $p < 0.001$, $n = 4$.

used another stem cell phenotypic marker Sox2 [21]. Sox2 expression decreased after exposure to MR438 by western blot (Supplementary data, Supplementary Figure 1 and Table 3). On the contrary, there was an increase in NF-M expression for DAOY-MS and D283-MS after exposure to MR438 (Figure 5A and 5F, Supplementary Table 3). These results were confirmed by qRT-PCR. We observed that the mRNA expression of CD15 and CD133 decreased significantly for the 3 cell lines after treatment with MR438 except for CD133 mRNA of D283-MS cell line (Figure 5G). Transcription factors Sox2, Oct4 and Nanog were also detected to supplement the impact of peptidomimetic on MB

stem cells, whereas only a significant decrease of Sox2 for the D283-MS cell line was detected after the exposure to MR438 (Supplementary data, Supplementary Figure 3).

Effect of peptidomimetic MR438 on invasive capacity of medullosphere cells

As NRP-1 is also involved in cell migration, we evaluated the effects of Tuftsin and MR438 on the invasive capacity of stem cells using the Boyden chamber model (Figure 6). MR438 induced a decrease in the capacity of invasion of MB stem cells derived from DAOY and

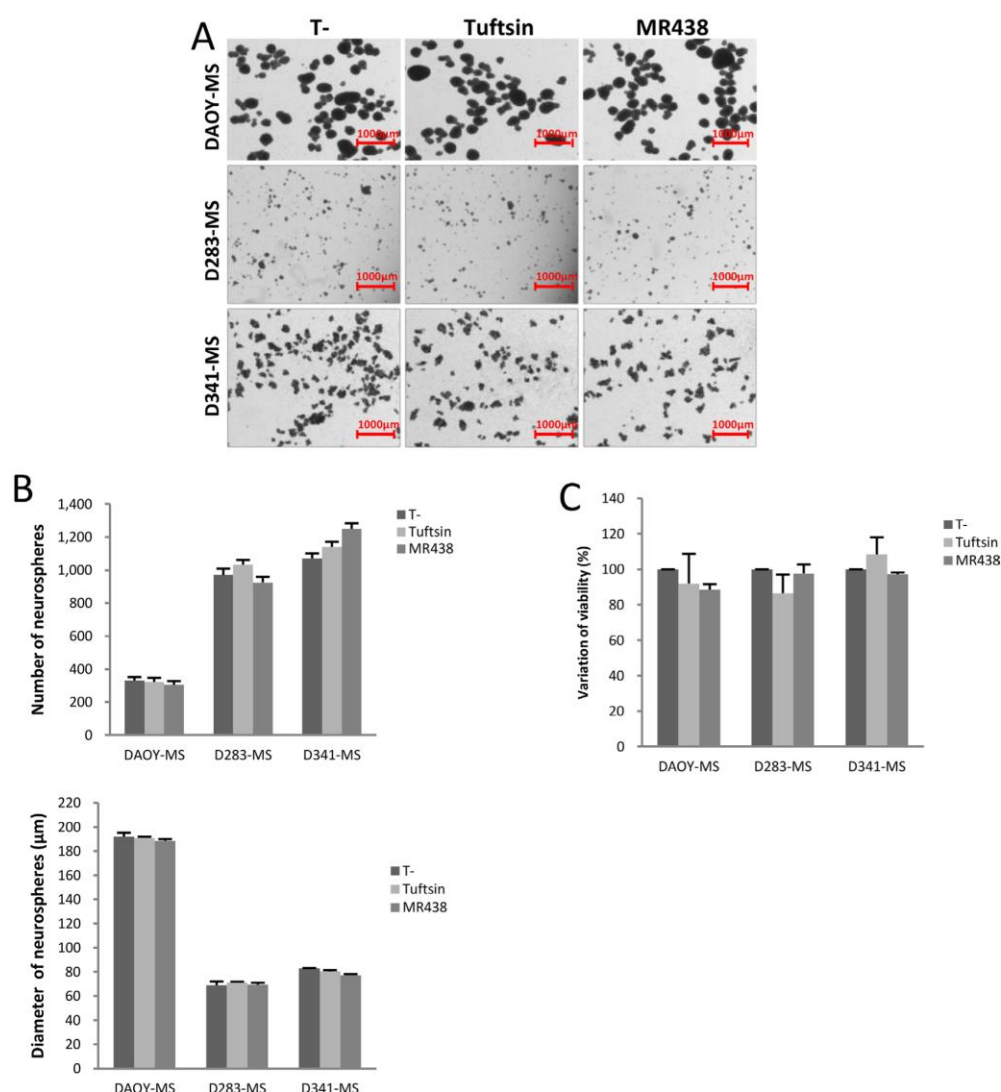


Figure 3: Effects of MR438 or Tuftsin on cytotoxicity and on spheres formation for MB stem cell models of DAOY, D283-Med and D341-Med. (A) Representative images of medullospheres from the different cell lines exposed to MR438 and Tuftsin evaluating the sphere formation ability (Bars:1000 μm). (B) Effect of MR438 and Tuftsin on number and diameter of medullospheres. (C) Viability of cells contained in the medullospheres treated by MR438 and Tuftsin after 72 hours of exposition for three cell lines. MS: Medullosphere, $p > 0.05$, $n = 6$.

D283 cell lines. Tuftsin is only able to inhibit invasion for D283 cell line. It was not possible to perform the invasion assay for D341 cells due to the limitations of these cells to adhere to Matrigel® despite the use of chemoattractant factors in the bottom chamber.

Effect of peptidomimetic MR438 on the key proteins involved in the neuropilin pathways

The study of the main signaling pathways known to be regulated by NRP-1 was carried out by the analysis of the phosphorylation state of key proteins of PI3K/AKT, RAS/MAPK and SMAD signaling pathways (Figure 7 and Supplementary Table 4). According to the activation state of the RAS/MAPK pathway, the expression of phospho-ERK1/2 showed a significant decrease for DAOY-MS cells after treatment with MR438 and Tuftsin compared to the untreated cells (Figure 7A and 7B). However, this difference in phosphorylation was not found for the 2 other models, probably because of a low level of expression of this protein (Figure 7A). Similarly, phosphorylated AKT expression also appeared to be significantly decreased for

DAOY-MS cells after exposure to MR438 and Tuftsin, but no difference was observed for the two other cell models (Figure 7A and 7C). As for the signaling pathway of AKT and ERK, there was no difference in the expression of phospho-SMAD2/3 after treatment with Tuftsin or MR438 whatever the cell models. There is a trend of increase of phospho-SMAD2/3 expression after treatment with Tuftsin or MR438 for D341 cells (Figure 7A and 7D).

DISCUSSION

A better understanding of the molecular characteristics involved in MB allowed to subdivide this pediatric brain tumor into four molecular subgroups: WNT, SHH, Group 3 and Group 4, with different molecular characteristics and clinical outcomes and thus to consider new therapeutic approaches [4, 5]. The WNT and SHH groups were thus named in connection with signaling pathways which appear to play important roles in the pathogenesis of these subgroups. Subgroup 3 and 4 MB are related to a high incidence of metastasis and lead to a

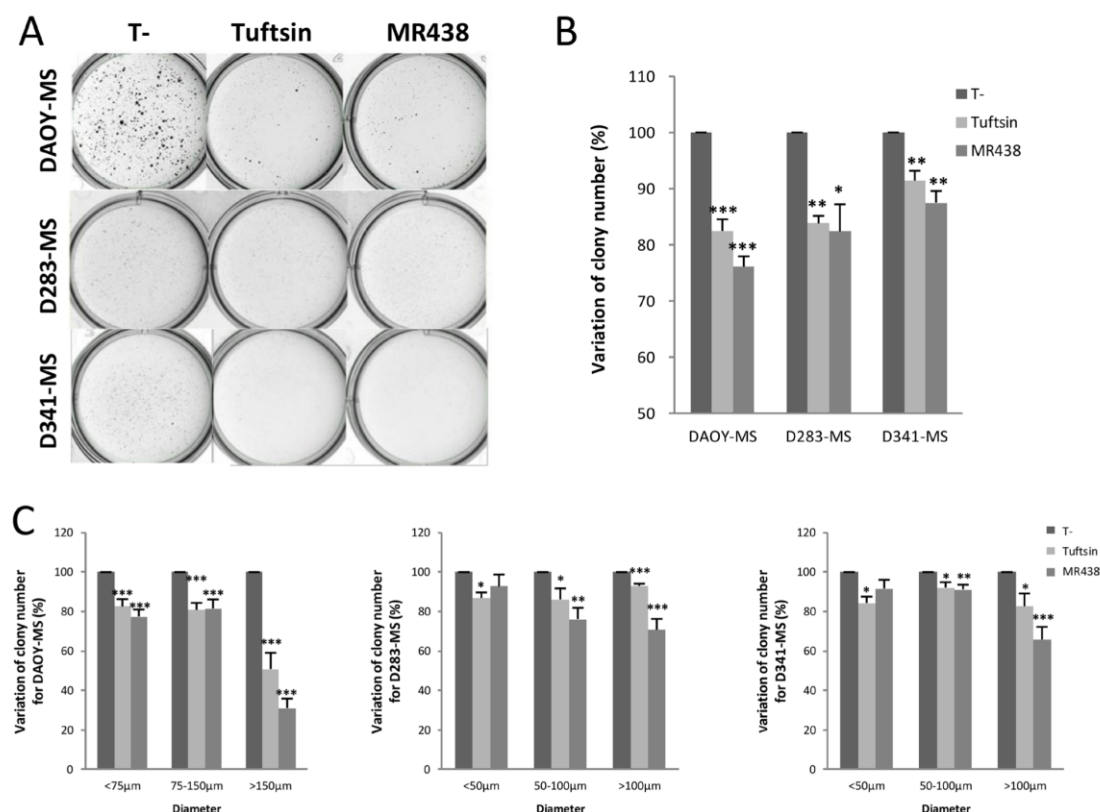


Figure 4: Effects of MR438 or Tuftsin on self-renewal ability by clonogenic assay for DAOY, D283 and D341 stem cells. (A) Representative images of medullospheres treated with MR438 or Tuftsin by clonogenic assay using methylcellulose culture medium for three cell lines: 2×10^4 cells/well for DAOY-MS and 5×10^4 cells/well for D283-MS and D341-MS. (B) Ratio of colony number compared to control group. (C) Ratio of colony number compared to control group depending on different ranges of diameter for DAOY-MS, D283-MS and D341-MS. MS: Medullosphere, * $p < 0.05$, ** $p < 0.01$, *** $p < 0.001$, $n = 6$.

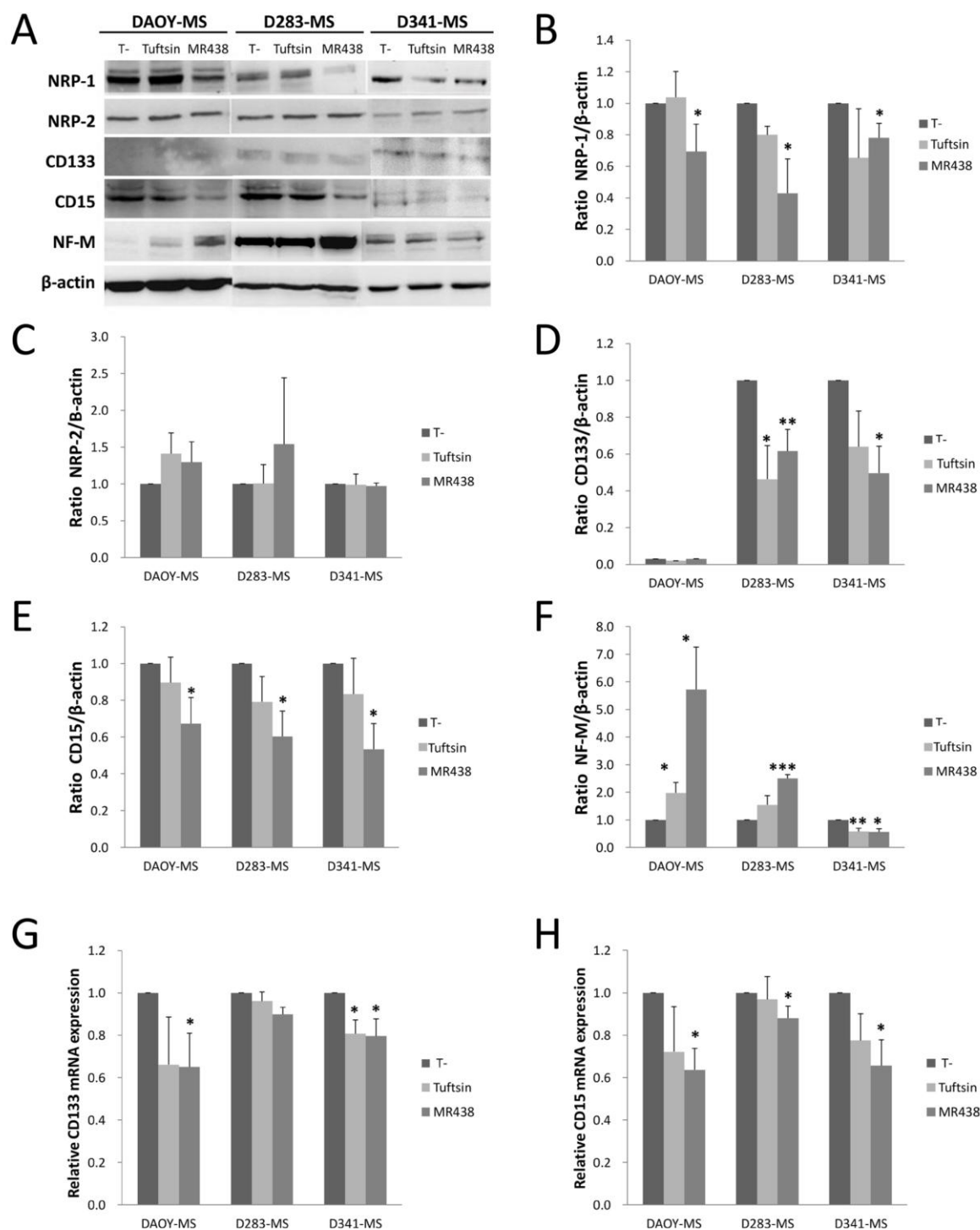


Figure 5: Effects of MR438 or Tuftsin on proteins and transcripts expression of neuropilin receptors and stem cell markers. (A) Representative blots of expression of neuropilins and phenotype markers for MB stem cells exposed to MR438 or Tuftsin by western blot. Ratio of NRP-1 (B), NRP-2 (C), CD133 (D), CD15 (E) and NF-M (F) protein expression normalized by β-actin expression for MB stem cells treated by MR438 or Tuftsin. Effects of compounds on mRNA expression of CD15 (G) and CD133 (H) for MB stem cells by qRT-PCR. * $p < 0.05$, ** $p < 0.01$, *** $p < 0.001$, $n = 3$.

poorer prognosis. Thus, it is important to study as much as possible all the molecular subgroups of MB for a better understanding of this disease. Therefore, in our study, we analyzed the three most frequent used cell lines of MB: DAOY, D283-Med and D341-Med, corresponding to the subgroup SHH, subgroup 4 and subgroup 3, respectively [12, 19].

NRP-1 is a single-pass transmembrane glycoprotein, which acts as a co-receptor by complexing with many transmembrane receptors such as VEGFR and Semaphorin receptor, or with TGF- β 1 receptor, as it has been recently demonstrated [20]. NRP-1 is involved in cell survival and proliferation and has been reported to be over-expressed in various cancers, which have also been correlated with poor prognosis [22–25]. More recently, Snuderl *et al.* found that MB patients with high NRP-1 expression level have a decrease of 50% in survival. Moreover, targeting placental growth factor (PlGF)/NRP1 with monoclonal antibodies induced a direct antitumor effect in MB, resulting in tumor regression, decrease of metastasis and increase of survival in mouse models [12]. In the context of a peptide based approach, Tuftsin, a natural peptide produced by enzymatic cleavage of the Fc domain of the immunoglobulin G heavy chain, was found to bind specifically to NRP-1 [18]. However, Tuftsin is not an ideal agent for use in clinical practice because of several limiting points including size, stability (susceptible to degradation by peptidases), lack of effective methods for delivery, low oral bioavailability, rapid excretion and poor transport properties through biologic membranes [26, 27]. Thus, we developed a novel peptidomimetic named

MR438 which has been built by molecular modeling based on well-known A7R peptide [16, 28].

Recent studies report that cancer stem cells (CSCs) are considered to be the origin of tumor proliferation and involved in the tumor recurrence because of their resistance to radiotherapy and chemotherapy [29]. CD133 is the most commonly used stem cell marker used for the identification of brain cancer stem cells [6, 30], but it was also shown that CD15+ MB cells could recur and lead to poor prognosis in mouse models [7]. Indeed, CD15 is a carbohydrate antigen that is expressed on both progenitors and stem cells in the embryonic and adult central nervous system and was also recently considered as a marker of brain cancer stem cells especially for Sonic hedgehog (SHH) MB subgroup cells [7, 31]. As expected, our MB stem cells obtained in serum free conditions characterized by overexpression of stem cell markers, in particular CD15 for DAOY stem cells (SHH subgroup) and CD133 for D283 cells (subgroup 4) compared to cell lines cultured under classic conditions. Interestingly, the *in vitro* enrichment of cancer stem cells induced a NRP-1 overexpression for all cell lines, which is encouraging to consider NRP-1 targeting as a strategy applicable to different MB subgroups.

MBs are poorly differentiated tumors containing a large proportion of cancer stem cells, so acting on their differentiation could also play an assisting role in the therapeutic management of MBs [32]. Cao *et al.* found that NRP-1 helps in maintaining an undifferentiated phenotype in renal cell carcinoma [13]. In our study, we have not observed early effects of NRP-1 targeting on cell

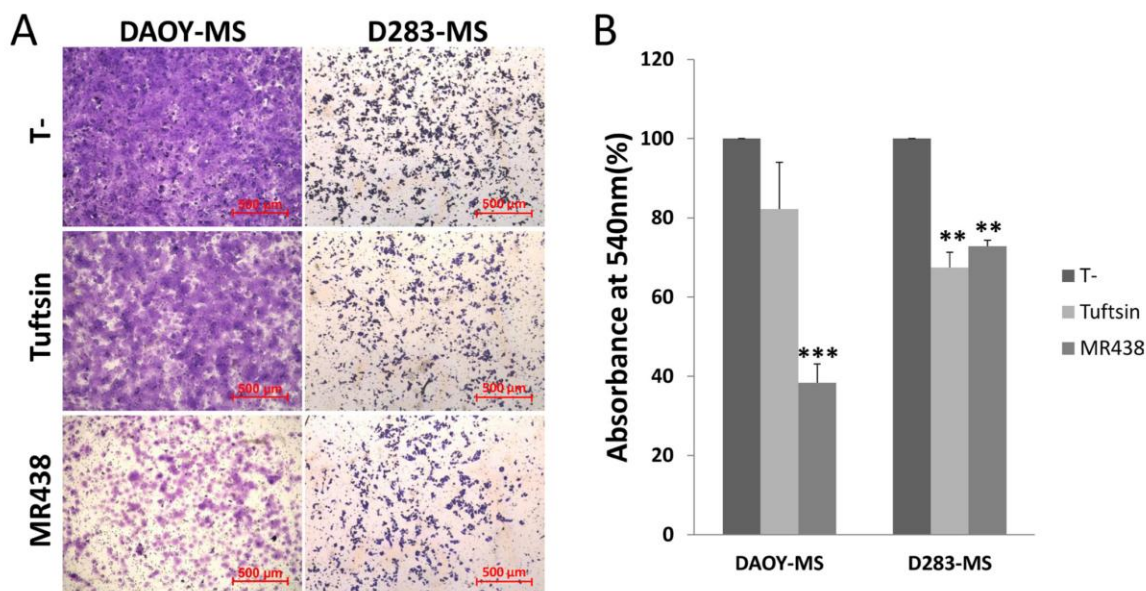


Figure 6: Effects of MR438 or Tuftsin on invasive ability of MB stem cells derived from DAOY and D283 cell lines. (A) Images of invasive cells exposed to MR438 or Tuftsin on the membrane surface of Boyden chamber (Bars: 500 µm). **(B)** Ratio of invasive cells exposed to MR438 or Tuftsin compared with the no treated cells. *** $p < 0.01$, $n = 3$.

viability nor on the ability of cells to form medullospheres. However, we observed a decrease in self-renewal capacity in the presence of MR438 and to a lesser extent in presence of Tuftsin indicating that cancer stem cells probably enter in a differentiation way. This seems more efficient for SHH sub-group cells.

The dissemination of MB stem cells in hematomenigeal space is a real clinical problem leading to metastasis occurrence and tumor recurrence [33]. Cao *et al.* showed also that the knockdown of NRP-1 by short hairpin RNA reduced migration and invasion of renal carcinoma cells [13] which was also found in our results with a decrease of invasion ability of MB stem cells after exposure to MR438. In the same way, it was recently shown that MiR-148a, a MiRNA which decreased NRP-1 expression, also inhibited invasion and tumorigenic potential of MB cells in the WNT subgroup [34].

Subsequently, we have endeavored to understand which signaling pathways of NRP-1 are preferably involved in the differentiation of MB stem cells. The precise signaling pathways of NRP-1 action are still unclear as they interact with many cancer associated

molecules. It has been demonstrated that overexpression of NRP-1 in cancer cells promotes tumor angiogenesis and stimulates cancer stem cell feature that depends on the complex NRP-1/VEGFR-2 for the CD133(+) human glioma stem-like cells (GSCs) [35, 36]. VEGFR and other VEGFR co-receptors of NRP-1 are involved in neoangiogenesis, tumor progression and differentiation by activating signaling pathways like PI3K/AKT, MAPK and SMAD. Thus, the most marked effect of MR438 as well as Tuftsin was the inactivation of PI3K/AKT and MAPK pathways for the SHH subgroup cells (DAOY). Frasson *et al.* have also recently proposed that the most important pathway involved in cell differentiation of MB stem cells is the PI3K/AKT/mTOR pathway [37]. Although TGF-beta-dependent SMAD signaling pathway did not appear to be disrupted in our study, Nissen *et al.* reported that Tuftsin promotes Smad3 phosphorylation and reduces AKT phosphorylation by TGF-beta-dependent signaling pathway [38]. In addition, we did not observe the effect of MR438 on the expression of SHH, although the expression of NRP-1 is known to activate the SHH signaling pathway [39]. Other unknown functions of NRP-1 could explain

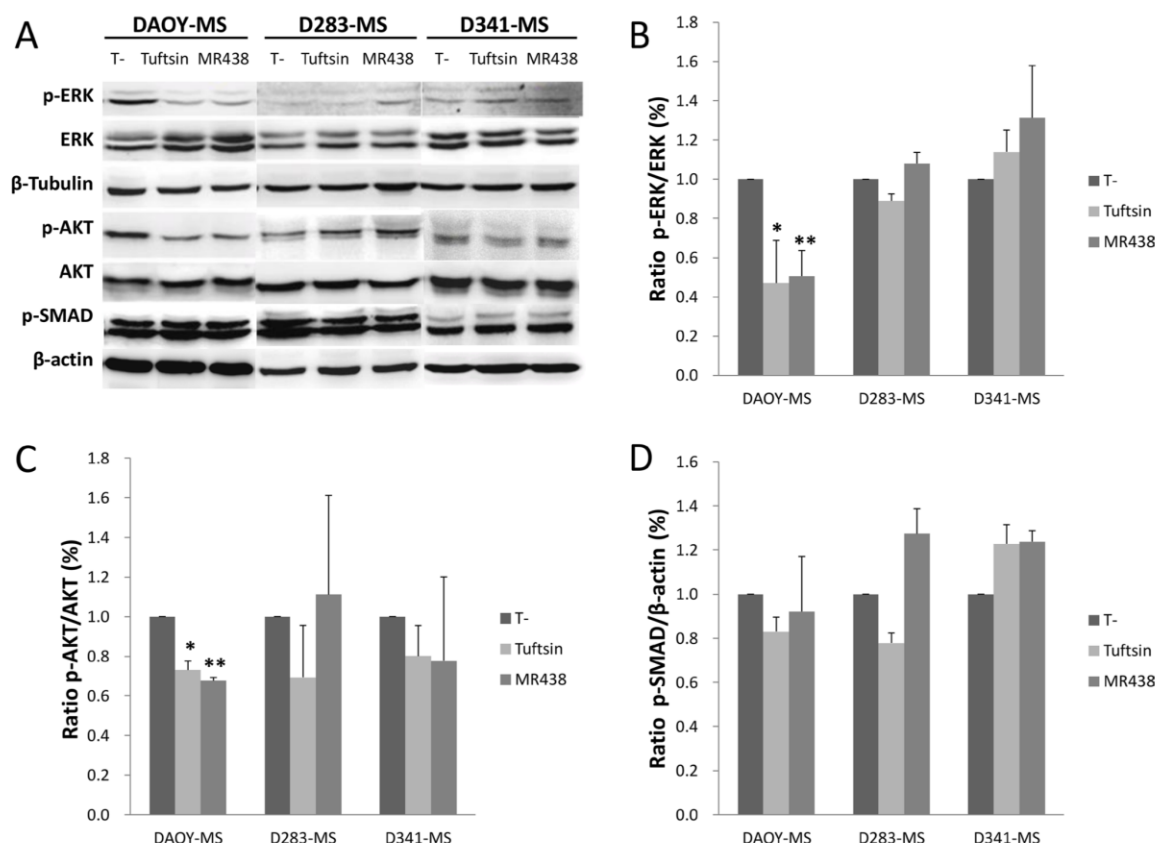


Figure 7: Effects of MR438 or Tuftsin on the key proteins involved in the neuropilin pathways. (A) Representative blots of p-ERK, ERK, p-AKT, AKT, p-SAMAD2/3, β-actin and β-tubulin by Western blot. (B) Ratio of p-ERK to ERK for MB stem cells treated by MR438 or Tuftsin. (C) Ratio of p-AKT to AKT for MB stem cells treated by MR438 or Tuftsin. (D) Ratio of p-SMAD to β-actin protein for MB stem cells treated by MR438 or Tuftsin. * $p < 0.05$, ** $p < 0.01$, $n = 3$.

the decrease in self-renewal capacity observed for the subgroups 3 and 4 and will have to be elucidated by unsupervised transcriptomic approaches.

In conclusion, by using models of MB stem cells, we found that inhibition of NRP-1 via the peptidomimetic MR438 seems to stimulate stem cell differentiation for different subgroups of MB, which can ultimately reduce the progression of MB, with an implication of the PI3K/AKT and MAPK signaling pathways for subgroup SHH. The use of NRP-1 targeting molecules seems relevant to target MB stem cells, notably by promoting their differentiation. Further molecular studies could help us understand the involved mechanisms and we will confirm these results in the future in *in vivo* medulloblastoma xenograft models.

MATERIALS AND METHODS

Cell culture of MB stem like cells

The human MB cell line DAOY [40], D283-Med [41] and D341-Med [42] were purchased from ATCC cell biology collection (Manassas VA, USA). Cells

were maintained in MEM (Gibco, Life Technologies Corporation, UK) including 10% fetal bovine serum (FBS, SIGMA, USA) for DAOY and D283, 20% FBS for D341-Med, 1% L-glutamine (SIGMA, UK), 1% non-essential amino acids (Gibco, UK), 1% penicillin/streptomycin (Gibco, UK) and 1% Sodium pyruvate (GibcoUK) at 37°C and 5% CO₂. MB stem like cells cultures were maintained in DMEM/F12 medium (GibcoUK) containing B27 and N2 supplement (Gibco, Life Technologies Corporation, USA), 20 ng/mL of human recombinant epidermal growth factor (EGF) and basic fibroblast growth factor (bFGF) (EGF and FGF from Miltenyi Biotec, Germany). After a 3-day culture in hydrophobic flasks at 37°C with 5% CO₂ in a humidifier atmosphere, spheres were obtained. MB stem like cells were dissociated from spheres using Accumax (Gibco, Life Technologies Corporation, UK) and seeded in 75 cm² or 25 cm² flasks depending on the experiment. The MB dissociated stem like cells were then exposed to MR438 (Molecular weight: 527.20 g/mol, supplied by the SRSMC laboratory-UMR 7565 in powder form) and Tuftsin (Molecular weight: 500.60 g/mol, BACHEM, Switzerland) at 25 µmol/L during 72 h (Figure 8).

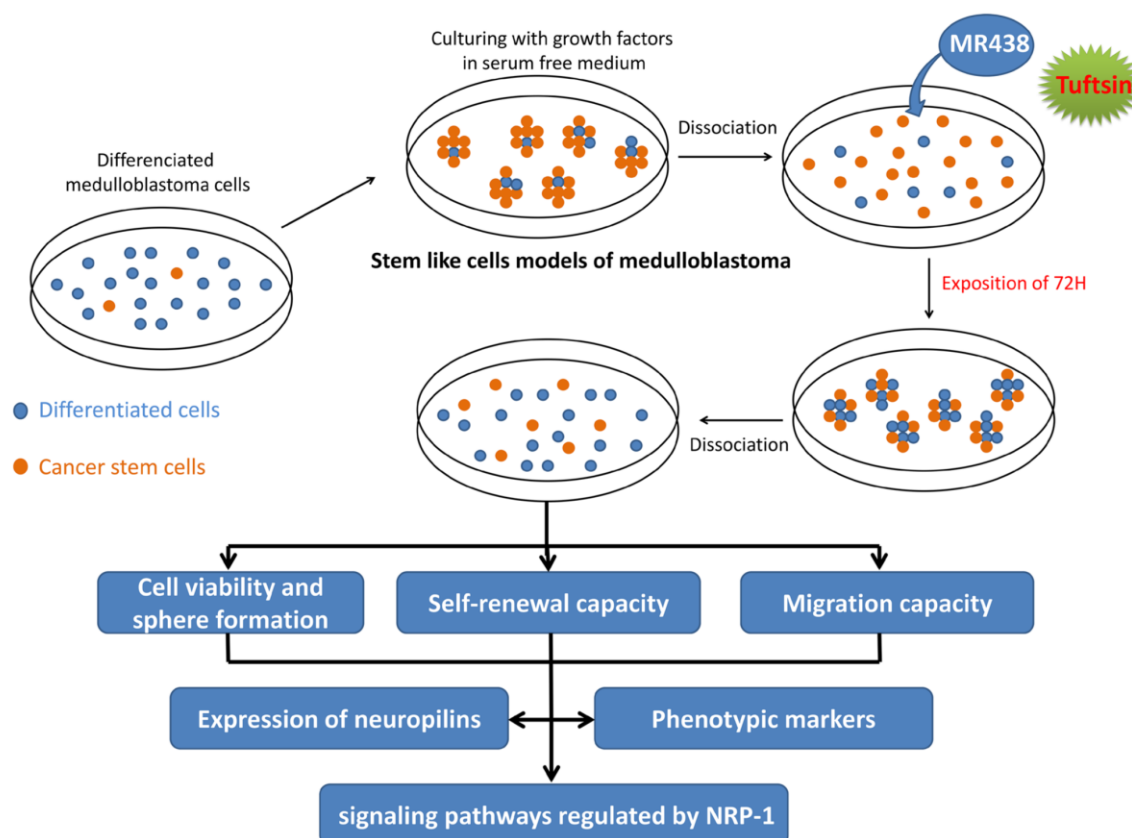


Figure 8: Design of the experimental procedures to evaluate the peptidomimetic effects on MB stem cells models obtained by *in vitro* enrichment methods.

Sphere formation and cells viability

We observed the sphere formation of the MB cells after a 72 h incubation with the compounds Tuftsin and MR438 at the concentration of 25 μ M. The cells were seeded in 6 wells plates at a density of 60 000 cells/mL for DAOY-MS and D341-MS and 75 000 cells/mL for D283-MS. The number of neurospheres larger than 30 μ m was quantified using GelCount™ (Oxford Optronix, UK) to count the number of spheres and to evaluate the efficacy of medullosphere formation. Each experiment was repeated 3 times with 3 independent wells.

The viability of MB stem like cells was evaluated by automated cell counter TC20 (Biorad, France) using the trypan blue exclusion assay in 24 well plates at the same condition of cell density like sphere formation assay. Spheres were previously dissociated with Accumax and cell suspension then rapidly stained with the same volume of 0.4% trypan-blue solution and deposited in counting chamber slides (TC20, Biorad). The percentage of surviving cells was counted twice and experiment was repeated 6 times.

Clonogenic assay

After exposure of MB stem like cells to MR438 and Tuftsin, clonogenic growth assay using methylcellulose based media was done. Briefly, MB stem like cells (20000 cells/well for DAOY-MS and 50000 cells/well for D283-MS and D341-MS) were suspended in 2 ml of DMEM/F12 containing 1% methylcellulose (SIGMA, USA). The cell suspension was then plated onto 6 well plates and allowed to grow for 8–12 days. Colonies were incubated with 0.5% MTT solution (Thiazolyl blue tetrazolium bromide, 98%, Acros Organics™) and colonies larger than 30 μ m in diameter were quantified using GelCount™ (Oxford Optronix, UK). Each experiment was repeated 6 times with 3 independent wells.

Transwell invasion assays

Transwell invasion assays were performed using a transwell insert (Corning Incorporated, Corning, USA) with 4.4% Matrigel® (BD Biosciences, France) coated onto the transwell membrane (8 μ m pore size, 6.5mm diameter). The lower chambers of the transwell plates were filled with 700 μ L DMEM/F12 containing 10% FBS. Cells were cultured in the higher chambers (200 000 cells/chambre for DAOY-MS and 1000 000 cells/chambre for D283-MS) onto 24-well plate with 500 μ L serum free DMEM/F12. After 16 h for DAOY-MS and 48 h for D283-MS in incubator at 37°C, cells on the upper surface of filters were removed using cotton swabs and those on the lower surface were fixed 10 minutes with 4% paraformaldehyde and staining with 0.05% crystal violet of 30 minutes. Photomicrographs of whole culture surface

were taken (Nikon AZ100, Digital Sight DS-Qi1Mc camera, Nikon, France). The coloration was solubilized 10 minutes by placing the inserts in 150 μ L of 4% acetic acid and then transferred into 96 well plates, the absorbance was read at 540 nm with a spectrophotometer (Thermo Electron Corporation, Finland).

Analysis of proteins expression by western blot

Western blot was carried out for analysis of NRP-1, NRP-2, CD133, CD15, NF-M and Sox2 protein expression. Total protein cell lysis buffer containing 10% protease (Roche, Germany), 1% Cocktail 2 and 3 (Sigma-Aldrich, Germany) was used to lysis of cells to extraction proteins. Kit Pierce BCA Protein Assay (Thermo scientific, USA) was used to determine protein concentration that read the absorbance at 540 nm with a spectrophotometer. Protein aliquots (50 μ g) were denatured in the Laemmli buffer containing β mercaptoethanol prior to resolution by SDS polyacrylamide gel electrophoresis. The separated proteins were transferred onto PVDF membranes (Biorad, USA). After blocking the PVDF membrane with Tris base-buffered saline prepared with 0.1% Tween-20 containing 5% bovine serum albumin within 1 hour, the following primary antibodies against NRP-1 (#3725, Cell Signaling, 1:1000 dilution), NRP-2 (#32241, Novus Biologicals, 1:1000 dilution), CD133 (#130-090-422, Miltenyi Biotec, 1:500 dilution), CD15 (#14-0159, eBioscience, 1:1000 dilution), Sox2(#SAB5500176, SIGMA, 1:1000 dilution), NF-M (#2838, Cell Signaling, 1:1000 dilution), p-ERK (#9106, Cell Signaling, 1:2000 dilution), ERK (#9102, Cell Signaling, 1:1000 dilution), p-AKT (#9271, Cell Signaling, 1:1000 dilution), AKT (#9272, Cell Signaling, 1:1000 dilution), p-SMAD (#8828, Cell Signaling, 1:1000 dilution), β -tublin (#2128, Cell Signaling, 1:1000 dilution) and β -actin (#4970, Cell Signaling, 1:1000 dilution) were incubated overnight at 4°C. Quantification of relative band densities was performed using densitometer (LAS Imager FujiFilm) and β -actin or β -tublin was used as internal control.

Gene expression of phenotypic markers by qRT-PCR

To confirm the protein expression, the gene expression of Sox2, Oct4, Nanog, CD133 and CD15 (Table 1) for the differentiated cells and stem cells in medullospheres, as well as the impact of MR438 and Tuftsin, were analyzed by quantitative reverse-transcription PCR (qRT-PCR). Total RNA was extracted with All Prep-DNARNA-Mini Kit (Omega). Reverse transcribed to cDNA was synthesized using the iScript™ cDNA synthesis Kit (BioRad) with conditions of 25°C for 5 minutes, 42°C for 30 minutes, 85°C for 5 minutes, and 12°C forever. Quantitative PCR amplification was performed with SyberGreen PCR supermix (BioRad)

Table 1: Sequences and annealing temperatures of primers used in qRT-PCR

Gene	Primer sequence (5'–3')	Tm (°C)
CD133 Fwd	TCCGGGTTTTGGATACACCCTA	68
CD133 Rev	CTGCAGGTGAAGAGTGCCGTAA	
CD15 Fwd	AGGAGGTGATGTGGACAGCG	67
CD15 Rev	AACTACGAGCGCTTTGTGCC	
Sox2 Fwd	TTTCACGTTTGCAACTGTCC	63
Sox2 Rev	AGTCTCCAAGCGACGAAAAA	
Oct4A Fwd	ACCTGGAGTTTGTGCCAGGGTT	68
Oct4A Rev	CTCCCCTGCCCCCACCCTTT	
Nanog Fwd	GATGGGAGGAGGGGAGAGGA	68
Nanog Rev	TTTGAAGCTGCTGGGGAAG	
RNA pol II Fwd	TGGGCAAAAGAGTGGACTTC	64
RNA pol II Rev	TTGAAGGGGGTGACAATCTC	

Fwd: forward, Rev: reverse, Tm: melting temperature, pol: polymerase.

using the CFX96 Real-Time System (BioRad). The qPCR conditions were 95°C for 2 minutes and 39 cycles of 95°C for 5 seconds and 63–68°C for 30 seconds, the hybridization temperature was depended on primers (Table 1). All values were normalized to RNA pol II and the $\Delta\Delta C_t$ method was used to estimate the fold change expression over control samples.

Statistical analysis

All results were given as mean \pm standard error of the mean (SEM). Nonparametric test was employed to determine the statistical significance using SPSS Statistics 5 (SPSS Statistics 19.0, USA) with a minimum of 3 repetitions. For all figures, $p < 0.05$ (marked by *) was considered significant and $p < 0.01$ and $p < 0.001$ were marked by ** and ***, respectively.

ACKNOWLEDGMENTS

The authors thank Chinese Scholarship Council for PhD support of Caifeng Gong. The authors thank for their help Valerie Jouan-Hureau for technical assistance in flow cytometry experiments.

CONFLICTS OF INTEREST

The authors declare that they have no conflicts of interest.

GRANT SUPPORT

This study was supported by research funds of the Société Française de Lutte contre les Cancers et Leucémies de l'Enfant et de l'Adolescent (SFCE), Association

pour la Recherche dans les Maladies Infantiles Graves (AREMIG), and French Ligue Contre le Cancer.

REFERENCES

- Orbach D, Chastagner P, Bourdeaut F, Doz F. Medulloblastoma in childhood: an heterogeneous disease requiring treatment adjustments to known risk factors. *Rev Prat.* 2012; 62:989–990.
- Bourdeaut F, Miquel C, Alapetite C, Roujeau T, Doz F. Medulloblastomas: update on a heterogeneous disease. *Curr opin oncol.* 2011; 23:630–637.
- Grill J, Sainte-Rose C, Jouvett A, Gentet JC, Lejars O, Frappaz D, Doz F, Rialland X, Pichon F, Bertozzi AI, Chastagner P, Couanet D, Habrand JL, et al. Treatment of medulloblastoma with postoperative chemotherapy alone: an SFOP prospective trial in young children. *Lancet oncol.* 2005; 6:573–580.
- Taylor MD, Northcott PA, Korshunov A, Remke M, Cho YJ, Clifford SC, Eberhart CG, Parsons DW, Rutkowski S, Gajjar A, Ellison DW, Lichter P, Gilbertson RJ, et al. Molecular subgroups of medulloblastoma: the current consensus. *Acta neuropathol.* 2012; 123:465–472.
- Northcott PA, Korshunov A, Witt H, Hielscher T, Eberhart CG, Mack S, Bouffet E, Clifford SC, Hawkins CE, French P, Rutka JT, Pfister S, Taylor MD. Medulloblastoma comprises four distinct molecular variants. *J clin oncol.* 2011; 29:1408–1414.
- Singh SK, Clarke ID, Terasaki M, Bonn VE, Hawkins C, Squire J, Dirks PB. Identification of a cancer stem cell in human brain tumors. *Cancer res.* 2003; 63:5821–5828.
- Read TA, Fogarty MP, Markant SL, McLendon RE, Wei Z, Ellison DW, Febbo PG, Wechsler-Reya RJ. Identification of CD15 as a marker for tumor-propagating cells in a mouse model of medulloblastoma. *Cancer cell.* 2009; 15:135–147.

8. Vescovi AL, Galli R, Reynolds BA. Brain tumour stem cells. *Nat rev cancer*. 2006; 6:425–436.
9. Singh SK, Hawkins C, Clarke ID, Squire JA, Bayani J, Hide T, Henkelman RM, Cusimano MD, Dirks PB. Identification of human brain tumour initiating cells. *Nature*. 2004; 432:396–401.
10. Bao S, Wu Q, McLendon RE, Hao Y, Shi Q, Hjelmeland AB, Dewhirst MW, Bigner DD, Rich JN. Glioma stem cells promote radioresistance by preferential activation of the DNA damage response. *Nature*. 2006; 444:756–760.
11. Prud'Homme GJ, Glinka Y. Neuropilins are multifunctional coreceptors involved in tumor initiation, growth, metastasis and immunity. *Oncotarget*. 2012; 3:921–939.
12. Snuderl M, Batista A, Kirkpatrick ND, Ruiz DAC, Riedemann L, Walsh EC, Anolik R, Huang Y, Martin JD, Kamoun W, Knevels E, Schmidt T, Farrar CT, et al. Targeting placental growth factor/neuropilin 1 pathway inhibits growth and spread of medulloblastoma. *Cell*. 2013; 152:1065–1076.
13. Cao Y, Wang L, Nandy D, Zhang Y, Basu A, Radisky D, Mukhopadhyay D. Neuropilin-1 upholds dedifferentiation and propagation phenotypes of renal cell carcinoma cells by activating Akt and sonic hedgehog axes. *Cancer Res*. 2008; 68:8667–72.
14. Pernot M, Vanderesse R, Frochot C, Guillemin F, Barberi-Heyob M. Stability of peptides and therapeutic success in cancer. *Expert Opin Drug Metab Toxicol*. 2011; 7:793–802.
15. Benachour H, Seve A, Bastogne T, Frochot C, Vanderesse R, Jasniowski J, Miladi I, Billotey C, Tillement O, Lux F, Barberi-Heyob M. Multifunctional Peptide-conjugated hybrid silica nanoparticles for photodynamic therapy and MRI. *Theranostics*. 2012; 2:889–904.
16. Richard M, Chateau A, Jelsch C, Didierjean C, Manival X, Charron C, Maigret B, Barberi-Heyob M, Chapleur Y, Boura C, Pellegrini-Moise N. Carbohydrate-based peptidomimetics targeting neuropilin-1: Synthesis, molecular docking study and *in vitro* biological activities. *Bioorg Med Chem*. 2016; 24:5315–5325.
17. Nissen JC, Selwood DL, Tsirka SE. Tuftsin signals through its receptor neuropilin-1 via the transforming growth factor beta pathway. *J neurochem*. 2013; 127:394–402.
18. Von Wronski MA, Raju N, Pillai R, Bogdan NJ, Marinelli ER, Nanjappan P, Ramalingam K, Arunachalam T, Eaton S, Linder KE, Yan F, Pochon S, Tweedle MF, et al. Tuftsin binds neuropilin-1 through a sequence similar to that encoded by exon 8 of vascular endothelial growth factor. *J biol chem*. 2006; 281:5702–5710.
19. Xu J, Margol A, Asgharzadeh S, Erdreich-Epstein A. Pediatric brain tumor cell lines. *J cell biochem*. 2015; 116:218–224.
20. Wild JR, Staton CA, Chapple K, Corfe BM. Neuropilins: expression and roles in the epithelium. *Int j exp pathol*. 2012; 93:81–103.
21. Becher OJ, Holland EC. Sox2, a marker for stem-like tumor cells in skin squamous cell carcinoma and hedgehog subgroup medulloblastoma. *Embo j*. 2014; 33:1984–1986.
22. Osada H, Tokunaga T, Nishi M, Hatanaka H, Abe Y, Tsugu A, Kijima H, Yamazaki H, Ueyama Y, Nakamura M. Overexpression of the neuropilin 1 (NRP1) gene correlated with poor prognosis in human glioma. *Anticancer res*. 2004; 24:547–552.
23. Jubb AM, Strickland LA, Liu SD, Mak J, Schmidt M, Koeppen H. Neuropilin-1 expression in cancer and development. *J pathol*. 2012; 226:50–60.
24. Chu W, Song X, Yang X, Ma L, Zhu J, He M, Wang Z, Wu Y. Neuropilin-1 promotes epithelial-to-mesenchymal transition by stimulating nuclear factor-kappa B and is associated with poor prognosis in human oral squamous cell carcinoma. *Plos one*. 2014; 9:e101931.
25. Peng Y, Liu YM, Li LC, Wang LL, Wu XL. MicroRNA-338 inhibits growth, invasion and metastasis of gastric cancer by targeting NRP1 expression. *Plos one*. 2014; 9:e94422.
26. Vagner J, Qu H, Hruby VJ. Peptidomimetics, a synthetic tool of drug discovery. *Curr opin chem biol*. 2008; 12:292–296.
27. Recio C, Maione F, Iqbal AJ, Mascolo N, De Feo V. The Potential Therapeutic Application of Peptides and Peptidomimetics in Cardiovascular Disease. *Front Pharmacol*. 2016; 7:526.
28. Bechet D, Tirand L, Faivre B, Plenat F, Bonnet C, Bastogne T, Frochot C, Guillemin F, Barberi-Heyob M. Neuropilin-1 targeting photosensitization-induced early stages of thrombosis via tissue factor release. *Pharm Res*. 2010; 27:468–479.
29. Eyler CE, Rich JN. Survival of the fittest: cancer stem cells in therapeutic resistance and angiogenesis. *J clin oncol*. 2008; 26:2839–2845.
30. Singh SK, Hawkins C, Clarke ID, Squire JA, Bayani J, Hide T, Henkelman RM, Cusimano MD, Dirks PB. Identification of human brain tumour initiating cells. *Nature*. 2004; 432:396–401.
31. Ward RJ, Lee L, Graham K, Satkunendran T, Yoshikawa K, Ling E, Harper L, Austin R, Nieuwenhuis E, Clarke ID, Hui CC, Dirks PB. Multipotent CD15+ cancer stem cells in patched-1-deficient mouse medulloblastoma. *Cancer res*. 2009; 69:4682–4690.
32. Burger PC, Grahmann FC, Bliedle A, Kleihues P. Differentiation in the medulloblastoma. A histological and immunohistochemical study. *Acta neuropathol*. 1987; 73:115–123.
33. Garg N, Bakhshinyan D, Venugopal C, Mahendram S, Rosa DA, Vijayakumar T, Manoranjan B, Hallett R, McFarlane N, Delaney KH, Kwiecien JM, Arpin CC, Lai PS, et al. CD133+ brain tumor-initiating cells are dependent on STAT3 signaling to drive medulloblastoma recurrence. *Oncogene*. 2017; 36:606–617.
34. Yogi K, Sridhar E, Goel N, Jalali R, Goel A, Moiyadi A, Thorat R, Panwalkar P, Khire A, Dasgupta A, Shetty P, Shirsat NV. MiR-148a, a microRNA upregulated in the WNT subgroup tumors, inhibits invasion and tumorigenic

- potential of medulloblastoma cells by targeting Neuropilin 1. *Oncoscience*. 2015; 2:334–348.
35. Hamerlik P, Lathia JD, Rasmussen R, Wu Q, Bartkova J, Lee M, Moudry P, Bartek JJ, Fischer W, Lukas J, Rich JN, Bartek J. Autocrine VEGF-VEGFR2-Neuropilin-1 signaling promotes glioma stem-like cell viability and tumor growth. *J exp med*. 2012; 209:507–520.
 36. Beck B, Driessens G, Goossens S, Youssef KK, Kuchnio A, Caauwe A, Sotiropoulou PA, Loges S, Lapouge G, Candi A, Mascré G, Drogat B, Dekoninck S, et al. A vascular niche and a VEGF-Nrp1 loop regulate the initiation and stemness of skin tumours. *Nature*. 2011; 478: 399–403.
 37. Frasson C, Rampazzo E, Accordi B, Beggio G, Pistollato F, Basso G, Persano L. Inhibition of PI3K Signalling Selectively Affects Medulloblastoma Cancer Stem Cells. *Biomed res int*. 2015; 2015:973912.
 38. Nissen JC, Selwood DL, Tsirka SE. Tuftsin signals through its receptor neuropilin-1 via the transforming growth factor beta pathway. *J neurochem*. 2013; 127:394–402.
 39. Hillman RT, Feng BY, Ni J, Woo WM, Milenkovic L, Hayden GM, Teruel MN, Oro AE, Chen JK, Scott MP. Neuropilins are positive regulators of Hedgehog signal transduction. *Genes Dev*. 2011; 25:2333–2346.
 40. Jacobsen PF, Jenkyn DJ, Papadimitriou JM. Establishment of a human medulloblastoma cell line and its heterotransplantation into nude mice. *J Neuropathol Exp Neurol*. 1985; 44:472–485.
 41. Friedman HS, Burger PC, Bigner SH, Trojanowski JQ, Wikstrand CJ, Halperin EC, Bigner DD. Establishment and characterization of the human medulloblastoma cell line and transplantable xenograft D283 Med. *J Neuropathol Exp Neurol*. 1985; 44:592–605.
 42. Friedman HS, Burger PC, Bigner SH, Trojanowski JQ, Brodeur GM, He XM, Wikstrand CJ, Kurtzberg J, Berens ME, Halperin EC, Et A. Phenotypic and genotypic analysis of a human medulloblastoma cell line and transplantable xenograft (D341 Med) demonstrating amplification of c-myc. *Am j pathol*. 1988; 130:472–484.

Titre : Intérêt de l'utilisation d'un peptidomimétique ciblant le récepteur NRP-1 pour le traitement du médulloblastome

Le médulloblastome (MB) est la plus fréquente des tumeurs cérébrales malignes pédiatriques qui représentent la première cause de mortalité par cancer chez l'enfant. Malgré les avancées des nouveaux traitements, les risques de récurrence, séquelles et décès après traitement restent importants. Le récepteur de neuropiline-1 (NRP-1) a été récemment impliqué dans la progression tumorale des MBs et semble jouer un rôle important dans le phénotype des cellules souches cancéreuses (CSCs). Le ciblage de cette molécule pourrait ainsi présenter un intérêt thérapeutique dans le traitement des MBs. Nous avons sélectionné des cellules souches de MB capables de former des médullosphères (MS) à partir de 3 lignées cellulaires (DAOY, D283-Med et D341-Med). Ces modèles ont été caractérisés par l'expression de neuropilines (NRP-1 and NRP-2) et de marqueurs phénotypiques (CD133, CD15 et NF-M). Les résultats ont montré une augmentation significative de l'expression de NRP-1 par les cellules cultivées en médullosphères confortant notre stratégie de ciblage. L'impact du traitement de ces cellules par un composé innovant ciblant spécifiquement NRP-1, le MR438, a été ensuite évalué *in vitro* seul et en association avec la radiothérapie notamment sur l'étude de la capacité d'auto-renouvellement des CSCs de MBs. Nous avons mis en évidence une diminution de la capacité d'autorenouvellement des cellules souches de MBs après exposition au MR438 avec une radiosensibilité augmentée pour les 3 modèles cellulaires. *In vivo*, le composé MR438 a été évalué sur des modèles de xénotransplantes hétéotopiques chez la souris nude et montre un effet radiopotentialisant significatif pour les tumeurs issues de la lignée DAOY avec une tendance à la diminution de la progression tumorale pour les 2 autres lignées. De façon intéressante, le composé MR438 induit une diminution significative du nombre de cellules souches pour l'ensemble de nos modèles. Par conséquent, le composé semblerait induire les cellules souches vers un phénotype différencié au moins pour la lignée DAOY, même si les mécanismes n'ont pas pu être clairement élucidés. En conclusion, l'inhibition de NRP-1 via MR438 semble stimuler la différenciation des cellules souches cancéreuses pouvant à terme réduire la progression du MB et apporter un bénéfice en association avec la radiothérapie. L'évaluation du composé sur des modèles orthotopiques de MB permettrait d'obtenir des informations quant à son efficacité sur des modèles plus proches de la physiopathologie tenant compte de sa distribution au niveau cérébral.

Mots-clés: Médulloblastome; Neuropiline-1; Cellule souche cancéreuse; Peptidomimétique; Radiothérapie

Title: Evaluation of a peptidomimetic targeting the receptor NRP-1 for treatment of medulloblastoma

Medulloblastoma (MB) is the most common malignant pediatric brain tumors which is the leading cause of cancer death in children. Despite the progress of new treatments, the risk of recurrence, morbidity, and death after treatment remain important. The neuropilin-1 receptor (NRP-1) has recently been implicated in tumor progression of MBs, which seems to play an important role in the phenotype of cancer stem cells (CSCs). Targeting this molecule could thus present an interesting therapeutic value in the treatment of MB. We have selected cancer stem like cells of MBs in the form of medullospheres (MSs) from 3 cell lines (DAOY, D283-Med and Med-D341). These models were characterized by expression of neuropilins (NRP-1 and NRP-2) and phenotypic markers (CD133, CD15 and NF-M). Results showed a significant increase of the expression of NRP-1 by our CSCs models cultured in MSs that confirms our targeting strategy. The impact of the treatment of these cells with an innovative compound specifically targeting NRP-1, MR438, was then evaluated *in vitro* alone and in association with radiotherapy, especially on the study of the capacity for self-renewal. A decrease of self-renewal capacity for MB stem cells after exposition of MR438 with an increase of radiosensitivity for the 3 cell models *in vitro* was demonstrated. *In vivo*, MR438 was evaluated on heterotopic xenograft models in nude mice and showed a significant augmentation of radiosensitivity for DAOY tumors with a tendency to decrease tumor progression for the other 2 cell lines. Interestingly, the compound MR438 induced a significant decrease in the number of stem cells for all of our models. The compound appeared to induce CSCs to a differentiated phenotype at least for the DAOY cells, although mechanisms could not be clearly elucidated. In conclusion, inhibition of NRP-1 via MR438 seems to stimulate the differentiation of CSCs that may eventually reduce the progression of MB and bring a benefit in association with radiotherapy. Evaluation of this compound on orthotopic models of MB would provide information on its effectiveness on models closer to the physiopathology taking into account its distribution at the cerebral level.

Key words: Medulloblastoma; Neuropilin-1; Cancer stem cells; Peptidomimetic; Radiotherapy